Louisiana State University
LSU Digital Commons

LSU Master's Theses | Graduate School

2014

Exploring Invariant Hybrid Color Image Features for Face Recognition Under Illumination Variation

Jayesh Mohan
Louisiana State University and Agricultural and Mechanical College, jmohan3@tigers.lsu.edu

Follow this and additional works at: https://digitalcommons.lsu.edu/gradschool_theses

 Part of the Electrical and Computer Engineering Commons

Recommended Citation
Mohan, Jayesh, "Exploring Invariant Hybrid Color Image Features for Face Recognition Under Illumination Variation" (2014). *LSU Master's Theses*. 628.
https://digitalcommons.lsu.edu/gradschool_theses/628

This Thesis is brought to you for free and open access by the Graduate School at LSU Digital Commons. It has been accepted for inclusion in LSU Master's Theses by an authorized graduate school editor of LSU Digital Commons. For more information, please contact gradetd@lsu.edu.

EXPLORING INVARIANT HYBRID COLOR IMAGE FEATURES FOR FACE RECOGNITION UNDER ILLUMINATION VARIATION

A Thesis

Submitted to the Graduate Faculty of the
Louisiana State University and
Agricultural and Mechanical College
in partial fulfillment of the
requirements for the degree of
Master of Science

in

The Department of Electrical and Computer Engineering

by
Jayesh Mohan
B.E., Visvesvaraya Technological University, 2010
August 2014

Acknowledgments

Matha Pitha Guru Deivam

Meaning: The meaning of this adage is the greatest truth according to the Vedic scriptures, and is the order in which one should offer reverence. Mother (Matha) who gives birth to the child and brings the child to this earth. Next comes the father (Pitha). The mother and father then take us to the teacher (Guru), and it is the guru, through his or her teachings, points us to God (Deivam). Here God represent the consciousness or self-awareness or our real self.

I dedicate this above verse to the most prominent entities in my life. First, I profusely thank my parents, Mrs.Rathi and Dr.N.Mohan for the immense motivation, emotional and financial support throughout my graduate studies at LSU. I am ever grateful to them for encouraging my interests and braving the decision to let me study at LSU despite the anxiousness of sending me all alone to Louisiana. At LSU, I deeply thank my advisor, mentor, professor and role model, Dr.Omer Soysal. He has been extraordinary in invigorating my interest in this research and has served as a role model in transforming my perspective of looking at academia. I have adopted intricate research skills from Dr.Soysal which are priceless. He has been an exemplary guru to realize my passion towards computer vision which now has become an entity of my real self. I believe that my profuse thankfulness will never suffice and I will remain indebted to Dr.Soysal for all his generous and valuable teachings.

I, further thank Dr.Bahadir Gunturk, my co-chair and professor for agreeing to be in my committee and also teaching wonderful courses in image processing. I have always enjoyed Dr.Gunturk's classes. I take this opportunity to thank Dr.Xin Li for his instant approval to be in my exam committee and also for appreciating the research.

I thank Professor Abdenour Hadid, University of Oulu, Finland for sending the compact disks containing the face database and also granting permission to use them in my thesis.

The International Cultural Center has been a strong pillar to support my education at LSU. I bow with respect and thank Ms.Maureen Hewitt and the ICC for the stupendous financial support throughout the assistantship.

I would like to take this opportunity to appreciate and thank my fiancée Anusha for her invincible endurance. She has been immensely supportive in all the walks of my graduate studies at LSU. My roommate Pratik has been a wonderful friend and companion for all the years at LSU. I also would like to thank, Abhilash for the generous help with some of the key technical aspects and valuable suggestions with my research. My friends, Anil, Sujeet, Chinmay, Asish, Ishan, Dinesh, Priyanka, Narendra have all played an important role at certain times during my studies here at LSU. I thank them all. I thank the almighty for infusing the strength to successfully complete my research.

Table Of Contents

Abstract

In this thesis, a novel analysis framework is presented in order to automate testing response of an image-feature descriptor algorithm for face recognition under different illumination conditions and white balance calibration over intra- and inter-color space. The method initially analyzes the robustness of keypoints that will be used to form image features. This analysis is conducted by exploring sensitivity of each channel of a color space against variation in illumination, white balance, and the both. In the second part, a robustness analysis is performed for the image features utilizing principal component analysis. Finally, we explore sensitivity of hybrid channels. The SIFT image descriptor is used in our experiments. The experimental results on the OPFD database show that our analysis framework finds the least sensitive channel of a color space for recognizing a face under unknown illumination, unknown white balance, and the both unknown illumination and white balance conditions. The results also show the combination of channels in a color space which are best suited face recognition.

Chapter 1 : Introduction and Motivation

1.1 Introduction

Face recognition is one of the primary research areas in image analysis and has applications not limited to the field of public security, military, personal mobile devices. The research on face recognition has made significant progress in recent years with a number of emerging accurate face recognition algorithms [1]. Despite the advancement in face recognition algorithms, many issues are yet to be addressed. There are challenges in face recognition when conditions like illumination, pose, and expression vary. We narrow down our scope in this research to explore the effect of illumination variation on detection of keypoints and image descriptors for face recognition.

1.2 Problem Statement

Practical applications for illumination invariant face recognition systems can be ranging from mobile phones to security cameras. For instance, if a law enforcement agency is trying to track a person travelling from one airport to another, how can they recognize the facial images of a person from the surveillance camera footages of two airports, taken during different times of the day? There is constant need for illumination invariant face recognition systems in real world.

1.3 Motivation and Objectives

In this thesis, we aim to present implementation results of the framework proposed to test robustness of color-space channels under varying illumination and white balance conditions for face recognition. The objectives of this thesis are

1. Automation of sensitivity-testing of an image-feature descriptor,
2. Measuring sensitivity of hybrid color spaces

We analyzed the robustness of keypoints and features of an image descriptor under different illumination and white balance conditions for three color spaces. The method of analysis is organized into three sections. First, the analysis is conducted for exploring the robustness of the keypoints. Secondly, we analyze the robustness of features. And, finally we propose the method of analyzing the salient keypoints in combination of color channels.

The robustness analysis of the keypoints and features rendered by an image descriptor are conducted to explore the stability of each channel of a color space against varying illumination, white balance, and the both together. For each varying condition, stability at local, global and most global perspectives are analyzed. The robustness of image features are analyzed using principal component analysis by examining the redundancy in feature dimensions.

The salient keypoints between two channels are analyzed by a ranking method which rates the degree of matching keypoints in a combination of channels. We utilized the proposed framework to test the SIFT image descriptor algorithm over the face images. The results are analyzed to find the stability of each channel in a color space. The images from the OPFD database show the performance of our framework. The results present the least sensitive channel in a color space for recognizing the face in unknown illumination conditions, unknown white balance conditions and both unknown illumination and white balance conditions. The combination of channels in a color space best suited for face recognition are also shown in our results. The algorithms presented in this thesis are proposed by Dr. Omer M. Soysal.

Chapter 2 : Related Work

Human face is one of the most complex three-dimensional structure due to its non-rigidity. The facial appearance is affected by many factors like illumination, pose, expression, age, occlusions and facial hair. The numerous face recognition algorithms are striving to deal with all these challenges. We will focus on the previous studies relating to illumination effects for face recognition.

The change in illumination variation has very complex effects on the image of an object. The effect of illumination on face has been studied by early psychobiologists [2]. They have observed that change in the direction of illumination on a familiar face leads to shifts in the location and shape of shadows, highlights and reversal of contrast gradients. The study emphasized that face recognitions is illumination dependent and the face recognition systems are sensitive to either direction of lighting or resultant pattern of shading [2]. A report of Face Recognition Vendor Test (FRVT 2006) [3] shows that varying illumination will greatly affect the performance of face recognition.

Many methods have been proposed to deal with the illumination variation problem, which can be roughly classified into three categories [4].

1. Illumination normalization, which use image processing techniques, such as histogram equalization (HE), Gamma correction, and homomorphic filtering [5], to normalize human face image in order to obtain face image's stability under illumination changes. However, these methods have limited success in handling arbitrary illumination changes.
2. Extraction illumination invariant, which attempts to extract robust facial features insensitive to illumination variations, such as Edge maps, Gabor-like filters methods, quotient image, Gradientfaces[4]. These methods are known to achieve good results.
3. Face modeling method, try to construct a generative 3-D face model that can be used to render face images with different poses and under varying illumination.

Further, [8] discusses method to restore a face image captured under arbitrary lighting conditions to one with frontal illumination by using a ratio-image between the face image and a reference face image. This study did not need to estimate the face surface normals and the light source directions and eliminates the need for many images captured under different lighting conditions for each person. Using color information in face recognition has been studied in [7]. It was shown in [7] that color information was helpful in improving the recognition and explored the discriminating power of different color spaces to perform reliable classification.

To our knowledge, an extensive analysis on illumination and white balance conditions on facial images has not yet been rigorously investigated. Also, there hasn't been a lot of study in exploring the effect of face recognition with a hybrid color channels in a color space and across color spaces. In this thesis, we carry out an extensive systematic analysis to explore the response of an image-feature descriptor for face recognition under effect of illumination, white balance and both illumination and white balance on frontal pose facial images. We automate the testing of the sensitivity for an image-feature descriptor. We also study the hybrid channels by examining the saliency of image-features between two channels of the same and different color spaces.

Chapter 3 : Background

3.1 Overview

In this chapter, we wish to convey brief information about some of the essential concepts used in this thesis. We will discuss the following concepts:

1. White balance
2. Scale Invariant Feature Transform
3. Principal Component Analysis
4. Color Spaces

3.2 White Balance

The various sources of light produce light differently. Ideally, we expect the white light to contain an uniform distribution across the visible spectrum. But the light which appears white does not usually contain even distribution of colors [6]. Our eyes are quick to compensate for the change in lighting conditions, like moving from indoor room to bright sunlight. The cameras, on the other hand, produce some unrealistic color casts [6]. In order to eliminate these artificial casts and get good image, we need to set the white balance of the camera to match the source temperature. Figure 3.1 shows two images, one with a blue color cast and the other with the color cast eliminated using the right white balance calibration settings for the camera. The objective of white balance is to calibrate the white balance settings of the camera to make white objects look white. Digital cameras usually have automatic white balance estimation to correct color casts. But, most camera manufacturers provide options for setting the white balance of the camera manually by setting the color temperature.

Color temperature, perceptually, is the warmness or coolness of the source light. Candle light, sunset are typical examples of the warm or reddish light and clear skies is an example of cool or bluish light.

Figure 3.1: Camera compensating for color casts [6]

In digital cameras, we can set the white balance of the camera by using the K or the Kelvin setting. This setting allows the user to input the color temperature of the image to be captured. Setting the color temperature precisely will produce an image without any color casts. In this work, it is important for us to understand the importance of color temperature and white balance. We will see the use of the terms color temperature, white balance and illumination in Section 5.3 while describing the creation of the database.

3.3 Scale Invariant Feature Transform (SIFT)

Image matching has become one of the most rudimentary parts of computer vision. The process of extracting invariant features is often sought as the quintessential aspect in recent research to facilitate image matching. The method for extracting distinctive image features through SIFT was proposed by David Lowe [9]. The features in this method are invariant to change in image scaling and rotation, partially invariant to change in illumination and 3D camera viewpoint [9]. The ability of SIFT features being highly distinctive has

3.3.1 Overview of finding the Scale Invariant Features

The steps in finding the SIFT features are as shown in Figure 3.2. We will now skim through each stage of the SIFT algorithm as described in [9].

(a) Creating a scale space and finding the scale space extrema: The process of progressively generating blurred out images results in a scale space. The locations invariant to scale change can be accomplished by searching for stable features across all possible scales [9]. The locations and scales are then repeatedly assigned to differing views of the same object. For instance, we first progressively generate blurred out images from the original image, then create scale space to resize the original image to 50% of its size and generate another set of progressively blurred images for the resized image. This process is repeated to create successive octaves of scale space. [9] suggests the use of four octaves and five blur levels for ideal performance of the SIFT.

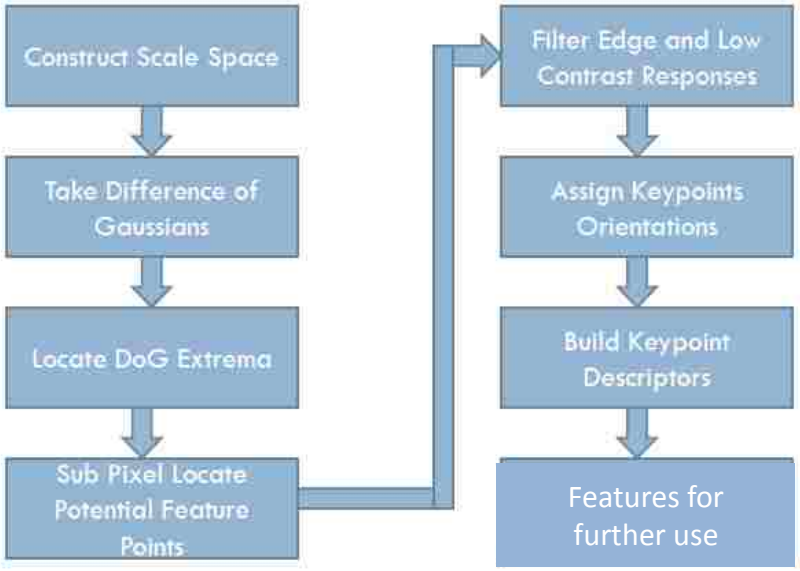

Figure 3.2: Steps in finding features of SIFT features

The function describing the scale space of an image $L(x, y, \sigma)$ is defined as the convolution of two elements. It can be written as

$$L(x, y, \sigma) = G(x, y, \sigma) * I(x, y) \tag{3.1}$$

Where $I(x, y)$ is the image with the location coordinates as x and y and $G(x, y, \sigma)$ is the variable scale Gaussian defined as

$$G(x, y, \sigma) = \frac{1}{2\pi\sigma^2} e^{\frac{-(x^2+y^2)}{2\sigma^2}} \tag{3.2}$$

[9] showed that the difference of Gaussian function provides a close approximation to the normalization of the Laplacian, $\sigma^2\nabla^2 G$, with the factor σ^2 required for true scale invariance. The Laplacian of Gaussian is computationally intensive and sensitive to noise too. Hence difference of Gaussian is used as an approximation for Laplacian of Gaussian. The process of obtaining difference of Gaussian for several scales is shown in Figure 3.3.

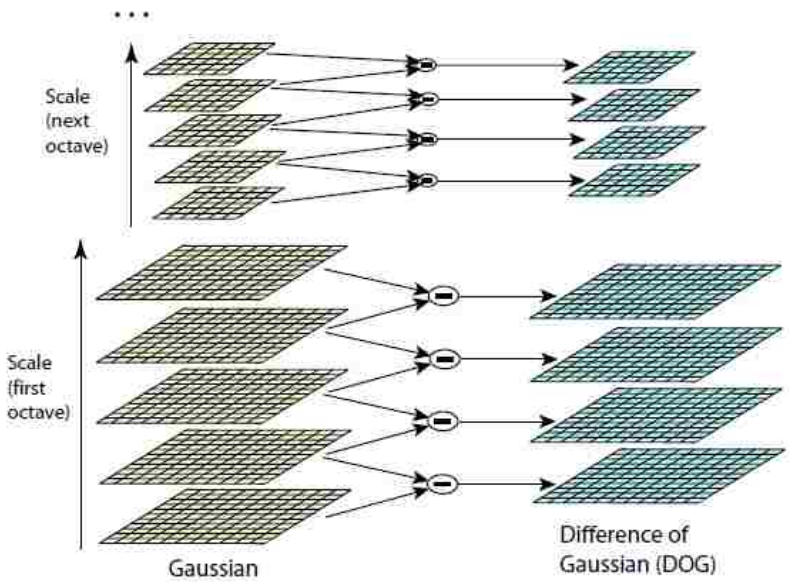

Figure 3.3: Finding the Difference of Gaussian from the scale spaces [9]

[16] showed that maxima and the minima of $\sigma^2\nabla^2 G$ produce the most stable image features compared to the other image functions. The maxima and minima are initially located in an image by iterating through each pixel and comparing it with all its neighbors and also with the same image in upper and lower scale spaces. After locating the gross maxima or minima, the sub-pixel maxima or minima is found mathematically by solving for the Taylor series as shown in [17].

$$D(x) = D + \frac{\partial D^T}{\partial x} + \frac{1}{2}\, x^T \frac{\partial^2 D}{\partial x^2} x \tag{3.3}$$

(b) Filtering the edge and low contrast points: Finding the sub-pixel maxima or minima generates a lot of keypoints even along the edges and in the regions of low contrast. These keypoints cannot be rendered useful and are eliminated. The magnitude of intensity at each candidate point in $L(x, y, \sigma)$ is compared against a threshold, which sets the bound for low contrast, noise susceptible keypoints. If the keypoint is below the threshold, it is eliminated. For edges, the poor peaks points depicting the difference of Gaussian function can be evaluated using their principal curvatures. [6] borrows the concept of finding edge responses from [18] who introduced finding of gradients to estimate a corner, edge and a flat region. An unsuitable keypoint will have a large principal curvature along the edge and a smaller value in the perpendicular direction. The ratio of both these principal curvatures serves as the threshold to eliminate poor edges. If the ratio is high then the principal curvature perpendicular to the edge is larger than the principal curvature along the edge. If that ratio for a keypoint is below the threshold, then it is retained, else eliminated.

(c) Assigning keypoints with orientation: Assignment of orientation makes the keypoints invariant against rotation. The local image gradient directions and magnitudes around each keypoint are collected and the direction of gradient for a certain keypoint is assigned to be the most prominent orientations in that region.

(d) Generating the SIFT features: After the assignment of keypoint orientation, a 16×16 window is created around the keypoint. The window is further disintegrated into sixteen 4×4 windows and local gradients magnitudes and orientations are computed and stored in an eight bin histogram. The amounts added to the bin are not only dependent on the magnitude of the gradient, but also dependent on the distance from the keypoint computed using weighted Gaussian function. The end result for 16 pixels will be 16 random orientations in eight predetermined bins. The feature vector for each keypoint will be the product of 4×4 array of histograms $\times 8$ bins resulting in 128 dimension vector.

We will use A.Vedaldi [19] implementation of SIFT in Chapter 4. This implementation produces keypoints and descriptors as similar to [9].

3.4 Principal Component Analysis (PCA)

Principal Component Analysis is the way of identifying patterns of data to find the similarities and differences. The objective of PCA is to reduce dimensionality by extracting the smallest number of components that represent most variation [10]. PCA summarizes the variation in a correlated multi-attribute to a set of uncorrelated components, each of which is a particular linear combination of the original variables. The extracted uncorrelated components are called principal components. These are estimated from the eigenvectors of the covariance or the correlation matrix of the original variables. PCA is commonly used to represent data in high dimensional space where graphical representation of data is not feasible. PCA also facilitates in compressing of high dimensional data into a lower dimensional space with minimum loss in information [10]. The application of PCA is widespread in computer vision and image processing. Image reconstruction and image compression are some of the applications in image processing.

3.4.1 PCA Terminology

In our work, eigenvalues play an important role in carrying out analysis on the SIFT features. Here we illustrate more about eigenvalues and eigenvectors from the perspective of PCA [10].

1. Eigenvalues: Measure the amount of variation given by each principal component. These will be the largest for the first principal component which indicates a lot of variation in the data points projected on it. Subsequent principal components will have lesser eigenvalues.
2. Eigenvectors: These values provide the weights to compute the uncorrelated principal components. They are linear combination of center standardized or center non standardized original variables.

3.5 Color Spaces

Light is reduced to three color components by the eye. These values are called tristimulus values [11]. The set of all possible tristimulus values determines the human color space. It is estimated that humans can distinguish around 10 million colors (See Figure 3.4).

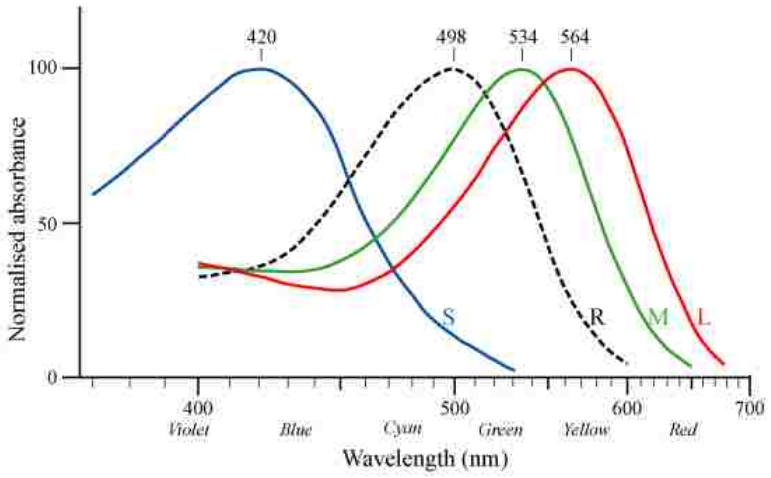

Figure 3.4: Color components as perceived by human retina [11]

The mechanisms of color vision within the retina are explained well in terms of tristimulus values. A dominant theory says that color is sent out of the eye in three opponent channels: a red-green channel, a blue-yellow channel and a black-white "luminance" channel. These channels are constructed from the tristimulus values.

Colors consisting of a single wavelength are called pure spectral or monochromatic colors. Most light sources are mixtures of various wavelengths of light. If they produce a similar stimulus in the eye, a non-monochromatic light source can be perceived as a monochromatic light. For a non-monochromatic light source there exists a dominant wavelength (or color) which identifies the single wavelength of light that produces the most similar sensation [11]. There are many color perceptions that cannot be identified by pure spectral colors, such as pink, tan, magenta, achromatic colors (black, gray, white). Two different light spectra that have the same effect on the three color receptors will be perceived as

the same color. Most human color perceptions can be generated by a mixture of three colors, called primaries. This is used to reproduce color in photography, printing, TV, etc.

The purpose of the color space is to retain the intricacies of an image such as shadow and lighting when an image is reproduced in another device other than the one with which the image was captured. For instance, the amount of color information compromised when an image is printed on the printer which clips the colors outside its color space. Figure 3.5 represents the color space conversions.

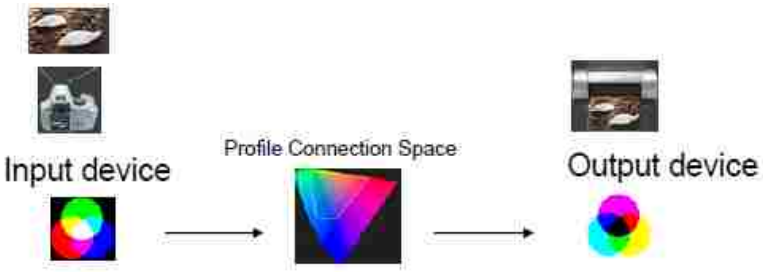

Figure 3.5: Color space conversion [12]

Each direction in a color space represents aspect of the color, such as lightness, saturation or hue, depending on the type of color space. A color gamut represents the most extreme colors which are reproducable within a particular color space [12].

3.5.1 Types of Color Space

There are three types of color spaces [12]:

a. Device dependent spaces: These color spaces can express color relative to some other reference space. It can define the subset of colors which can be displayed or captured on a particular device.
b. Device independent spaces: These color spaces express color in terms of absolute terms. These are mostly useful in comparing the devices.
c. Working spaces: These color spaces are usually confined to image editing programs and file formats. These follow a defined color palette.

We use three color spaces in our work.

1. RGB
2. YCbCr
3. HSV

3.5.1.1 RGB color space

The colors in this color space are obtained by the additive combination of three primary chromaticities. The primary chromaticities are red, green and blue. The three primary chromaticities can be visualized as shown in Figure 3.6 when they are mapped onto a 3-D Cartesian coordinate system. The RGB color space can be either device dependent or independent.

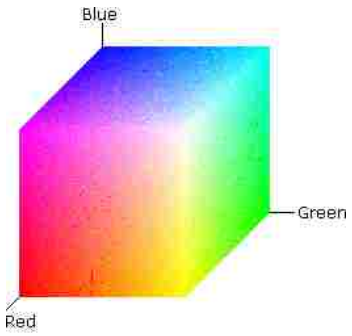

Figure 3.6: Visualization of the RGB color space on a 3-D Cartesian coordinate system [12]

3.5.1.2 YCbCr color space

This is a part of the family of color spaces used in the color image pipeline in video and digital photography systems. The Y represents the luminance information and the chrominance information is stored as Cb and Cr which are the blue difference and the red difference chroma components respectively.

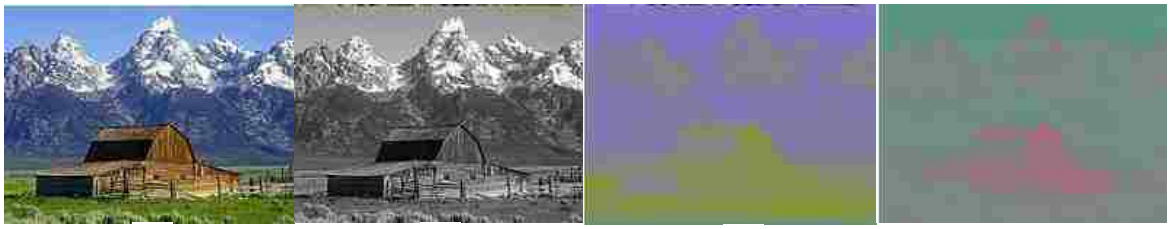

(a) (b) (c) (d)

Figure 3.7: The components of YCbCr color space. (a) Original image (b) Y component (c) Cb component (d) Cr component [13]

YCbCr is a device dependent color space. An example of the original image and the Y, Cb and Cr components are shown in Figure 3.7.

3.5.1.3 HSV color space

HSV as shown in Figure 3.8 is one of the cylindrical coordinate representations of the RGB color model. This color space is said to be the most intuitive and perceptually relevant. It is often used by artists.

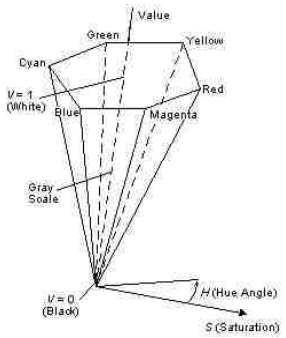

Figure 3.8: The HSV color space

The ‘H’ in the HSV represents the hue which is often referred to as the attribute of visual sensation and is used to definitively name a color such as ‘blue’ or ‘red’. The ‘V’ in the HSV represents the value, which can be described as the lightness attribute of color. The value represents any color equivalent to some shade of gray between black and white. Saturation is a measure of how different a color appears from a gray of the same lightness. Saturation can be defined as the ratio of colorfulness to brightness.

Chapter 4 : Method

4.1 Overview

In this chapter we will discuss our method of implementation and also the intuition behind each experiment. There are four primary experiments done on the keypoints and features. All these experiments are based on a set of rationale which will provide the foundation to design a face recognition system under varying illumination and white balance conditions. Following are the set of four rationales on which we model our experiments:

1. If we know the white balance condition of the camera from which an image was captured, and we do not know the illumination condition, then which color channel in a color space can we use for face recognition? For example: Let's say that we know the white balance settings of two cameras and we want to recognize if two facial images from these cameras correspond to the same person. We do not have any information about the time during which the image was captured and hence the illumination conditions. We can apply our analysis to find an appropriate channel which is best suited for recognizing the face in unknown illumination conditions.
2. If we know the illumination condition of a certain image, but we do not know the white balance condition of the camera used to capture the image, then which color channel in a color space can we use for face recognition? For example: If we have two images of a person captured at almost the same time of a day from two different cameras, and let us say that we know the illumination condition from the time of the day, but we do not have information about the type of camera and its white balance settings. If we want to recognize the person's face in this situation, we can apply our analysis to find a channel in the color space which is best suited for recognizing the face.

3. If we have no information about the white balance and illumination conditions of an image, then which color channel can we use for face recognition?
4. Which combination of channels in a color space is best suited for face recognition.

We will compare our results of all these four experiments with classification.

The following four terminologies will be referred frequently in this chapter.

1. Object: The person in an image is referred as an object. There are 16 images for each object and there are 35 objects.
2. White Balance: The preset white balance of the camera used as given by the specifications of the database.
3. Illumination condition: The set illumination condition for a certain image as given by the specifications of the database.
4. Channel: A certain channel which is a subset of a color space.

4.2 Keypoint Based Robustness Analysis

In this section we present the keypoint based stability analysis framework. As mentioned earlier, we use SIFT to obtain the number of keypoints for each image. The SIFT output for the each keypoint gives us the (x, y) location coordinates, scale and rotation quadruplets. For each image there will be several keypoints as detected by SIFT. The total count of the number of quadruplets is the number of keypoints in an image. This count will be used repeatedly throughout the following three experiments.

4.2.1 Effect of Illumination

In this experiment, we study the effect of change in illumination on the keypoint detection keeping the white balance of the image constant. Let c represents the channel, w represents the white balance, o represents the object and i represents the illumination condition; the total effect of channel, white balance, object and illumination can be represented by the variable $N_{(c,w,o,i)}$ as:

$$N_{(c,w,o,i)} = \bar{N}_{(c,w,o)} + \in_{(c,w,o,i)} \tag{4.1}$$

$$\bar{N}_{(c,w,o)} = \frac{\sum_{i=1}^{N_I} N_{(c,w,o,i)}}{N_I} \tag{4.2}$$

where $\bar{N}_{(c,w,o)}$ reflects the effect of facial structure and $\in_{(c,w,o,i)}$ represents the effect of illumination on the number of keypoints given a channel and white balance. In this experiment we utilize $\in_{(c,w,o,i)}$ to observe the effect of illumination.

Table 4.1 shows an example for an object in the H white balance condition. The illumination is changed from H through D and $N_{(c,w,o,i)}$ is the number of keypoints as detected by SIFT. The average of detected number of keypoints under all the illumination conditions is represented by $\bar{N}_{(c,w,o)}$. The value of $\bar{N}_{(c,w,o)}$ in this example is computed to be 101. We are interested in exploring $\in_{(c,w,o,i)}$ which represents the effect of illumination alone. Figure 4.1 elucidates the example shown in Table 4.1. Notice that $N_{(c,w,o,i)}$ reflects the total effect of channel, white balance, object and illumination. We are primarily interested in $\in_{(c,w,o,i)}$ to experiment the effect of illumination.

Table 4.1: Effect of illumination on keypoint detection

Channel	**WB**	**OBJ**	**ILLUM**	$N_{(c,w,o,i)}$	$\bar{N}_{(c,w,o)}$
R	H	1	H	100	101
R	H	1	A	110	101
R	H	1	T	90	101
R	H	1	D	105	101

Let N_I represent the number of illumination conditions; the value of N_I is four in our experiments. The Intra-object Stability Index, $IaOSI_{(c,w,o)}$ of the variable $N_{(c,w,o,i)}$ that varies due to the illumination i, for a channel c, white balance condition w, and object o can be represented as:

$$IaOSI_{(c,w,o)} = STD\{N_{(c,w,o,i)}\} = \sqrt{\frac{1}{N_I - 1}\sum_{i=1}^{N_I}\left(N_{(c,w,o,i)} - \bar{N}_{(c,w,o)}\right)^2} \tag{4.3}$$

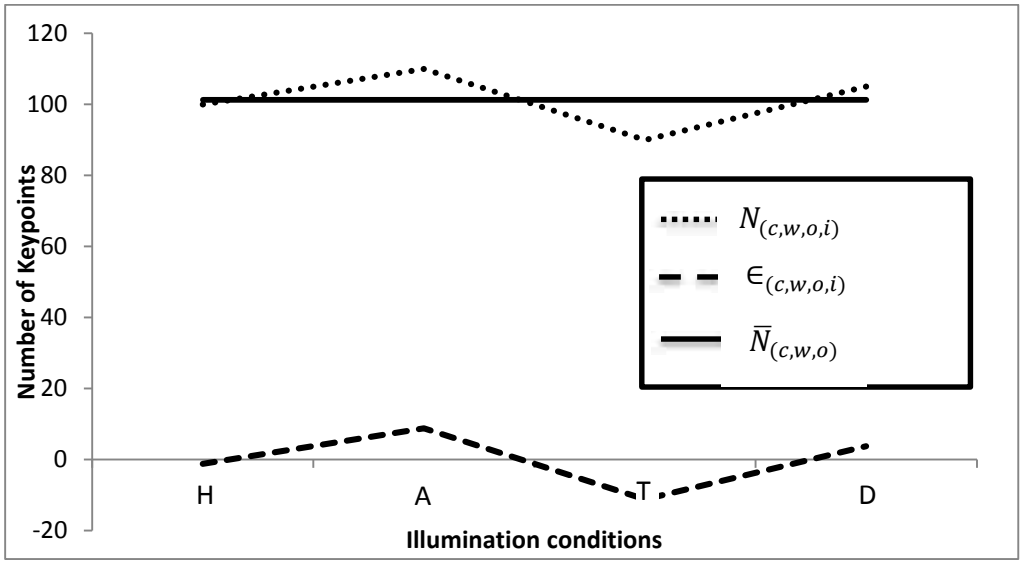

Figure 4.1: Illustration of number of keypoints and the effect of illumination

The equation (4.3) can be rewritten after substituting the value of N_{I} as follows:

$$IaOSI_{(c,w,o)} = \sqrt{\frac{1}{3}\sum_{i=1}^{4}\left(\in_{(c,w,o,i)}\right)^2} \tag{4.4}$$

The equation (4.4) measures the effect of illumination change. Exploring variation in $N_{(c,w,o,i)}$ will show us the effect of illumination change on the number of keypoints detected when the white balance is kept constant. By analyzing the variation in $N_{(c,w,o,i)}$ for each channel, we can find the most robust channel in a color space.

In the sequel, we present our framework to analyze effect of illumination on the keypoint detection. The analysis will be conducted on 3 stages: 1) Analysis of intra-object variation by measuring the effect of the illumination for a facial structure given a channel and a white balance, 2) Analysis of inter-object variation by the *inter-object stability index* (IOSI) as described below, 3) Overall analysis by means of the *overall stability index* (OSI) as given below. At the stage 2, we can decide which color channel to use for detection of keypoints for a specific type of camera system whose white balance

calibration is known. The stage 3 leads us to the most suited channel for the cases where the white balance calibration is not known. Figure 4.2 illustrates the proposed analysis stages of the framework.

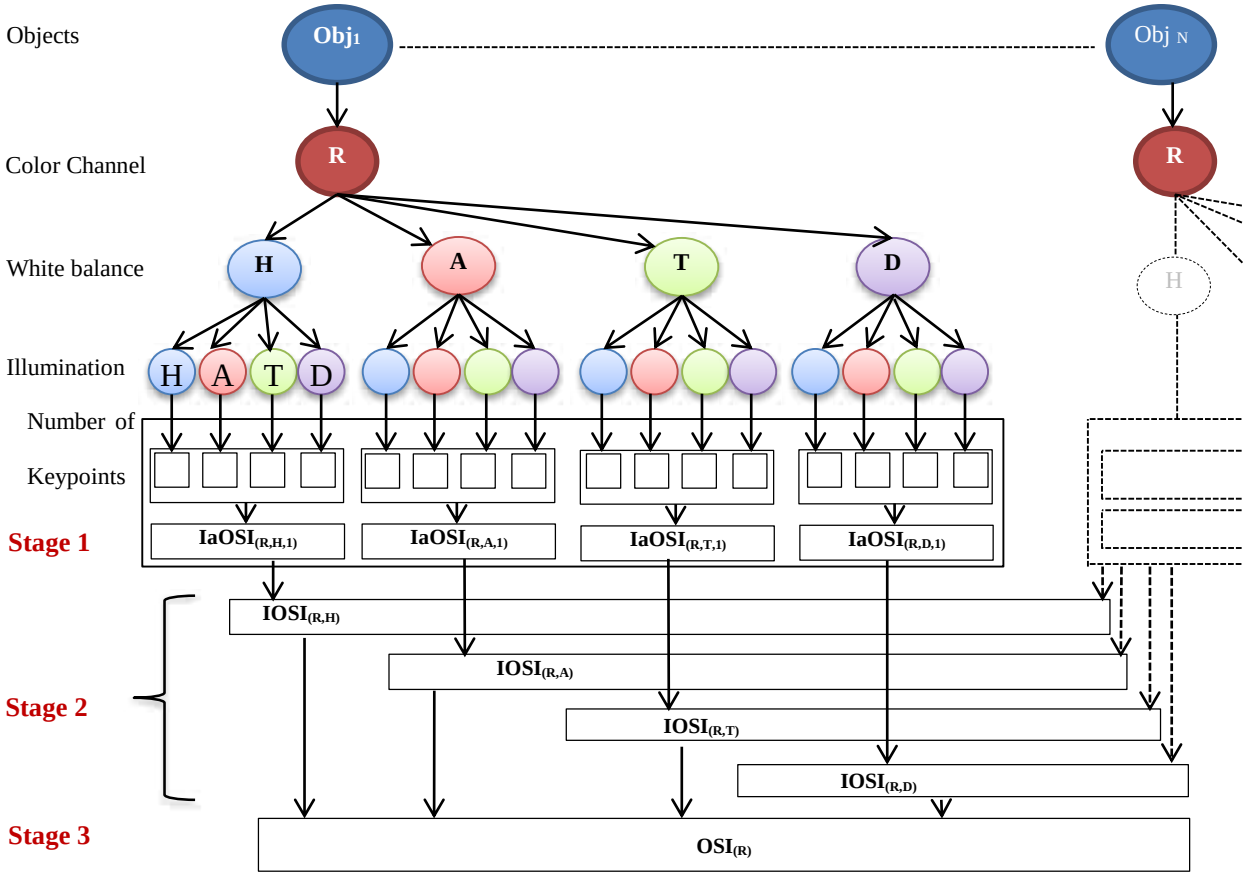

Figure 4.2: Framework for exploring the stability of keypoints against illumination for intra-object and inter-object variations

4.2.1.1 The algorithm to measure the effect of illumination variation

1. Set the color space to, say, RGB, YCbCr and HSV.
2. For a single channel, set the white balance of the input image from the database to one of H (2300K), A (2856K), T (4000-5000K) or D (6500K).
3. Obtain the input image from the database with the illumination condition set to one of H (2300K), A (2856K), T (4000-5000K) and D (6500K).
4. Apply the keypoint detector to the image rendered by each channel of the same object captured under a set white balance and illumination condition.

5. Repeat step 4 for all the four illumination conditions and obtain the detected keypoints. For each object calculate the standard deviation of the number of keypoints under the four illumination conditions keeping white balance and channel constant.
6. Repeat steps 2 – 5 for all the objects.
7. The inter-object stability index $IOSI_{(c,w)}$ is computed as average standard deviation of all objects in a certain color channel and white balance condition.

$$IOSI_{(c,w)} = \frac{\sum_{o=1}^{N_O} IaOSI_{(c,w,o)}}{N_O} \tag{4.5}$$

where N_O is the number of objects and $IaOSI_{(c,w,o)}$ is the intra-object stability index for each object under four illumination conditions defined above.

8. Repeat step 7 for all the channels in the color space.
9. Tabulate the results for further analysis.
10. Repeat steps 1 – 9 for all the color spaces.

We can compare the stability of a channel under varying illuminations for different white balance conditions by observing the inter-object stability indices .If the inter-object stability index varies little from one white balance to the other, we can say that illumination change does not significantly affect the detection of keypoints for a particular channel. Also, we can say that the keypoints rendered by the channel are more stable across variation in illumination.

We can analyze the stability of a channel across the white balance conditions by finding the variation in the stability index $IOSI_{(c,w)}$ for the four white balance conditions. The overall stability index for illumination change (OSII) of a channel *c* is given by:

$$OSII_c \triangleq STD\{IOSI_{(c,w)}\} = \frac{\sum_w \left(IOSI_{(c,w)} - \overline{IOSI_c}\right)^2}{N_W - 1} \tag{4.6}$$

The overall stability index across white balance conditions leads us to the channel which is the least sensitive to illumination variation irrespective of the white balance conditions. Figure 4.2 is a representation of the process of computing inter-object stability index and the overall stability index across white balance conditions for the red channel.

At stage 1, we explore the effect of illumination by equation (4.3) for each object under a fixed white balance condition for the red channel. At stage 2, we explore the inter-object stability index of all objects under a white balance condition as in equation (4.5). Comparing the inter-object stability indices from different white balance conditions in Stage 2 can show the effect of illumination variation from one white balance to another. At this stage we can analyze the effect of image structures under different white balance conditions to illumination variation. At stage 3, we can analyze the overall sensitivity of a particular channel to the variation in illumination considering all the white balance conditions as in equation (4.6). This stage shows us the overall stability of each channel to illumination variation. Hence, we will be comment on the most stable channel under illumination variation in a color space.

We look at the effect of illumination from a comparatively global perspective by analyzing the inter-object variation grouped according to the white balance conditions.

For a channel *c* and a white balance *w* condition, the normalized total number channel $NT_{(c,w)}$ keypoints, is computed as follows:

$$NT_{(c,w)} \triangleq \frac{\sum N_{(o,i)}}{N_{\mathrm{I}}\, N_{\mathrm{O}}} \tag{4.7}$$

where $N_{(o,i)}$ is the total of number of keypoints for all objects and illuminations for a particular white balance condition. The normalization factors in the denominator represent the number of illumination conditions N_{I} and the number of objects N_{O}. The overall standard deviation and normalized total will

be used in 6.1 to compare the different results to analyze the performance of various channels in a color space.

4.2.2 Effect of White Balance

In this experiment, we study the effect of change in white balance on the keypoint detection keeping the illumination of the image constant. Let *c* represents the channel, *w* represents the white balance, *o* represents the object and *i* represents the illumination condition; the total effect of channel, white balance, object and illumination similar to equation (4.1) can be represented by the variable $N_{(c,i,o,w)}$ as:

$$N_{(c,i,o,w)} = \bar{N}_{(c,i,o)} + \in_{(c,i,o,w)} \tag{4.7}$$

$$\bar{N}_{(c,i,o)} = \frac{\sum_{w=1}^{N_W} N_{(c,i,o,w)}}{N_W} \tag{4.8}$$

where $\bar{N}_{(c,i,o)}$ reflects the effect of facial structure and $\in_{(c,i,o,w)}$ represents the effect of white balance on the number of keypoints given a channel and illumination. In this experiment we utilize $\in_{(c,i,o,w)}$ to observe the effect of white balance.

We can use the equations (4.3) and (4.4) to explore $\in_{(c,i,o,w)}$, the effect of white balance on the number of keypoints under fixed illumination condition. The intra-object Stability Index, $IaOSI_{(c,i,o)}$ of the variable $N_{(c,i,o,w)}$ that varies due to the illumination *i*, for a channel *c*, white balance condition *w*, and object *o* can be represented as:

$$IaOSI_{(c,i,o)} = STD\{N_{(c,i,o,w)}\} = \sqrt{\frac{1}{N_W - 1}\sum_{w=1}^{N_W}\left(N_{(c,i,o,w)} - \bar{N}_{(c,i,o)}\right)^2} \tag{4.9}$$

The equation (4.9) can be rewritten after substituting the value of N_W as:

$$IaOSI_{(c,i,o)} = \sqrt{\frac{1}{3}\sum_{w=1}^{4}\left(\in_{(c,i,o,w)}\right)^2} \tag{4.10}$$

The equation (4.10) measures the effect of white balance change. Exploring variation in $N_{(c,i,o,w)}$ will show us the effect of white balance change on the number of keypoints detected when the illumination is kept constant. By analyzing the variation in $N_{(c,i,o,w)}$ for each channel, we can find the most robust channel in a color space.

We present our framework to analyze effect of white balance on the key point detection. The analysis will be conducted on 3 stages: 1) Analysis of intra-object variation by measuring the effect of the white balance for a facial structure given a channel and an illumination, 2) Analysis of inter-object variation by the *inter-object stability index* (IOSI) as described below, 3) Overall analysis by means of the *overall stability index* (OSI) as given below. At the stage 2, we can decide which color channel to use for detection of key points for a circumstance where illumination condition is known. The stage 3 leads us to the most suited channel for the cases where the illumination condition is not known. Figure 4.3 illustrated the proposed analysis stages of the framework.

4.2.2.1 The algorithm to measure the effect of white balance variation

1. Set the color space to, say, RGB, YCbCr and HSV.
2. For a single channel, set the illumination condition of the input image from the database to one of H (2300K), A (2856K), T (4000-5000K) or D (6500K).
3. Obtain the input image from the database with the white balance condition set to one of H (2300K), A (2856K), T (4000-5000K) and D (6500K).
4. Apply the keypoint detector to the image rendered by each channel of the same object captured under a set illumination and white balance condition.
5. Repeat step 4 for all the four white balance conditions and obtain the detected keypoints.

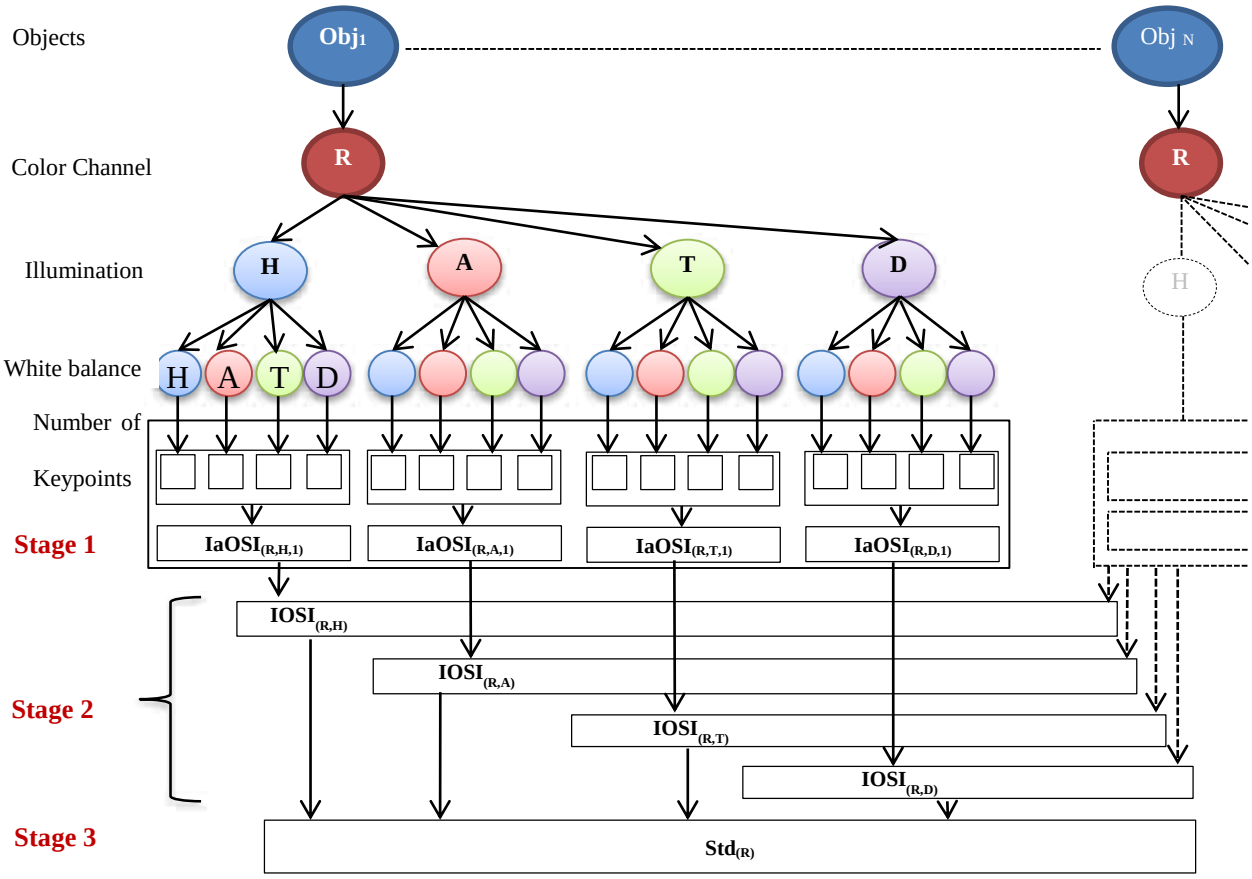

Figure 4.3: Framework for exploring the stability of keypoints against white balance variation for intra-object and inter-object variations

For each object calculate the standard deviation of the number of keypoints under the four white balance conditions keeping illumination condition and channel constant.

6. Repeat steps 2 – 5 for all the objects.
7. The inter-object stability index $IOSI_{(c,i)}$ is computed as average standard deviation of all objects in a certain color channel and illumination condition.

$$IOSI_{(c,i)} = \frac{\sum_{o=1}^{N_O} IaOSI_{(c,i,o)}}{N_O} \tag{4.11}$$

where N_O is the number of objects and $IaOSI_{(c,i,o)}$ is the intra-object stability index for each object under four white balance conditions.

8. Repeat step 7 for all the channels in the color space.

9. Tabulate the results for further analysis
10. Repeat steps 1 – 9 for all the color spaces.

The stability of a channel under varying white balance conditions can be analyzed by comparing the inter-object stability index. If the inter-object stability index varies little from one illumination to the other, we can say that white balance change does not significantly affect the detection of keypoints for a particular channel. Also, we can say that the keypoints rendered by the channel are more stable across variation in white balances.

We can analyze the stability of a channel across the illumination conditions by exploring the variation in the inter-object stability index $IOSI_{(c,i)}$ for the four illumination conditions. The standard deviation for illumination change is given by:

$$OSIW_c \triangleq STD\{IOSI_{(c,i)}\} = \frac{\sum_i \left(IOSI_{(c,i)} - \overline{IOSI_c}\right)^2}{N_{\mathrm{I}} - 1} \tag{4.12}$$

At stage 1, we explore the effect of white balance by equation (4.9) for each object under a fixed illumination condition for the red channel. At stage 2, we explore the inter-object stability index of all objects under an illumination condition as in equation (4.11). Comparing the inter-object stability indices from different illumination conditions in Stage 2 can show the effect of white balance variation from one illumination to another. At this stage we can analyze the effect of image structures under different illumination conditions to white balance variation. At stage 3, we can analyze the overall sensitivity of a particular channel to the variation in white balance considering all the illumination conditions as in equation (4.12). This stage shows us the overall stability of each channel to white balance variation. Hence, we will be comment on the most stable channel under white balance variation in a color space.

We look at the effect of white balance from a comparatively global perspective by analyzing the inter-object variation grouped according to the illumination conditions. For each channel and white balance condition, the normalized total number of keypoints $NT_{(c,w)}$, is computed as follows:

$$NT_{(c,w)} \triangleq \frac{\sum N_{(o,w)}}{N_W\, N_{\mathrm{O}}} \tag{4.13}$$

where $N_{(o,w)}$ is the total of number of keypoints for all objects and white balance conditions for a particular illumination. The normalization factors in the denominator represent the number of white balance conditions N_{W} and the number of objects N_{O}.

4.2.3 Effect of Illumination and white balance

In this experiment, we study the effect of change in white balance and illumination on the keypoint detection. Let *c* represents the channel, *w* represents the white balance, *o* represents the object and *i* represents the illumination condition; the total effect of channel, white balance, object and illumination can be represented similar to the equation (4.1) by the variable $N_{(c,w,o,i)}$:

$$N_{(c,o,w,i)} = \bar{N}_{(c,o)} + \in_{(c,o,\mathrm{w},i)} \tag{4.14}$$

$$\bar{N}_{(c,o)} = \frac{\sum_{w=1}^{N_{\mathrm{W}}} \sum_{i=1}^{N_{\mathrm{I}}} N_{(c,o,w,i)}}{N_{\mathrm{W}} N_{\mathrm{I}}} \tag{4.15}$$

where $\bar{N}_{(c,o)}$ reflects the effect of facial structure in addition to the channel and white balance under different illumination conditions and $\in_{(c,o,\mathrm{w},i)}$ represents the effect of variation due to white balance and illumination conditions on the number of keypoints.

We can use the equations (4.3) and (4.4) to explore $\in_{(c,o,\mathrm{w},i)}$, the effect of white balance and illumination on the number of keypoints for a given channel and object. The intra-object stability index, $IaOSI_{(c,o)}$ of the variable $N_{(c,o,w,i)}$ that varies due to the illumination *i*, for a channel *c*, white balance condition *w*, and object *o* as:

$$IaOSI_{(c,o)} = STD\{N_{(c,o,w,i)}\} = \sqrt{\frac{1}{N_{\mathrm{W}}N_{\mathrm{I}} - 1}\sum_{w=1}^{N_{\mathrm{W}}}\sum_{i=1}^{N_{\mathrm{I}}}\left(N_{(c,o,w,i)} - \bar{N}_{(c,o)}\right)^2} \tag{4.16}$$

Having $N_{\mathrm{W}} = N_{\mathrm{I}} = 4$,

$$IaOSI_{(c,o)} = \sqrt{\frac{1}{15}\sum_{w=1}^{4}\sum_{i=1}^{4}\left(\in_{(c,o,\mathrm{w},i)}\right)^2} \tag{4.17}$$

The equation (4.16) measures the effect of white balance and illumination change. Exploring variation in $N_{(c,o,w,i)}$ will show us the effect of white balance and illumination change on the number of keypoints detected.

4.2.3.1 Algorithm to compute the effect of illumination and white balance variation

1. Set the color space to, say, RGB, YCbCr and HSV.
2. Choose an object.
3. For a single channel in the color space, apply keypoint detector to the image rendered by each channel of the same object captured under all the illumination and white balance conditions.
4. Given the color channel, for each object calculate the standard deviation of keypoints under all the four white balance and illumination conditions. Repeat step 3 and 4 for other channels in the color space.
5. Repeat steps 2 – 4 for all the objects.
6. The inter-object stability index $IOSIWI_c$ is computed as average standard deviation of all objects for a certain color channel c under the change of white balance and illumination conditions.

$$IOSIWI_c = \frac{\sum_{o=1}^{N_O} IaOSI_{(c,o)}}{N_O} \tag{4.18}$$

where N_O is the number of objects and $IaOSI_{(c,o)}$ is the intra-object stability index of an object under all four white balance and illumination conditions. There will be 16 images per object in this case.

7. Repeat step 6 for all the channels in the color space.
8. Tabulate the results for further analysis.
9. Repeat steps 1 – 8 for all the color spaces.

Since this experiment does not compute the variations one object at a time, we expect inter-object stability index to be more unstable than the other two previous experiments. We will find the channel which is most robust to both illumination and white balance variations from this analysis.

We look at the effect of white balance and illumination from a comparatively global perspective by analyzing the inter-object variation. For each channel and object, the normalized total number of keypoints $NT_{(c)}$ is computed as follows:

$$NT_{(c)} \triangleq \frac{\sum N_{(o,w,i)}}{N_W N_I N_O} \tag{4.19}$$

where $N_{(o,w,i)}$ is the total of number of keypoints for all objects, white balance and illumination conditions. The normalization factors in the denominator represent the number of white balance conditions N_{W}, illumination conditions N_{I} and the number of objects N_{O}.

4.2.3.2 Overall Analysis

In the previous sections, we looked at the effect of illumination and white balance considering one object at a time for the number of keypoints. It was a localized way to look at all the objects. This experiment accounts for the inter-object variation and gives us the most global perspective of illumination and white balance variation considering all the objects at a time. Our objective of this

experiment is to explore the overall sensitivity of a channel to change in illumination, white balance and facial structure.

The overall inter-object stability index OSI_c of a channel is given by:

$$OSI_c \triangleq STD\{N_{(c,w,o,i)}\} = \frac{\sum(N_{(c,w,o,i)} - \bar{N}_{(c)})^2}{N_O N_W N_I} \quad (4.20)$$

where $N_{(c,w,o,i)}$ represents the number of keypoints for all objects in the database under all the illumination and white balance conditions for a given channel.

4.3 Feature Based Robustness Analysis

The SIFT feature vector for each keypoint has 128 dimensions. The number of dimensions of a feature vector is the most significant and a unique description of a keypoint. In order to measure the variation in the sensitivity of the features rendered by a channel, we look into its redundancy of dimensions. If there are more distinguishing feature dimensions in a channel, they can describe the keypoints very effectively. But, if the feature dimensions are redundant, they do not help in describing the keypoints uniquely. We use normalized number of dimensions as the redundancy index to measure the amount of redundancy in the feature vectors. We will elucidate more about normalized number of dimensions in the coming sections. By the end of this section, we will establish methodologies for the following objectives:

1. To measure the effect of change in illumination on the feature vectors when the white balance is kept constant.
2. To measure the effect of change in white balance on the feature vectors when the illumination is constant.
3. To measure the effect of change in illumination and white balance on the feature vectors.

4.3.1 Normalized number of dimensions

PCA finds a linear projection of high dimensional data into lower dimensional subspace. We will use PCA to analyze the redundancy in dimensions of the feature vectors. When PCA is applied to the a feature vector, the eigenvalues measure the amount of variation described by each principal component and the number of eigenvalues represent the number of principal components or in other words, the number of dimensions in the resultant feature vector.

We will illustrate the significance of number of dimensions and their reduction with an example. Let us consider two channels, blue and red of the RGB color space. The results after application of PCA to the blue and red channels of an image are as shown in

Table 4.2. The table also shows the number of feature points as detected by SIFT before applying PCA.

Table 4.2: Number of dimensions after PCA

	Number of Dimensions After applying PCA	Number of feature points
Blue channel	3	10
Red channel	2	10

Figure 4.4 shows a pictorial representation of the data in Table 4.2. We can see the projection of the key features on the dimensions after they have been reduced by PCA. The 10 feature points in the red channel can only be projected on 2 dimensions, whereas the blue channel is more effective in describing the features of 10 feature points on 3 dimensions. From this example we can infer that features from the blue channel have more distinguishing capability than the ones in the red channel for the same image.

Our objective throughout this experiment is to look for more distinguishing dimensions exhibited by the feature vectors.

Two important hypotheses can be drawn from the example described earlier:

1. More dimensions exist if feature vectors of the keypoints are dissimilar as they are sparsely scattered.

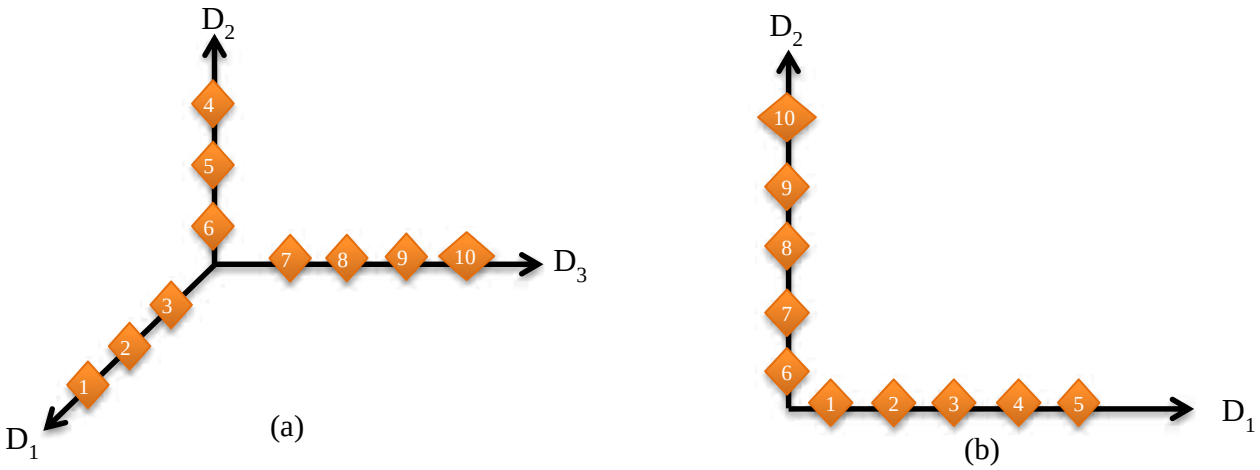

Figure 4.4: Illustration of number of dimensions

2. When keypoints are similar we can express the feature vectors associated with the keypoints in a space which has less number of dimensions. So, the features of these keypoints are densely populated on fewer dimensions indicating the presence of many similar, non-unique feature descriptions.

We have seen how the reduction in number of dimensions of feature vectors can be an important measure to help us find a channel with salient features. But, can we just compare the reduction in number of dimensions before and after PCA in all the cases? After further analysis, we proposed two redundancy indices to compare the reduction in the number of dimensions:

1. The ratio of the number of dimensions after applying PCA to the number of dimensions before the applying PCA, called the reduction ratio.
2. The normalized number of dimensions.

The reduction ratio as described earlier is a straightforward method of analyzing the reduction in number of dimensions post application of PCA. But, in some cases we cannot decide the efficiency of

the features in a channel by merely looking at the reduction ratio. We will illustrate the problem with an example shown in Figure 4.5. In Figure 4.5(a), the red channel has two dimensions with nine feature points and in Figure 4.5(b) the blue channel has three dimensions with 14 feature points. Both of these channels look efficient in expressing their key features if the reduction ratio is used; notice that the reduction ratio is 9/128 versus 14/128, respectively. To find the most efficient channel we propose to normalize number of dimensions obtained by PCA with the number of keypoints. The normalized number of dimensions can be expressed as follows:

$$Normalized\ number\ of\ dimensions\ (in\ percentage) = \frac{Number\ of\ dimensions\ (post\ PCA)}{Number\ of\ keypoints} \qquad (4.21)$$

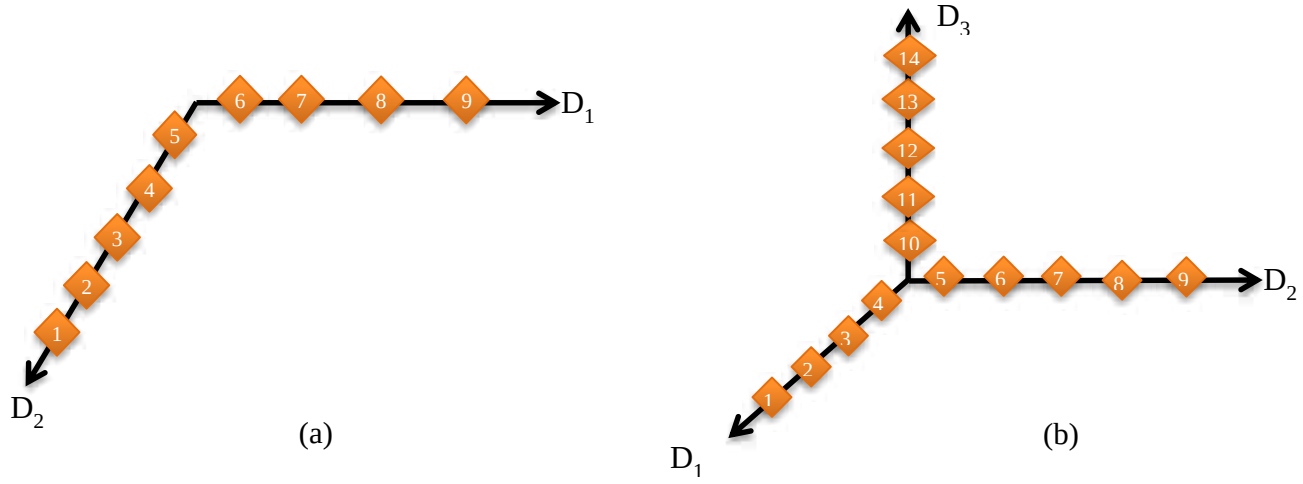

Figure 4.5: (a) Red channel with two dimensions and nine key features (b) Blue channel with three dimensions and 14 key features

Reduction ratio and normalized number of dimensions (NND) are the two redundancy indices proposed. We need to identify the ideal redundancy index to efficiently analyze the features in a channel. Table 4.3 shows an example of data from two channels. The last two columns show the results of NND and reduction ratio. From the data in Table 4.3 we can see that the reduction ratio for both the channels give the same results. Hence we cannot use reduction ratio as the redundancy index. But, when we normalize the PCA reduced dimensions with the number of feature points, we can clearly see that the channel 1 is more efficient in expressing its feature points than channel 2. Hence, the NND turns out to be a better method for measuring the redundancy index.

Further, let us say that there are million feature points for a channel and they are projected onto 10

Table 4.3: Normalized number of dimensions vs. Reduction Ratio

Channel	PCA reduced dimensions	Number of feature points detected	Normalized number of dimensions	Reduction Ratio
1	10	100	10%	$\frac{10}{128}$
2	10	200	5%	$\frac{10}{128}$

dimensions and compare it to another channel with 10 feature points projected onto 10 dimensions. For SIFT we know that each point in the feature space has 128 dimensions. When a million key features are projected onto just 10 dimensions, then we can say that there is some way to group the million data into clusters and project them to just 10 dimensions. Even though the dataset is large, the projection of dataset is in just few dimensions. It means that there are too many points in the dataset giving information about each dimension. In the second case, we have 10 points and there are 10 dimensions. Here, we can say that clustering was not possible with the points and each point defined a unique dimension. We are indeed looking for dataset which express the feature points of a channel uniquely as much as possible. From all the previous examples, we can conclude that NND suits for our purpose of measuring redundancy of the dataset. We will use it for the following experiments in this section.

4.3.2 Obtaining the cut values and setting a threshold on eigenvalues

In general, the number of non-zero eigenvalues are the same for all channels. On the other hand, when the eigenvalues get smaller, their significance to represent data also is reduced. The question "what would be the minimum best eigenvalue such that the dimensions up to this eigenvalue can be used to represent data?" In the sequel, we present a method to find this 'minimum best' eigenvalue.

We will use the eigenvalues which are arranged in descending order to compute the NND. As discussed earlier, the eigenvalues represent the number of principal components. To compute the number of

dimensions, we need to have a reference count. From each channel we create a column matrix of reference counts known as cut values from the eigenvalues as follows:

1. We will choose the first cut value to be half of the minimum value of the first and most significant eigenvalues from all the channels. For instance, Figure 4.6 shows the eigenvalues of R, G and B channels arranged in descending order. The first eigenvalues in all the channels represent the most significant principal component. The minimum eigenvalue of all the three channels is B channel with a value of 1.29. We will choose our first cut value to be half of 1.29.

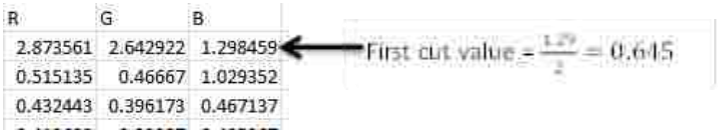

Figure 4.6: Choosing the first cut value

2. The consecutive cut values to form the column matrix are calculated by dividing the first cut value by 2. This division is carried on until the current cut value is greater than 0.000001. Table 4.4 shows an example of forming the column matrix of cut values and their indices. We know that the eigenvalues in our experiment are arranged in descending order from the most to the least significant ones. The cut value threshold was decided upon close examination of the range of the eigenvalues which are significant after applying PCA to the images. The eigenvalues lesser than 10^{-8} are considered to be insignificant.

Table 4.4: Cut values

Cut value index	0.6450
1	$\frac{0.6450}{2}$ =0.3225
2	$\frac{0.3225}{2}$ =0.1613
3	$\frac{0.1613}{2}$ =0.0806
4	$\frac{0.0806}{2}$ =0.0403
5	$\frac{0.0403}{2}$ =0.0202
6	$\frac{0.0202}{2}$ =0.0101

n^{th} cut value index	……. Greater or equal to 0.000001

4.3.3 Finding the Normalized Number of Dimensions

The data in the cut value column matrix is compared against the eigenvalues of all the channels in an image as follows:

1. We begin from the first cut value in the matrix. Let us consider it as the current cut value.
2. Count the number of eigenvalues or the cut value indices in each channel which are greater than or equal to the current cut value. Store the count in the resultant matrix. This count is called the number of dimensions.
3. Repeat step 2 for all the cut values in the cut value column matrix.

The normalized number of dimensions is computed by normalizing each value of the number of dimensions by the number of keypoints of the corresponding channel.

$$Normalized\ number\ of\ dimensions\ (in\ percentage) = \frac{Number\ of\ dimensions\ (post\ PCA)}{Number\ of\ keypoints} \qquad (4.22)$$

4.3.4 Finding the Maximum Normalized Number of Dimensions

Our core objective throughout this section is to find a channel which can express the feature points in maximum possible unique dimensions. The NND values are stored in a column matrix. We set an upper threshold to the NNDs by finding its maximum value. The maximum NND of each channel is a point at which two consecutive NNDs stop varying or in other words, it is the point at which the difference between consecutive NNDs is zero. Table 4.5 shows the computation of maximum NND's for sample data from the RGB channel. It should be noted that all the entries in Table 4.5 are NNDs Figure 4.7 shows the values of maximum NNDs for a RGB channel. The point at which the NND value stops varying is shown for G and B channels.

If we do not find the two consecutive non varying values, then the end value of NND is considered to be the maximum NND. In Figure 4.7, the end value of the R channel is taken as the maximum NND.

Table 4.5: Computing the maximum normalized number of dimensions

	R	G	B	
	15	13	14	
20-15	20	15	25	
22-20	22	18	25	25-25, Difference is '0'

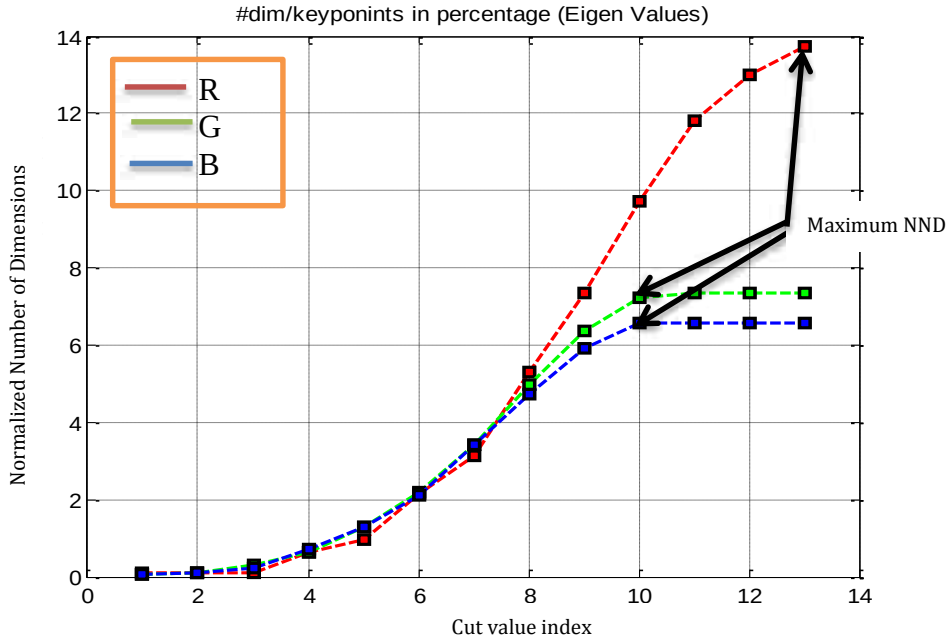

Figure 4.7: The maximum NND for RGB channel

4.3.5 Effect of illumination

In this experiment, we analyze the effect of illumination on the features rendered by an image. Our objective is to find a channel which produces the maximum dimensions to express the feature points despite the illumination change. We have seen how many dimensions are favorable for us as it describes the features uniquely. Maximum NND is the measure used to inspect the redundancy of the features in a channel. We study the effect of change in illumination on the maximum NNDs keeping the white balance of the image constant. The analysis is similar to effect of illumination on the number of keypoints. Here we use the maximum NND instead of the number of keypoints. Let *c* represents the channel, *w* represents the white balance, *o* represents the object and *i* represents the illumination

condition; the total effect of channel, white balance, object and illumination can be represented similar to equations (4.1) and (4.2) by the variable $N_{(c,w,o,i)}$ as:

$$N_{(c,w,o,i)} = \bar{N}_{(c,w,o)} + \in_{(c,w,o,i)} \tag{4.23}$$

$$\bar{N}_{(c,w,o)} = \frac{\sum_{i=1}^{N_I} N_{(c,w,o,i)}}{N_I} \tag{4.24}$$

where $\bar{N}_{(c,w,o)}$ reflects the effect of facial structure and $\in_{(c,w,o,i)}$ represents the effect of illumination change on the maximum NND given a channel and white balance. In this experiment we utilize $\in_{(c,w,o,i)}$ to observe the effect of illumination. Let N_I represent the number of illumination conditions; the value of N_I is four in our experiments. The intra-object stability index, $IaOSI_{(c,w,o)}$ of the variable $N_{(c,w,o,i)}$ that varies due to the illumination *i*, for a channel *c*, white balance condition *w*, and object *o* can be represented similar to equations (4.3) and (4.4) as:

$$IaOSI_{(c,w,o)} = STD\{N_{(c,w,o,i)}\} = \sqrt{\frac{1}{N_I - 1}\sum_{i=1}^{N_I}\left(N_{(c,w,o,i)} - \bar{N}_{(c,w,o)}\right)^2} \tag{4.25}$$

The equation (4.25) can be rewritten after substituting the value of N_I as follows:

$$IaOSI_{(c,w,o)} = \sqrt{\frac{1}{3}\sum_{i=1}^{4}\left(\in_{(c,w,o,i)}\right)^2} \tag{4.26}$$

Exploring variation in $N_{(c,w,o,i)}$ as seen in equation (4.25), will show us the effect of illumination change on the maximum dimensions detected when the white balance is kept constant. By analyzing the variation in $N_{(c,w,o,i)}$ for each channel, we can find the most robust channel in a color space.

The framework to analyze the effect of illumination was discussed in section 4.2.1. We follow this framework for effect of illumination on the features.

4.3.5.1 Algorithm to measure the effect of illumination variation

5. Set the color space to, say RGB, YCbCr and HSV.
6. For a single channel, set the white balance of the input image from the database to one of H (2300K), A (2856K), T (4000-5000K) or D (6500K).
7. Obtain the input image from the database with the illumination condition set to one of H (2300K), A (2856K), T (4000-5000K) and D (6500K).
8. Apply the feature detector to the image rendered by each channel of the same object captured under a set white balance and illumination condition.
9. Apply Principal Component Analysis (PCA) to feature vectors of all the channels of an image and obtain the eigenvalues.
10. Compute the cut value matrix with the starting cut value to be the half of the minimum value of the first eigenvalues from all channels.
11. Find the NNDs corresponding to each cut value as follows:
12. We will begin from the first cut value in the matrix and consider it as the current cut value.
13. Count the number of eigenvalues in each channel which are greater than or equal to the current cut value for all the channels and store the count in the resultant matrix.
14. Repeat step (b) for all the cut values in the cut value matrix.
15. Each value in the resultant matrix is normalized with the corresponding number of keypoints to get the value of NND
16. Find the maximum NND for each channel by locating a value of NND beyond which the NNDs remain constant.
17. Repeat steps 4 – 8 for all the four illumination conditions and obtain the maximum NNDs. For each object calculate the standard deviation of maximum NNDs under the four illumination conditions keeping white balance and channel constant.

18. Repeat steps 1 – 9 for all objects.
19. The inter-object stability index $IOSI_{(c,w)}$ is computed as average standard deviation of all objects in a certain color channel and white balance condition.

$$IOSI_{(c,w)} = \frac{\sum_{o=1}^{N_O} IaOSI_{(c,w,o)}}{N_O} \tag{4.27}$$

where N_O is the number of objects and $IaOSI_{(c,w,o)}$ is the intra-object stability index for each object under four illumination conditions.

20. Repeat step 11 for all the channels in the color space.
21. Tabulate the results for further analysis.
22. Repeat steps 1 – 13 for all the color spaces.

We can analyze the stability of a channel under varying illuminations for different white balance conditions by looking at the average standard deviation for maximum NNDs. If the average standard deviation does not change from one white balance to other, we can say that illumination change does not affect the number of dimensions in a feature vector for a particular channel. We can also say that the maximum NNDs rendered by a channel are more stable across variation in illumination.

We can analyze the stability of a channel across the white balance conditions by finding the variation in the stability index $IOSI_{(c,w)}$ for the four white balance conditions as seen in equation (4.6). The standard deviation $OSII_c$ for illumination change is given by:

$$OSII_c \triangleq STD\{IOSI_{(c,w)}\} = \frac{\sum_w \left(IOSI_{(c,w)} - \overline{IOSI_c}\right)^2}{N_W - 1} \tag{4.28}$$

The overall stability index leads us to the channel which is the least sensitive to illumination variation irrespective of the white balance conditions. Comparing the stability index across white balance conditions shows the overall stability of each channel to illumination variation. We will be able to find

the channel in a color space whose features are stable against illumination variation across all white balance conditions.

We look at the effect of illumination from a comparatively global perspective by analyzing the inter-object variation grouped according to the white balance conditions. For each channel and white balance condition, the normalized total of maximum NNDs $NT_{(c,w)}$ is computed as follows:

$$NT_{(c,w)} \triangleq \frac{\sum N_{(o,i)}}{N_{\mathrm{I}}\, N_{\mathrm{O}}} \tag{4.29}$$

where $N_{(o,i)}$ is the total of number of the maximum NNDs for all objects in a particular white balance condition. The normalization factors in the denominator are the product of N_I and N_O which represent the number of illumination conditions and the number of objects respectively.

4.3.6 Effect of White Balance

In this experiment, we study the effect of change in white balance on the maximum NNDs keeping the illumination of the image constant. Let *c* represents the channel, *w* represents the white balance, *o* represents the object and *i* represents the illumination condition; the total effect of channel, white balance, object and illumination similar to equation (4.1) can be represented by the variable $N_{(c,i,o,w)}$ as:

$$N_{(c,i,o,w)} = \bar{N}_{(c,i,o)} + \in_{(c,i,o,w)} \tag{4.30}$$

$$\bar{N}_{(c,i,o)} = \frac{\sum_{w=1}^{N_{\mathrm{W}}} N_{(c,i,o,w)}}{N_{\mathrm{W}}} \tag{4.31}$$

where $\bar{N}_{(c,i,o)}$ reflects the effect of facial structure and $\in_{(c,i,o,w)}$ represents the effect of white balance on the number of keypoints given a channel and illumination. In this experiment we utilize $\in_{(c,i,o,w)}$ to observe the effect of white balance.

We can apply the equations (4.3) and (4.4) to explore $\in_{(c,i,o,w)}$, the effect of white balance variation on the maximum NNDs when illumination is kept constant. The intra-object Stability Index, $IaOSI_{(c,i,o)}$ of the variable $N_{(c,i,o,w)}$ that varies due to the illumination *i*, for a channel *c*, white balance condition *w*, and object *o* can be represented similar to equation (4.9) as:

$$IaOSI_{(c,i,o)} = STD\{N_{(c,i,o,w)}\} = \sqrt{\frac{1}{N_{\mathrm{W}} - 1}\sum_{w=1}^{N_{\mathrm{W}}}\left(N_{(c,i,o,w)} - \bar{N}_{(c,i,o)}\right)^2} \tag{4.32}$$

The equation (4.32) can be rewritten after substituting the value of N_{W} as:

$$IaOSI_{(c,i,o)} = \sqrt{\frac{1}{3}\sum_{w=1}^{4}\left(\in_{(c,i,o,w)}\right)^2} \tag{4.33}$$

The equation (4.33) measures the effect of white balance change. Exploring variation in $N_{(c,i,o,w)}$ will show us the effect of white balance change on the number of feature dimensions when illumination is kept constant. By analyzing the variation in $N_{(c,i,o,w)}$ for each channel, we can find the most robust channel in a color space.

The framework to analyze the effect of white balance variation was presented in section 4.2.2. We follow a similar analysis in this section too.

4.3.6.1 Algorithm to measure the effect of white balance variation

1. Set the color space to, say, RGB, YCbCr and HSV.
2. For a single channel, set the illumination condition of the input image from the database to one of H (2300K), A (2856K), T (4000-5000K) or D (6500K).
3. Obtain the input image from the database with the white balance condition set to one of H (2300K), A (2856K), T (4000-5000K) and D (6500K).

4. Apply the feature detector to the image rendered by each channel of the same object captured under a set illumination and white balance condition.
5. Apply Principal Component Analysis (PCA) to feature vectors of all the channels of an image and obtain the eigenvalues.
6. Compute the cut value matrix with the starting cut value to be the half of the minimum value of the first eigenvalues from all channels.
7. Find the NNDs corresponding to each cut value.
8. Find the maximum NND for each channel by locating a value of NND beyond which the NNDs remain constant.
9. Repeat steps 4 – 8 for all the four white balance conditions and obtain the maximum NNDs. For each object calculate the standard deviation of maximum NNDs under the four white balance conditions keeping illumination and channel constant.
10. Repeat steps 1 – 9 for all objects.
11. The inter-object stability index $IOSI_{(c,i)}$ is computed as average standard deviation of all objects in a certain color channel and illumination condition.

$$IOSI_{(c,i)} = \frac{\sum_{o=1}^{N_O} IaOSI_{(c,i,o)}}{N_O} \tag{4.34}$$

where N_O is the number of objects and $IaOSI_{(c,i,o)}$ is the intra-object stability index for each object under four white balance conditions.

12. Repeat step 11 for all the channels in the color space.
13. Tabulate the results for further analysis.
14. Repeat steps 1 – 13 for all the color spaces.

The stability of the features rendered by the channel under varying white balance conditions can be analyzed by comparing the inter-object stability index for each illumination condition. If the inter-

object stability index varies little from one illumination to the other, we can say that white balance change does not significantly affect the detection of features for a particular channel. Also, we can say that the features rendered by the channel are more stable across variation in white balances.

We can analyze the stability of a channel across the illumination conditions by exploring the variation in the inter-object stability index $IOSI_{(c,i)}$ for the four illumination conditions. The standard deviation for illumination change is similar to (4.12) and is given by:

$$OSIW_c \triangleq STD\{IOSI_{(c,i)}\} = \frac{\sum_i \left(IOSI_{(c,i)} - \overline{IOSI_c}\right)^2}{N_{\mathrm{I}} - 1} \tag{4.35}$$

We analyze the inter-object variation by grouping according to the illumination conditions. The analysis is similar to the experiment described in section 4.2.1.1. For each channel and white balance condition, the normalized total of maximum NNDs $NT_{(c,w)}$ is computed as follows:

$$NT_{(c,w)} \triangleq \frac{\sum N_{(o,w)}}{N_W\, N_{\mathrm{O}}} \tag{4.36}$$

where $N_{(o,w)}$ is the total number of maximum NNDs for all objects in a particular illumination condition. The normalization factors in the denominator represent the number of white balance conditions N_{W} and the number of objects N_{O}.

4.3.7 Effect of Illumination and White Balance

In this experiment, we study the effect of change in white balance and illumination on the feature dimensions. Let *c* represents the channel, *w* represents the white balance, *o* represents the object and *i* represents the illumination condition; the total effect of channel, white balance, object and illumination can be represented as in equation (4.1) by the variable $N_{(c,w,o,i)}$:

$$N_{(c,o,w,i)} = \bar{N}_{(c,o)} + \in_{(c,o,\mathrm{w},i)} \tag{4.37}$$

$$\bar{N}_{(c,o)} = \frac{\sum_{w=1}^{N_{\mathrm{W}}} \sum_{i=1}^{N_{\mathrm{I}}} N_{(c,o,w,i)}}{N_{\mathrm{W}} N_{\mathrm{I}}} \tag{4.38}$$

where $\overline{N}_{(c,o)}$ reflects the effect of facial structure in addition to the channel and white balance under different illumination conditions and $\in_{(c,o,\mathrm{w},i)}$ represents the effect of variation due to white balance and illumination conditions on the number of dimensions.

Using the equations (4.3) and (4.4) to explore $\in_{(c,o,\mathrm{w},i)}$, the effect of white balance and illumination on the number of keypoints for a given channel and object . The intra-object stability index, $IaOSI_{(c,o)}$ of the variable $N_{(c,o,w,i)}$ that varies due to the illumination *i*, for a channel *c*, white balance condition *w*, and object *o* as:

$$IaOSI_{(c,o)} = STD\{N_{(c,o,w,i)}\} = \sqrt{\frac{1}{N_{\mathrm{W}}N_{\mathrm{I}} - 1}\sum_{w=1}^{N_{\mathrm{W}}}\sum_{i=1}^{N_{\mathrm{I}}}\left(N_{(c,o,w,i)} - \overline{N}_{(c,o)}\right)^2} \tag{4.39}$$

We have $N_{\mathrm{W}} = N_{\mathrm{I}} = 4$,

$$IaOSI_{(c,o)} = \sqrt{\frac{1}{15}\sum_{w=1}^{4}\sum_{i=1}^{4}\left(\in_{(c,o,\mathrm{w},i)}\right)^2} \tag{4.40}$$

The equation (4.39) measures the effect of white balance and illumination change. Exploring variation in $N_{(c,o,w,i)}$ will show us the effect of white balance and illumination change on the number of feature dimensions when channel and object are kept constant.

4.3.7.1 Algorithm to compute the effect of illumination and white balance variation

1. Set the color space to, say, RGB, YCbCr and HSV.
2. Choose an object.
3. For a single channel in the color space, apply feature detector to the image rendered by each channel of the same object captured under all the illumination and white balance conditions.

4. Given the color channel, for each object calculate the standard deviation of NNDs under all the four white balance and illumination conditions. Repeat step 3 and 4 for other channels in the color space.
5. Repeat steps 2 – 4 for all the objects.
6. The inter-object stability index $IOSIWI_c$ is computed as average standard deviation of all objects in a certain color channel. This computation is similar to equation (4.18).

$$IOSIWI_c = \frac{\sum_{o=1}^{N_O} IaOSI_{(c,o)}}{N_O} \tag{4.41}$$

   where N_O is the number of objects and $IaOSI_{(c,o)}$ is the intra-object stability index of an object under all four white balance and illumination conditions.There will be 16 images per object.

7. Repeat step 6 for all the channels in the color space.
8. Tabulate the results for further analysis.
9. Repeat steps 1 – 8 for all the color spaces.

This experiment does not compute the variations one object at a time, we expect the inter-object stability index for the number of dimensions to be more unstable than the other two previous experiments. We will explore the channel with the features which are most robust to both illumination and white balance variations from this analysis.

We look at the effect of white balance from a comparatively global perspective by analyzing the inter-object variation. For each channel and object, the normalized total of maximum NNDs is computed as follows:

$$NT_{(c)} \triangleq \frac{\sum N_{(o,w,i)}}{N_W \times N_I \times N_O} \tag{4.42}$$

where $N_{(o,w,i)}$ is the summation of the NNDs for all objects, white balance and illumination conditions. The normalization factors in the denominator represent the number of white balance conditions N_{W}, illumination conditions N_{I} and the number of objects N_{O}.

4.3.7.2 Overall Analysis

In the previous sections, we looked at the effect of illumination and white balance considering one object at a time for the feature dimensions. It was a localized way to look at all the objects. This experiment accounts for the inter-object variation and gives us the most global perspective of illumination and white balance variation considering all the objects at a time. Our objective of this experiment is to explore overall sensitivity of a channel to change in illumination, white balance and facial structure.

The overall inter-object stability index OSI_c of a channel is given by:

$$OSI_c \triangleq STD\{N_{(c,w,o,i)}\} = \frac{\sum\left(N_{(c,w,o,i)} - \bar{N}_{(c)}\right)^2}{N_{\mathrm{O}} N_{\mathrm{W}} N_{\mathrm{I}}} \tag{4.43}$$

where $N_{(c,w,o,i)}$ represents the number of feature dimensions for all objects in the database under all the illumination and white balance conditions for a given channel.

4.4 Finding the Salient Keypoints in Combination of Color Channels

After the analysis of the channels individually, we will analyze the combination of color channels in a color space and also across color spaces. Our objective for this experiment is to explore the keypoints which are not common in a pair of channels. In order to explore the least or non-redundant keypoints between two channels, our approach was to first find the keypoints which are common.

We know that the SIFT output for the each keypoint gives us the (x, y) location coordinates, scale and rotation quadruplets. We will use the (x, y) coordinates in the SIFT quadruplet to find the Euclidian distance and determine the common keypoints between two channels.

4.4.1 Overview of finding the common points

In order to find the common points, we have to compare all the keypoints of one channel to other. We will illustrate the process of finding the common points with an example. Consider two color channels of RGB color space as shown in Figure 4.8. Let us say that we are trying to find the common keypoints between the Red and Blue channel. At first, we make the R channel to be the reference channel and the B channel to be the test channel. We then start from the first keypoint location in the R channel and find the Euclidean distance to all the keypoint locations in the B channel. The keypoint location in the B channel which has the least Euclidean distance will be the one closest to the reference channel keypoint. The process is repeated for all the other keypoints in the R or the reference channel. At the end we will have a set of keypoints in the test channel which are closest to each of the keypoints in the reference channel.

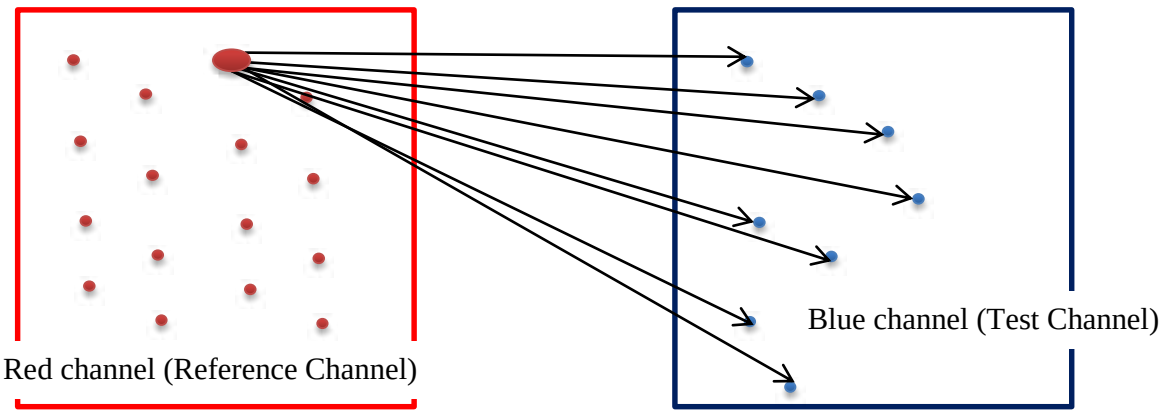

Figure 4.8: Finding the closest match for a keypoint in red channel to all the keypoints in blue channel

4.4.2 Setting Threshold and optimizing for speed and efficiency

Finding Euclidean distance is computationally intensive. Suppose we have 1000 keypoints each in the reference and the test channel, the Euclidean distance must be computed 1000 times for each keypoint in the reference channel.

We propose a better and computationally efficient way obtain the keypoints from the test channel which are in close range to any reference channel keypoint. We do this by setting a square threshold

window of 2 pixels around each reference channel keypoint. The 2 pixel window was chosen to be the ideal window to narrow down a set of prospective keypoints in the test channel close to the reference channel keypoint. We then apply Euclidean distance between a reference channel keypoint and a small set of keypoints in the test channel. This method of reducing the number of computations in the Euclidean distance has drastically improved the speed of execution of the program.

4.4.2.1 Illustration of threshold window

We have seen how threshold window can reduce the number of iterations in computing the Euclidean distance. Let us illustrate the working of threshold window for a pair of channels. Let red or R channel be the reference channel and green or G channel be the test channel. We are trying to find points which are closer to the keypoint R_1 as shown in Figure 4.9.

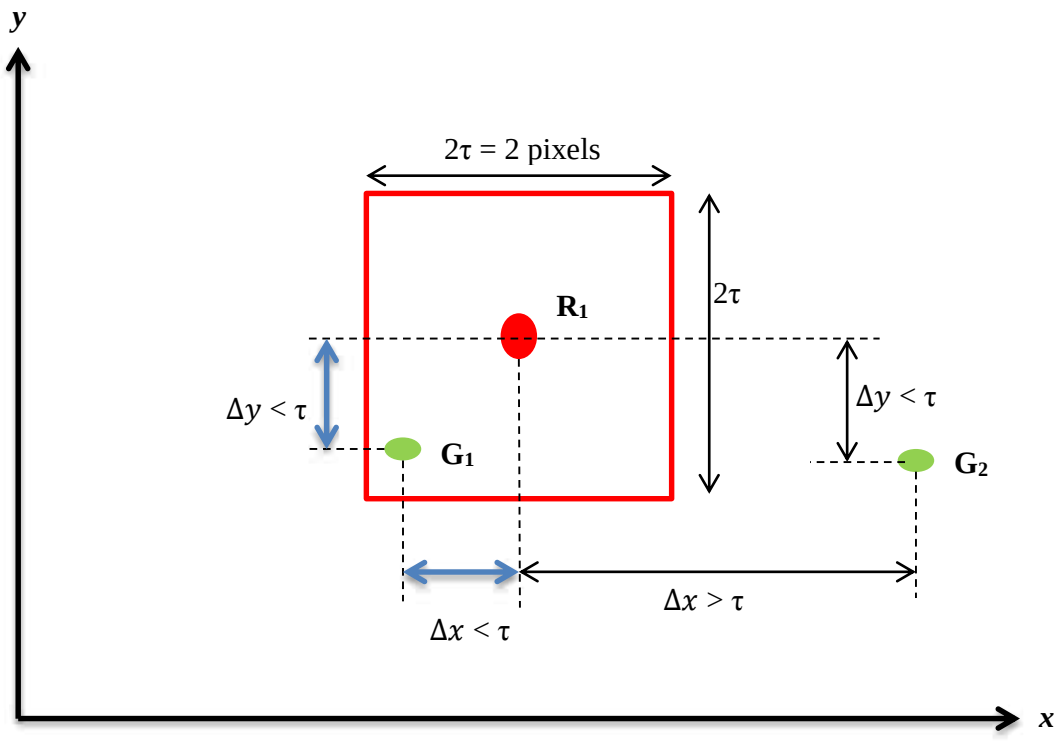

Figure 4.9: Two pixel threshold window

We first establish a 2 pixel threshold around R_1. Let 2τ represent the 2 pixel threshold. We want to check if the keypoints G_1 and G_2 in the G channel are in proximity to R_1. We do this by finding the x and y distances from R_1 to the two test channel keypoints.

In general we can express the distances between the reference channel and test channel keypoints as follows:

$$\Delta x = |x(reference\ channel\ keypoint) - x(test\ channel\ keypoint)| \quad (4.44)$$

$$\Delta y = |y(reference\ channel\ keypoint) - y(test\ channel\ keypoint)| \quad (4.45)$$

If both Δx and Δy are less than or equal to τ, then it can be readily concluded that the test channel keypoint is in the vicinity of the reference channel keypoint. When this rule is applied to the points G_1 and G_2, we can see from Table 4.6 that only G_1 satisfies our condition and becomes the point inside the 2 pixel threshold.

Table 4.6: Examining vicinity of test channel keypoints to the reference channel keypoint

	Δx	Δy	Result
G_1	$\Delta x < \tau$	$\Delta y < \tau$	Inside 2 pixel window
G_2	$\Delta x > \tau$	$\Delta y < \tau$	Outside 2 pixel window

We will apply the threshold to each keypoint in the reference channel. Since, finding the distance is a simple subtraction, the program runs much faster than the method described earlier.

4.4.2.2 Marking the used keypoints in the test channel

We employ marking to further optimize the program to find the matching keypoints. In this method we gradually reduce the number of available test channel keypoints for matching with the reference channel keypoints. Once a test channel keypoint has been identified as being closest to a reference channel keypoint, we mark it and make it unavailable for matching with the remaining reference channel keypoints. When a keypoint in the test channel is marked, the program will skip computing threshold window and Euclidean distance for it. This greatly improves the efficiency of the program and avoids unwanted iterations.

4.4.2.3 Ranking the number of matches

The objective of this experiment is to find the salient keypoints between a pair of channels. We need to compare the number of matches obtained by each channel pair combinations. The raw count values which indicate the number of matches could not be used for comparison as there were no common grounds from one channel combination to another. To overcome this, we devised a ranking method to rank the matching keypoints rendered by the combination of channels.

The criterion for ranking was to assign the rank 1 for combination of channels which yield the lowest number of keypoint matches and rank 3 to the channels with the highest number of keypoints. By using this method for ranking, we give priority to the channel combination which has least number of matches or in other words the non-redundant salient keypoints. The ranking is done for all the channels and the overall ranking percentage can be easily computed for all the objects and also for objects categorized by illumination condition. This method of ranking will help us analyze the objective of finding the salient keypoints in the combination of channels.

4.4.3 Steps in finding the salient keypoints for combination of channels

Most of the steps in finding the salient keypoints are to find the matching keypoints between two channels. Ranking is employed at the end to derive conclusions from the percentages.

1. Set the color space to, say, RGB, YCbCr and HSV. We set two color spaces if salient keypoints between two channels of different color spaces are to be analyzed.
2. Set the white balance of the input image from the database to one of H (2300K), A (2856K), T (4000-5000K) and D (6500K).
3. Obtain the input image from the database with the illumination condition set to one of H (2300K), A (2856K), T (4000-5000K) and D (6500K).

4. Apply the keypoint detector to the image rendered by each channel of the same object captured under the white balance and the illumination condition set.

5. For a combination of two channels, SIFT gives the (x,y) location of the keypoints. The steps to find the matching keypoints are as follows:

    a. Create a threshold window of 2 pixels.

    b. Out of the two channels taken, one is regarded as reference channel and the second as the test channel.

    c. We then compare the keypoints in the reference channel with the ones in the test channel. The process of comparison is summarized below:

        i. First, we try to narrow down the prospective matching points using the threshold window (See Figure 4.9).

$$\Delta x = |x(reference\ channel\ keypoint) - x(test\ channel\ keypoint)|$$

$$\Delta y = |y(reference\ channel\ keypoint) - y(test\ channel\ keypoint)|$$

        If both Δx and Δy are less than or equal to τ, then it can be readily concluded that the test channel keypoint being considered is in the vicinity of the reference channel keypoint. We increment the counter which keeps track of the matching points.

        ii. Step (i) is repeated for all the keypoints in test channel keeping the reference channel keypoint constant. The location of all the keypoints in vicinity of the reference channel keypoint marked by the threshold window is stored in a matrix called the matching matrix.

iii. Out of all the test channel keypoints in the matching matrix, the closest one to the reference channel keypoint should be found and marked. The closest keypoint is found by computing the Euclidian distance between each of points in the matching matrix with the reference channel keypoint. The test channel keypoint with the least Euclidian distance is considered to be the closest with the reference channel keypoint. This keypoint in the test channel is marked and made unavailable to the other keypoints in the reference channel.

d. Steps (b) and (c) are repeated for all the keypoints in the reference channel.

6. Step 4 is repeated for all channel combinations as required.

7. Steps 1 – 5 is repeated for all the objects.

8. Rank each channel combination based on the degree of matching. Channel combination which has the least matching count receives a ‘rank 1’ and the channel combination with the most matching points receives a ‘rank 3’.
9. Results are tabulated and analyzed.

In this experiment we find the salient keypoints using the concept of matching keypoints between two channels. By assigning higher rank to the channel combination which has the least match, we find the measure of saliency between two channels. From this analysis we can find if two channels have keypoints which are completely different from each other. In conclusion, we will be able to find the channel combination in a color space which yields the most salient keypoints.

Chapter 5 : Data Preparation

5.1 Requirements of the database

The primary requirement for our dataset was to have color face images with frontal pose in different illumination conditions. We further looked for consistency in the frontal pose across all the illumination conditions. We also expected the face images to have uncluttered plain background.

5.2 Face databases explored

Several available face databases were surveyed based on the described requirements. The following list enumerates some of the face databases which were explored during the process of selecting the right dataset for our experiment:

1. AR Face Database
2. CMU Face Detection Database
3. CMU Face Expression Database
4. CMU Face Pose, Illumination, and Expression (PIE) Database
5. FERET Color Database
6. Georgia Tech Face Database
7. MIT-CBCL Face Recognition Database
8. MIT-CBCL Face Databases
9. ORL Database of Faces
10. The University of Oulu Physics-Based Face Database
11. UMIST Face Database
12. UCD Color Face Image (UCFI) Database for Face Detection
13. Yale Face Database
14. Yale Face Database B

15. Indian Face Database
16. CVL Face Database
17. GTAV Face Database

We decided to use The University of Oulu Physics-Based Face Database as it met all our requirements.

5.3 The University of Oulu Physics-Based Face Database (OPFD)

This database contains 125 different faces each in 16 different camera calibration and illumination condition, an additional 16 if the person has glasses. The camera used to capture the images was a 3 charge coupled device (CCD) Sony DXC-755P [14]. Four types of illumination conditions used were provided by a commercially available Macbeth SpectraLight II Luminaire source [14]:

1. Horizon sunlight (incandescent, 2300 K; marked ‘H’).
2. Incandescent A (CIE A, 2856 K; marked ‘A’),
3. Fluorescent TL84 (4000 K; marked ‘T’), and
4. A daylight source (CIE D65, 6500 K; marked ‘D’).

The illuminants used in the dataset are comparable to the illumination conditions in the real world [14]. The conditions in which this dataset was created was a dark room with a large diffusing 80% gray screen behind the sitting subject and a white plate was used for setting the white balance of the camera [14]. The setup for acquiring the dataset is shown in Figure 5.1. The imaged person was seated such that his or her nose coincides with the main axis of the camera. During image acquisition, the person was asked to keep his or her face in the same position, with the same facial expression, and to keep eyes opened [14]. Our method in all experiments reiterates the conditions in which the dataset was created. Hence, it is important for us to understand the steps in constructing this dataset. Before we state the steps involved in creating the database, it is necessary to recall importance of white balance settings in a camera. Setting white balance of a camera removes pseudo color casts in the captured image such that the objects which appear perceptually white are rendered white in the image [6].

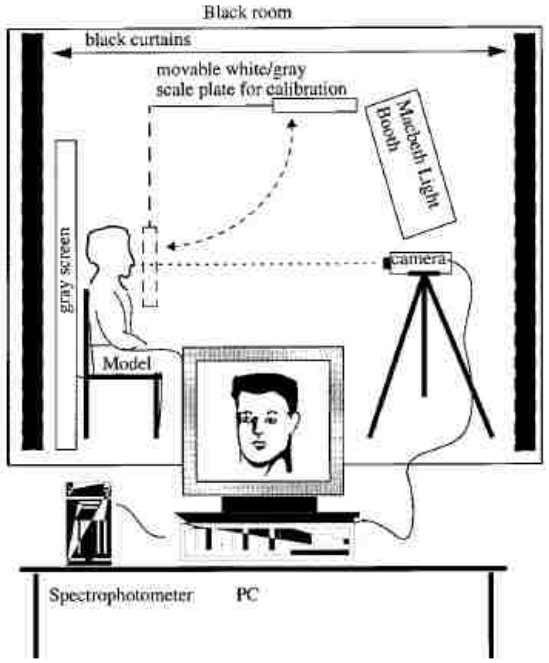

Figure 5.1: OPFD dataset creation setup [14]

The images in the OPFD were obtained in the following manner [14]:

1. Illuminant H is switched on.
2. The camera is white balanced for this illuminant.
3. The person's image is captured.
4. With the camera still white balanced for H, illuminants A, T, and D are switched on and the face is captured for each illuminant. Only one illuminant is switched on each time the image is taken.
5. Steps 1–4 are repeated using A, T, and D as reference illuminants for calibration thus for each person 16 images were captured.

The illumination source as described earlier is a light booth called the Macbeth SpectraLight II Luminaire.

The light booth is generally used to capture images of objects under different illumination. Figure 5.2 shows an image of the light booth used in the OPFD experiment. All the images in the database were recorded in the BMP format.

Figure 5.2: Macbeth SpectraLight II photo booth

5.4 Preprocessing of images

The images of the OPFD face database have headshots of objects under different illumination conditions. Our experiments deal with variation in the number of keypoints and features. We had to impose some restrictions and select images which are consistent in appearance. We do this to avoid any pseudo values of variation. If we are comparing the images of the same person in two different illumination conditions, the analysis on the number of keypoints should account for just the illumination variation. If we are trying to compare two images of the same person, one with normal pose in one illumination and another with eyes closed and head rotated in another illumination, the result of analyzing the variation in illumination is very likely to include the effect of head rotation and eye closure. This is not desirable. Hence we have gone through images of 125 people and chosen the ones which are consistent in the following aspects:

1. Head position
2. Retina position
3. No intensive occlusion of the face region by facial beard or hairs

4. Steady pose for the object in all illumination conditions
5. Eye is open in all the images for an object

Figure 5.3 shows 16 images of a person captured under different white balance and illumination conditions. If there was inconsistency in any one image out of the 16 images per object (person), the whole object was rejected. We use the images of 35 objects in all our experiments. There are 16 images per person and we use 140 images per white balance. A total of 560 images are used in total.

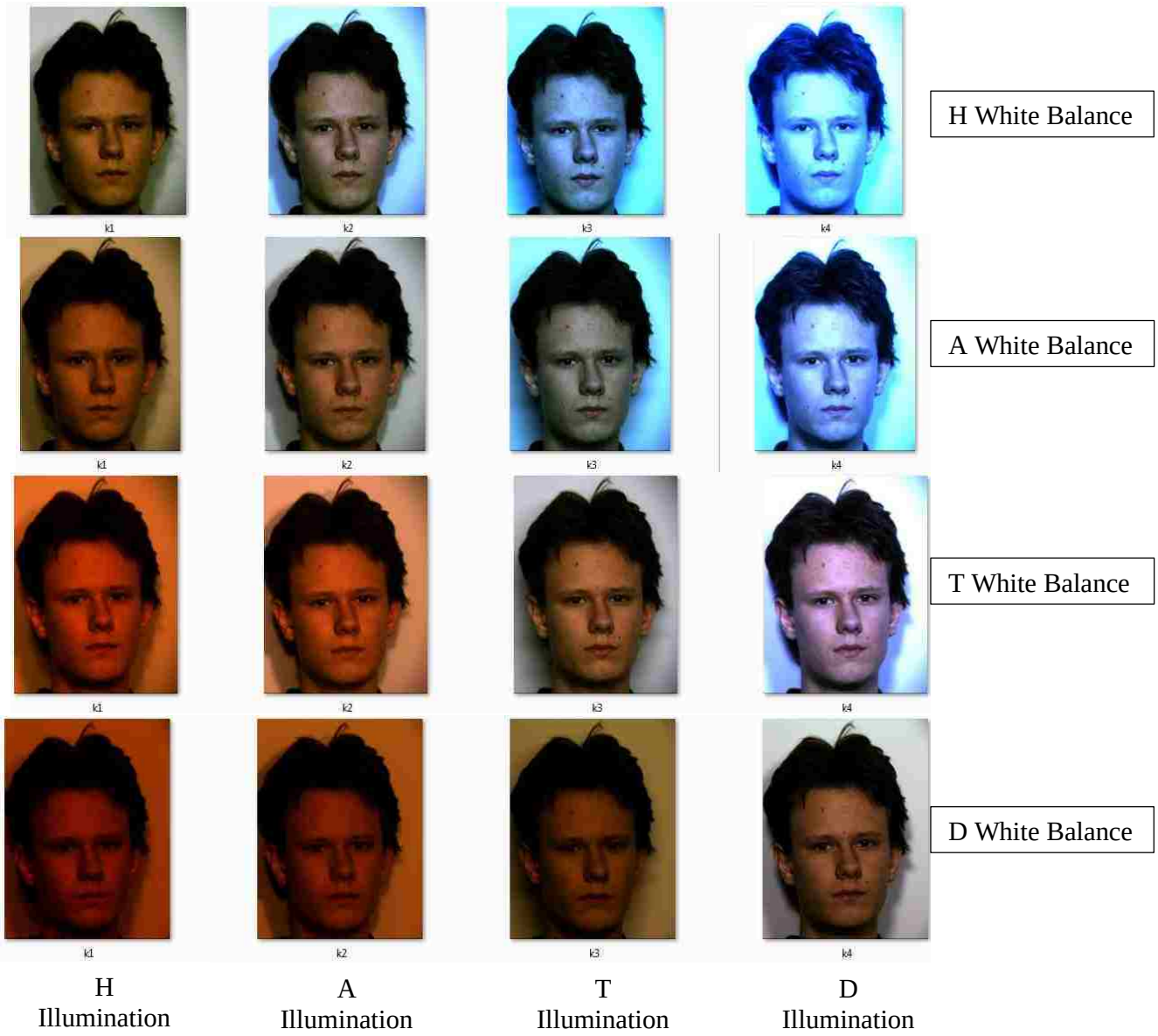

Figure 5.3: Images of a person from the OPFD face database. Used with permission from The University of Oulu, Center for Machine Vision Research, Finland.[14]

Once the suitable images were selected, the gray background and other non-essential aspects of the face were cropped using a Viola-Jones face detector.

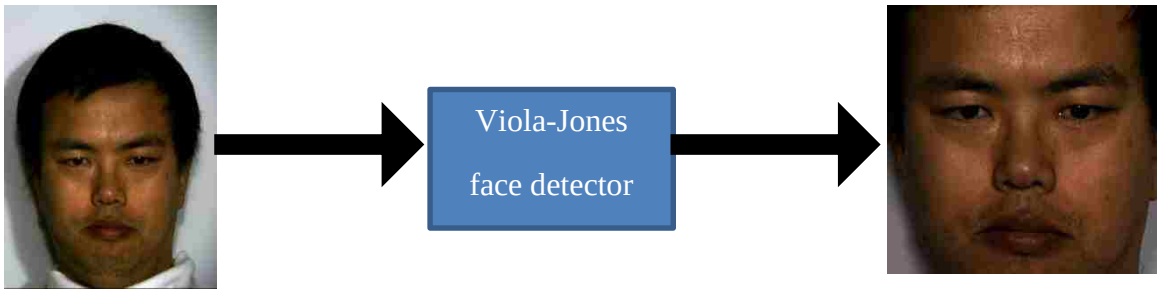

Figure 5.4: Removing the gray background and other non-essential aspects using Viola-Jones face detector

All the 560 images were renamed. The first part of the name is composed of one or two alphabets unique to each object. The second part of the name is a number which indicates the illumination condition; (1) H, (2) A, (3) T and (4) D. The illumination conditions were arranged in increasing order of temperature. The renaming was done to facilitate easier access of images from Matlab and for additional data log preparation for the number of keypoints and features.

Chapter 6 : Results and Discussion

6.1 Results for Keypoints Based Robustness Analysis

6.1.1 Effect of Illumination

6.1.1.1 RGB Color Space

The results for inter-object stability index for fixed white balance and the overall stability index across white balance conditions in the RGB color space are shown in Table 6.1. Table 6.2 shows the normalized total number of keypoints categorized by white balance conditions.

Table 6.1: Inter-object stability index and the overall stability index (OSII) for RGB color space

WB	R	G	B
H	90.5	164.7	303.7
A	88.5	137.5	275.1
T	70.2	183.3	419.5
D	69.7	197.4	456.3
OSII	11.3	25.9	87.8

Table 6.2: Normalized total number of keypoints by white balance for RGB color space

Normalized Total (WB)	H	A	T	D
R	880	882	838	723
G	988	1075	1094	834
B	541	669	720	373

Figure 6.1(a) shows the results for inter-object stability index which is the average variation in the number of keypoints under illumination change for all objects under a particular white balance condition categorized by channels of the RGB color space. Each point for a color channel gives the average of variations taken from all the objects under the fixed white balance and color channel. For each white balance condition, the value of average standard deviation shows the stability of keypoints for images belonging to that white balance condition. From Figure 6.1(a), for R channel, we can say that the images from the T and D white balance conditions have the least average standard deviation. Hence, the keypoints rendered by these images are less sensitive to illumination compared to the

images from H and A white balance conditions. Similarly, we can say that the images in the A white balance condition are less sensitive to illumination change in both G and B channels. To comment on the overall stability of the each channel, we look at the standard deviation across white balance conditions as shown in Figure 6.1(b). The R channel has the least variation and is the most stable across white balance conditions. The normalized total number of keypoints is shown in Figure 6.1(c). The inter-object variation gives a global perspective for multiple objects grouped by white balance condition. Higher normalized total number of keypoints show that the images of a channel and a white balance condition have higher overall efficiency in rendering the keypoints. From the Figure 6.1(c) we can say that the G channel has the highest normalized number of keypoints in all the white balance conditions. Hence, when we consider the inter-object variation, G channel is best suited for varying illumination and fixed white balance and channel.

6.1.1.2 YCbCr Color Space

The results for average standard deviation for fixed white balance and the standard deviation across white balance conditions in the YCbCr color space are shown in Table 6.3. Table 6.4 shows the normalized total number of keypoints categorized by white balance conditions.

Table 6.3: Inter-object stability index (IOSI) and the overall stability index (OSII) for YCbCr color space

WB	Y	Cb	Cr
H	100.2	262.5	292.1
A	149.3	319.5	281.2
T	172.4	195.6	126.7
D	165.7	84.0	68.3
OSII	32.6	101.2	111.9

Figure 6.2(a) shows the average variation in the number of keypoints under illumination change for all objects under a particular white balance condition categorized by channels of the YCbCr color space. We recall that the least value standard deviation is best suited given a channel and white balance condition.

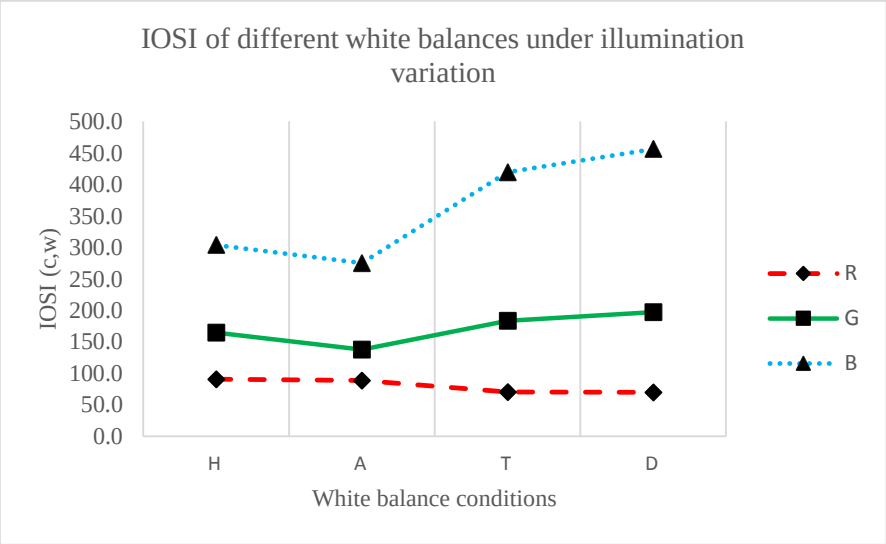

(a)

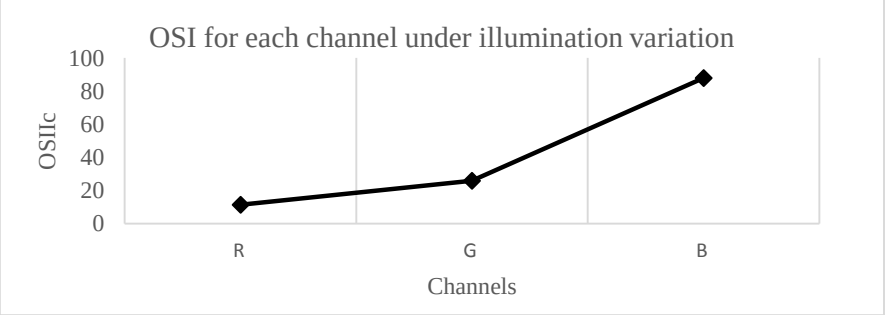

(b)

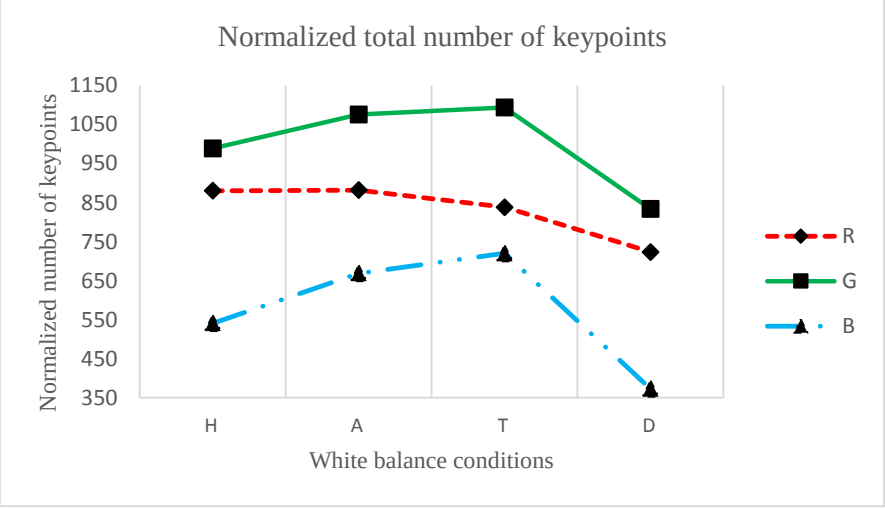

(c)

Figure 6.1: Sensitivity of individual color channels to illumination variation when white balance is constant (a) Inter-object stability index (IOSI) (b) Overall stability index (OSII) (c) The normalized total number of keypoints in RGB channel

Table 6.4: Normalized total number of keypoints by white balance for YCbCr color space

Normalized Total (WB)	H	A	T	D
Y	1077	1106	1077	854
Cb	810	789	777	703
Cr	757	677	579	484

Considering images from particular white balance conditions in Figure 6.2(a), we can observe the following:

1. The images from H white balance condition are most stable in Y channel
2. The images from D white balance condition are most stable in Cb channel
3. The images from D white balance condition are most stable in Cr channel

The normalized total number of keypoints is shown in Figure 6.2(c). The analysis of normalized total number keypoints is similar as in 6.1.1.1. From Figure 6.2(c) we see that the Y channel yields the highest normalized number of keypoints and is best suited from the perspective of inter-object variation.

6.1.1.3 HSV Color Space

The results for average standard deviation for fixed white balance and the standard deviation across white balance conditions in the HSV color space are shown in Table 6.5. Table 6.6 shows the normalized total number of keypoints categorized by white balance conditions.

Figure 6.3(a) shows the average variation in the number of keypoints under illumination change for all objects under a particular white balance condition categorized by channels of the HSV color space. When individual white balance conditions are considered, the images from white balance D, H and D are least sensitive to channels H, S and V respectively. Across white balances, we can observe from Figure 6.3(b) that the S channel is least sensitive to illumination variation. The normalized total number of keypoints is shown in Figure 6.3(c).

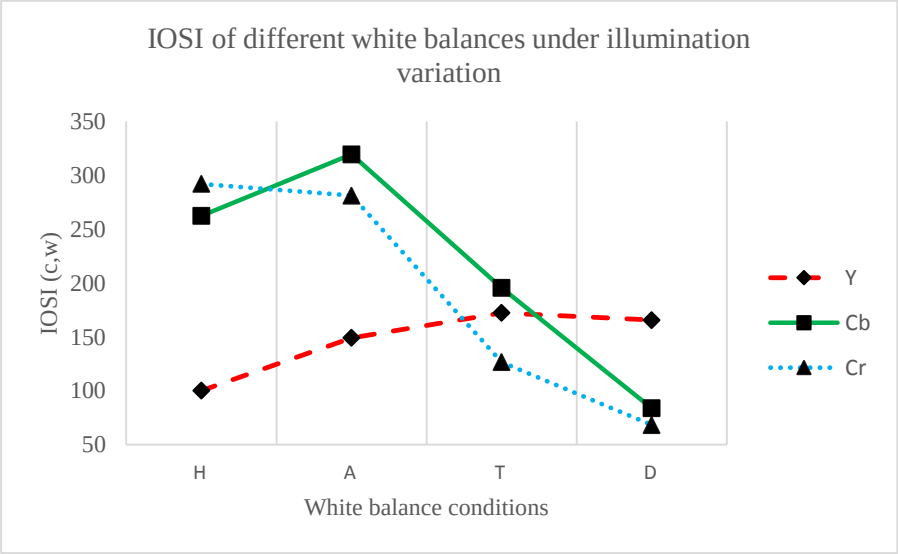

(a)

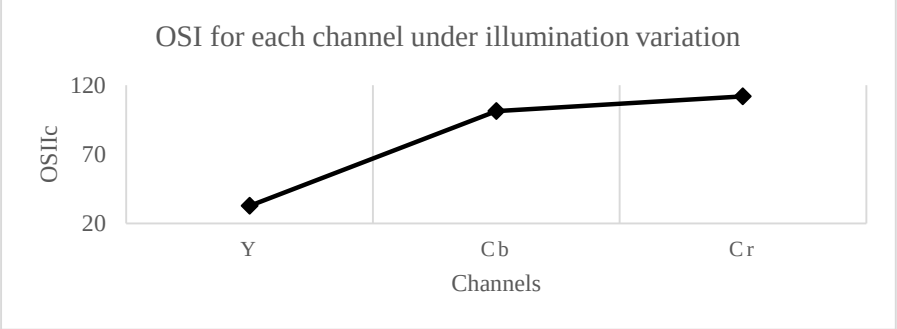

(b)

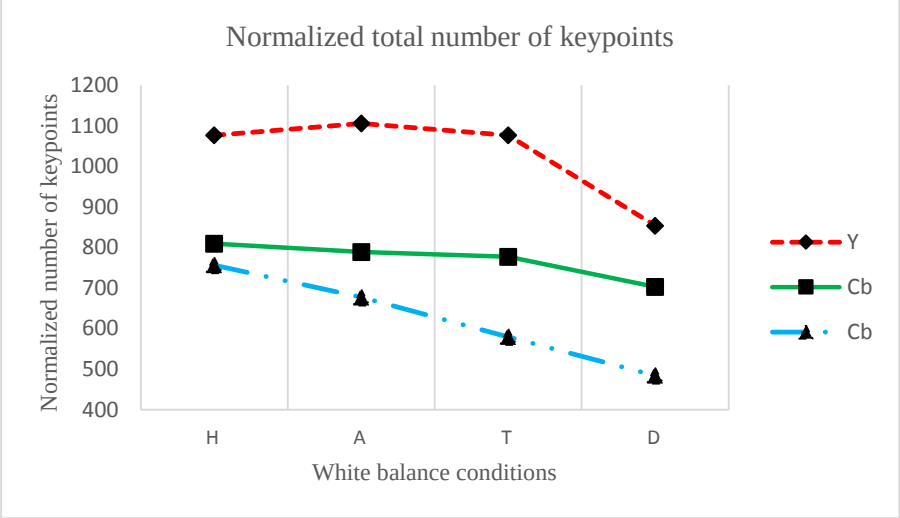

(c)

Figure 6.2: Sensitivity of individual color channels to illumination variation when white balance is constant (a) Inter-object stability index (IOSI) (b) Overall stability index (OSII) (c) The normalized total number of keypoints in YCbCr channel

Table 6.5: Inter-object stability index (IOSI) and the overall stability index (OSII) for HSV color space

WB	H	S	V
H	326.3	134.8	228.0
A	299.0	237.9	144.5
T	142.5	277.3	211.2
D	25.1	302.5	54.7
OSII	141.0	73.8	78.7

Table 6.6: Normalized total number of keypoints by white balance for HSV color space

Normalized Total (WB)	H	A	T	D
H	251	201	83	26
S	500	447	311	197
V	350	343	363	199

The analysis of normalized total number keypoints is similar as in 6.1.1.1. The S channel has the maximum normalized total number of keypoints for images in H and A white balance conditions. The V channel performs best for images in T and D white balance conditions.

6.1.2 Effect of White Balance

6.1.2.1 RGB Color Space

Table 6.7 shows the results of average standard deviation for fixed illumination and varying white balance conditions. It also shows the standard deviation across white balance conditions in the RGB color space. Table 6.8 shows the normalized total number of keypoints categorized by illumination conditions.

Table 6.7: Inter-object stability index (IOSI) and the overall stability index (OSIW) for RGB color space

Illumination	R	G	B
H	76.4	144.5	255.3
A	85.1	161.2	364.1
T	86.0	153.4	269.7
D	102.9	210.2	471.5
OSIW	11.1	29.4	100.0

Figure 6.4(a) shows the average variation in the number of keypoints under white balance change for

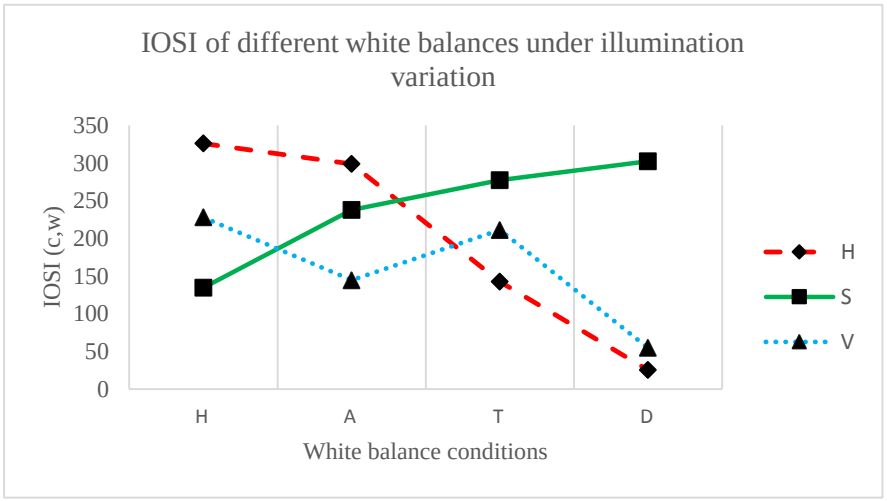

(a)

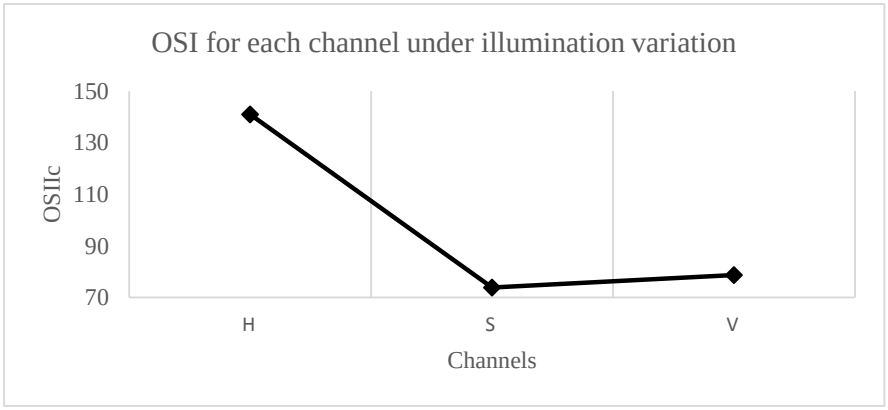

(b)

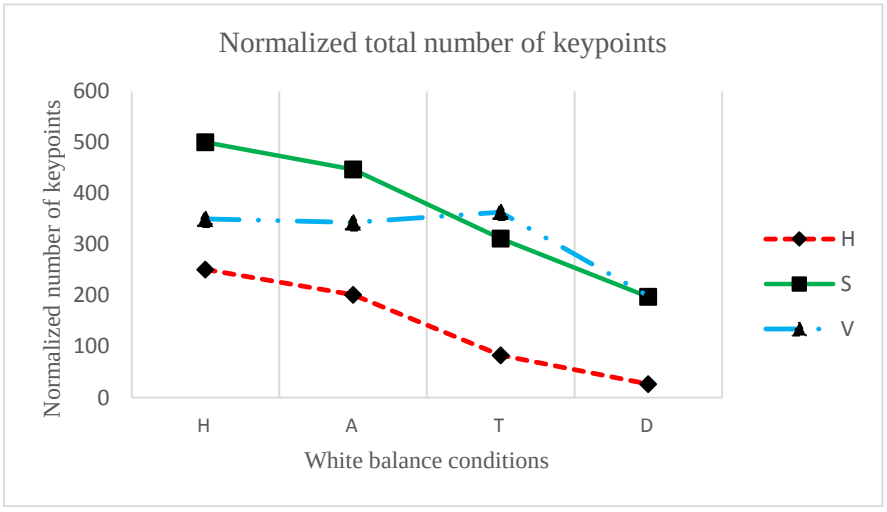

(c)

Figure 6.3: Sensitivity of individual color channels to illumination variation when white balance is constant (a) Inter-object stability index (IOSI) (b) Overall stability index (OSII) (c) The normalized number of keypoints in HSV channel

Table 6.8: Normalized total number of keypoints categorized by illumination condition for RGB color space

Normalized Total (ILL)	H	A	T	D
R	758	839	806	921
G	824	1000	1088	1079
B	300	585	757	661

all objects under a particular illumination condition categorized by channels in the RGB color space. Here the average standard deviation can show the stability of the keypoints rendered by the images to white balance variation. From Figure 6.4(a), we can observe that the images in the H illumination condition have the least average standard deviation for all the channels in the RGB color space. From this, we can conclude that the keypoints from images of the H illumination condition are least sensitive to white balance change for all the channels. Figure 6.4(b) shows us the comparison of different channels' sensitivity to change in white balance across the illumination conditions. We can see that the R channel is the least sensitive to white balance change across illumination conditions. The normalized total number of keypoints is shown in Figure 6.4(c). The analysis of normalized total number keypoints is similar as in 6.1.1.1. The normalized total number of keypoints are categorized for a given illumination and varying white balance conditions. The G channel has the highest number of keypoints from Figure 6.4(c) for the images in all the illumination conditions.

6.1.2.2 YCbCr Color Space

Table 6.9 shows the results of average standard deviation for fixed illumination and varying white balance conditions. It also shows the standard deviation across white balance conditions in the YCbCr color space. Table 6.10 shows the normalized total number of keypoints categorized by illumination conditions.

Figure 6.5(a) shows the average variation in the number of keypoints under white balance change for all objects under a particular illumination condition categorized by channels in the YCbCr color space. Figure 6.5(b) shows us the comparison of different channels' sensitivity to change in white balance across the illumination conditions.

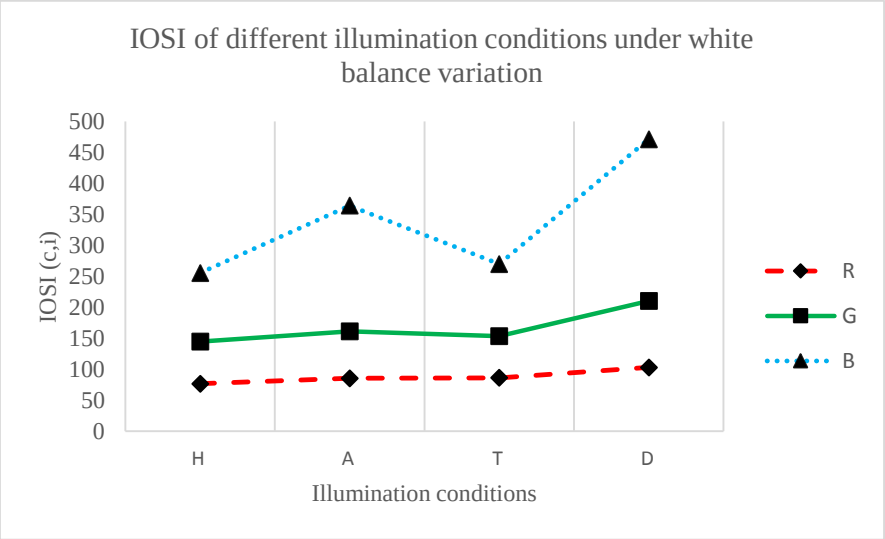

(a)

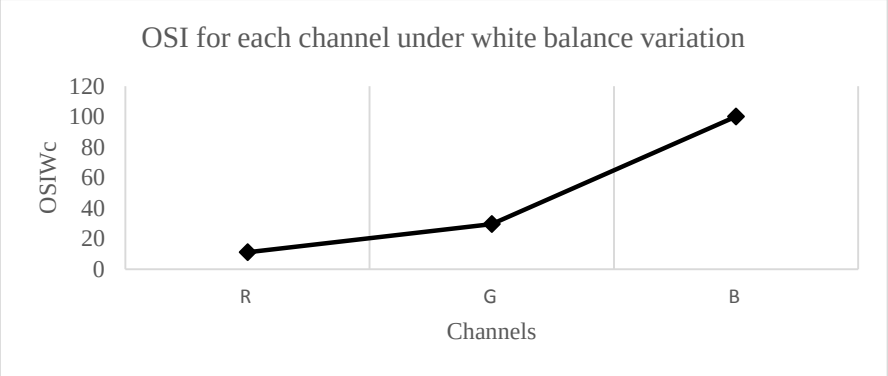

(b)

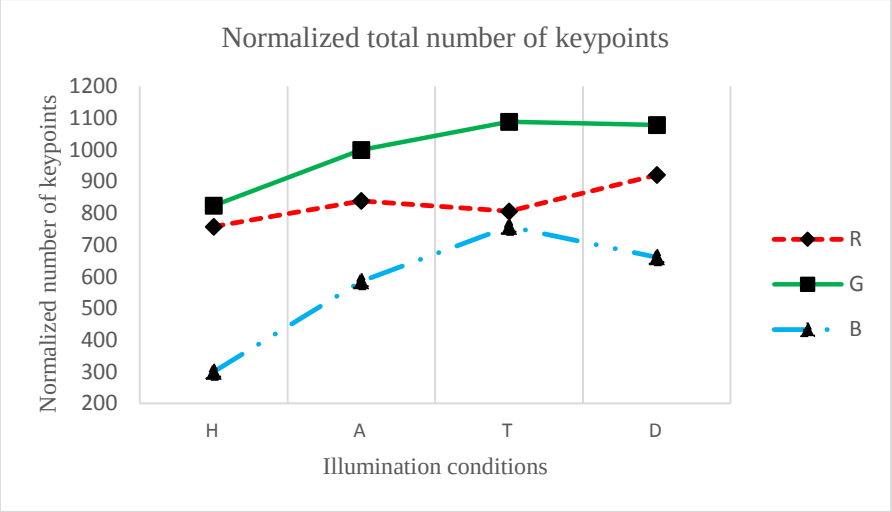

(c)

Figure 6.4: Sensitivity of individual color channels to white balance variation when illumination is constant (a) Inter-object stability index (IOSI) (b) Overall stability index (OSIW) (c) The normalized total number of keypoints in RGB channel

Table 6.9: Inter-object stability index (IOSI) and the overall stability index (OSIW) for HSV color space

Illumination	Y	Cb	Cr
H	126.5	104.8	76.5
A	148.8	109.0	87.5
T	158.5	139.7	248.4
D	118.0	281.7	290.1
OSIW	18.8	83.4	109.5

Table 6.10: Normalized total number of keypoints by white balance for YCbCr color space

Normalized Total (ILL)	H	A	T	D
Y	853	1016	1082	1163
Cb	674	657	741	1006
Cr	479	537	683	798

We can observe that the Y channel is the least sensitive to white balance change across illumination conditions. The normalized total number of keypoints is shown in Figure 6.5(c). By looking at the inter-object variation, the Y channel yields the highest normalized total number of keypoints for images in all the illumination conditions.

6.1.2.3 HSV Color Space

Table 6.11 shows the results of average standard deviation for fixed illumination and varying white balance conditions. It also shows the standard deviation across white balance conditions in the HSV color space. Table 6.12 shows the normalized total number of keypoints categorized by illumination conditions.

Table 6.11: Inter-object stability index (IOSI) and the overall stability index (OSIW) for HSV color space

Illuminations	H	S	V
H	27.6914	212.827	46.2087
A	359.4958	323.4001	82.6075
T	298.2344	254.94	228.4345
D	113.2428	114.4894	242.7104
OSIW	155.2477	87.4295	100.1026

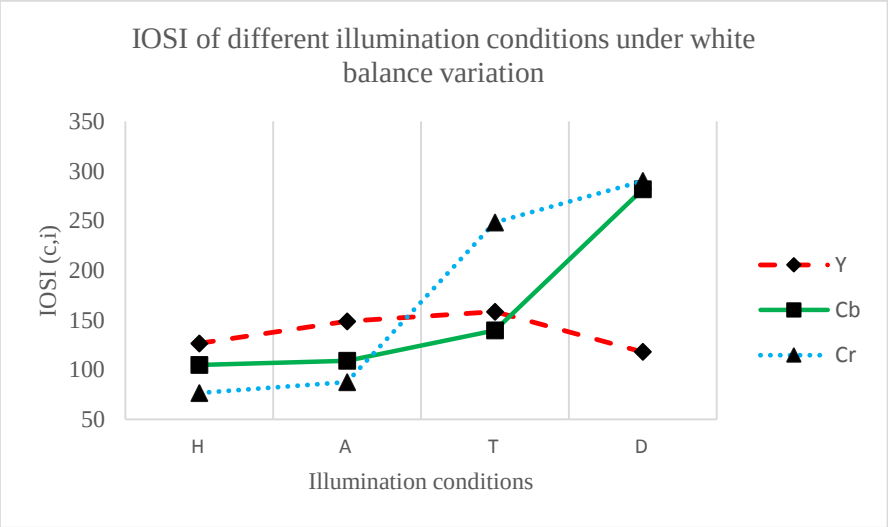

(a)

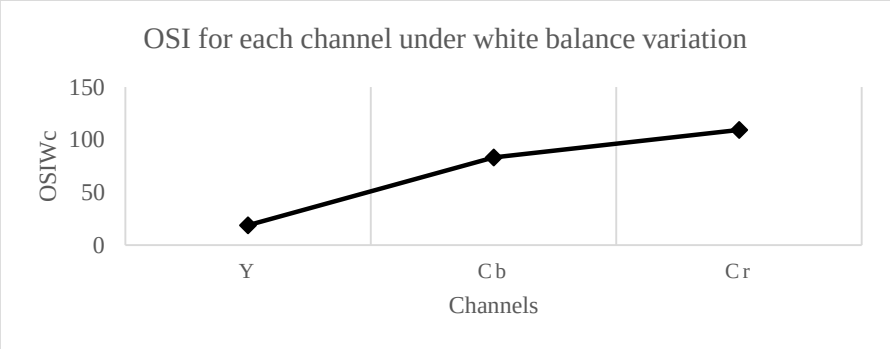

(b)

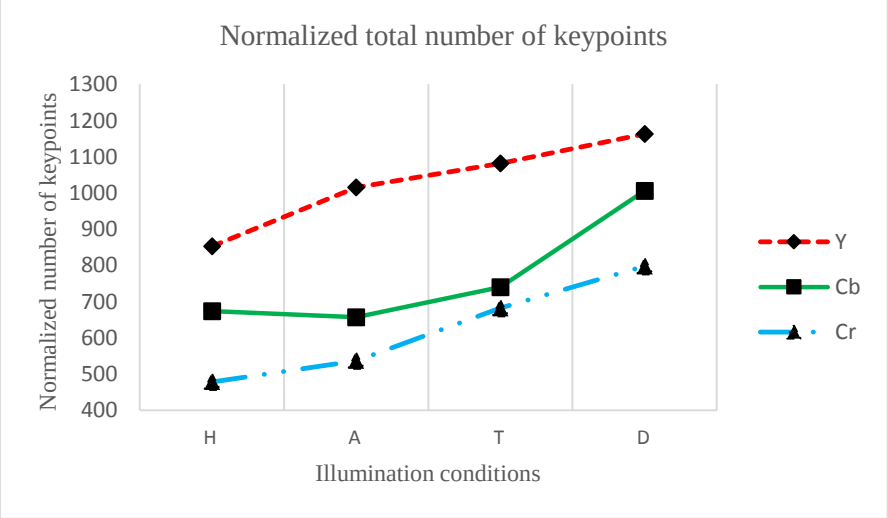

(c)

Figure 6.5: Sensitivity of individual color channels to white balance variation when illumination is constant (a) Inter-object stability index (IOSI) (b) Overall stability index (OSIW) (c) The normalized total number of keypoints in YCbCr channel

Table 6.12: Normalized total number of keypoints by white balance for HSV color space

Normalized Total (ILL)	H	A	T	D
H	25	197	205	134
S	160	365	425	505
V	218	286	384	367

Figure 6.6(a) shows the average variation in the number of keypoints under white balance change for all objects under a particular illumination condition categorized by channels in the HSV color space. Figure 6.6(b) shows us the comparison of different channels' sensitivity to change in white balance across the illumination conditions. We can observe that the S channel is the least sensitive to white balance change across illumination conditions. The normalized total number of keypoints is shown in Figure 6.6(c). The analysis of normalized total number keypoints is similar as in 6.1.1.1. It can be seen from Figure 6.6(c) that the V channel has the maximum total number of keypoints for the images in the H illumination condition and the S channel has most total number of keypoints for images in A T D illuminations.

6.1.3 Effect of White Balance and Illumination change

6.1.3.1 RGB Color Space

The effect of white balance and illumination change are analyzed in the RGB color space. The average standard deviation in this case is the mean variation in the number of keypoints considering all the illumination and white balance conditions together for each object, in a channel of the color space. From Figure 6.7(a), we can say that the channel R is least sensitive to white balance and illumination variation in overall. The most global analysis is given by the overall standard deviation in Figure 6.7(b). When the variation in number of keypoints is considered for all illuminations and white balances, we see that the overall inter-object stability of R channel is the best compared to other channels. Figure 6.7(c) shows the global perspective with the normalized total number of keypoints. It can be seen that the G channel yields the maximum normalized total number of keypoints.

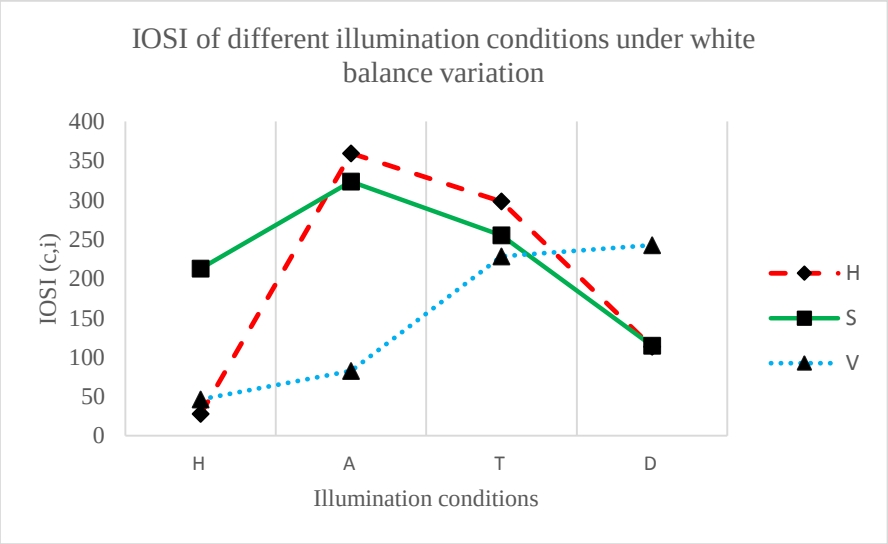

(a)

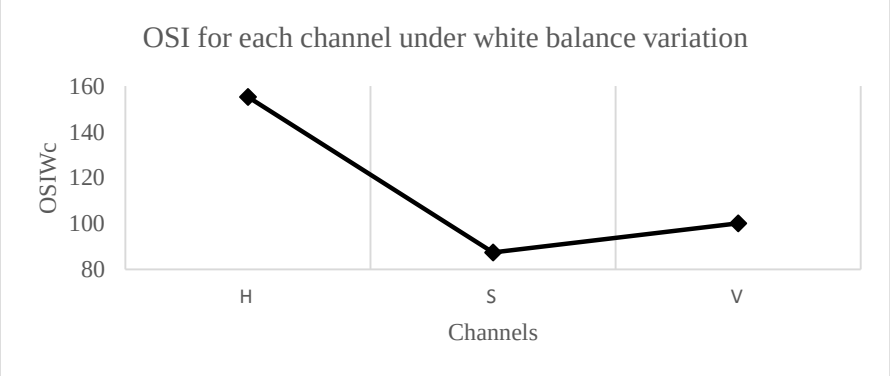

(b)

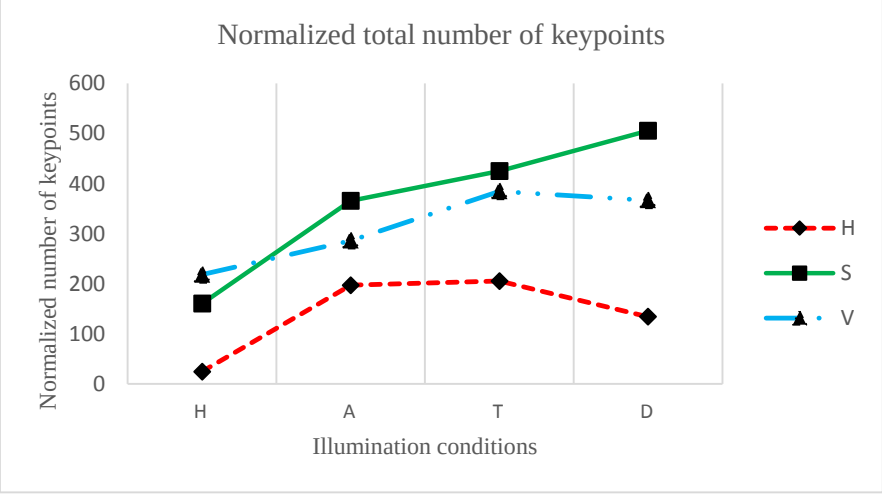

(c)

Figure 6.6: Sensitivity of individual color channels to white balance variation when illumination is constant (a) Inter-object stability index (IOSI) (b) Overall stability index (OSIW) (c) The normalized total number of keypoints in HSV channel

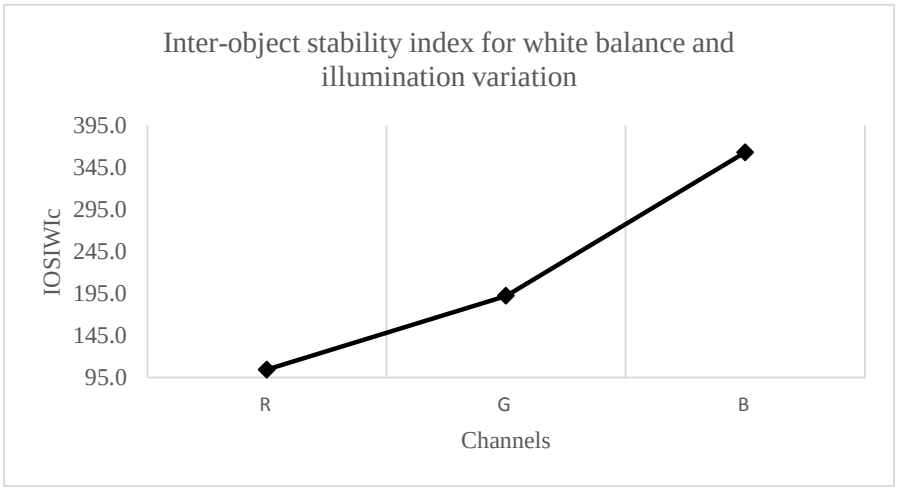

(a)

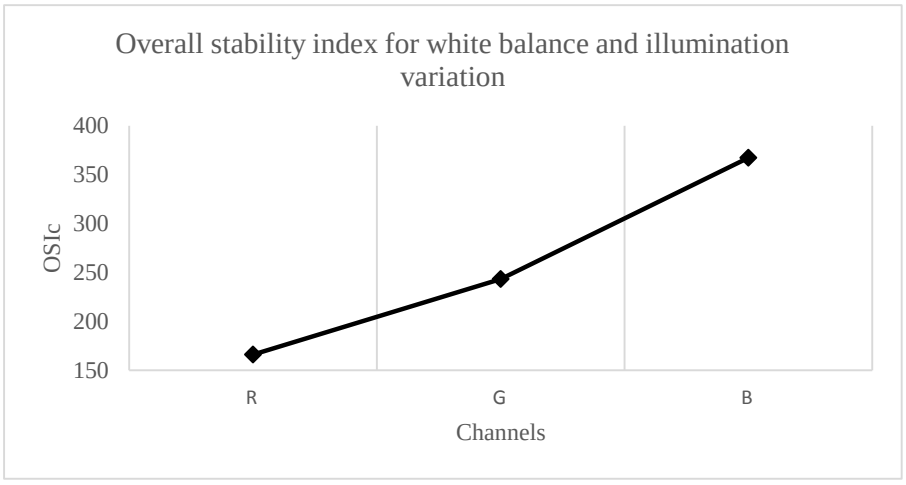

(b)

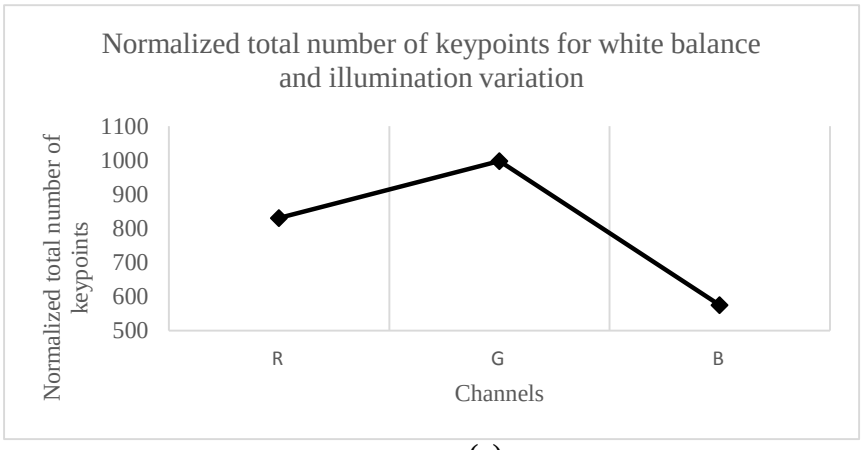

(c)

Figure 6.7: Sensitivity of color channels to change in white balance and illumination variation (a) Inter-object stability index (IOSI) (b) The overall stability index (OSI) and (c) The normalized total number of keypoints in RGB channel

6.1.3.2 YCbCr Channel

By examining the overall effect of white balance and illumination change, we can say that Y channel is least sensitive from Figure 6.8(a). The most global analysis is given by the overall standard deviation in Figure 6.8(b). The Cr channel has the most stability when overall inter-object stability is considered. Figure 6.8(c) shows the global perspective with the normalized total number of keypoints. It can be seen that the Y channel yields the most normalized total number of keypoints.

6.1.3.3 HSV Channel

By examining the overall effect of white balance and illumination change, we can say that V channel is least sensitive from Figure 6.9(a). The V channel is also least sensitive when the overall inter-object stability is considered in Figure 6.9(b). Figure 6.9(c) shows the global perspective with the normalized total number of keypoints. It can be seen that the S channel yields the most normalized total number of keypoints

6.2 Results for Feature Based Robustness Analysis

6.2.1 Effect of Illumination

6.2.1.1 RGB Color Space

The results for average standard deviation in the maximum NNDs for fixed white balance and the standard deviation across white balance conditions in the RGB color space are shown in Table 6.13. Table 6.14 shows the normalized total NNDs categorized by white balance conditions.

Figure 6.10(a) shows the average variation in the maximum NNDs under illumination change for all objects under a particular white balance condition categorized by channels of the RGB color space. Each point for a color channel gives the average of variations in the maximum normalized number of dimensions taken from all objects under the fixed white balance and color channel.

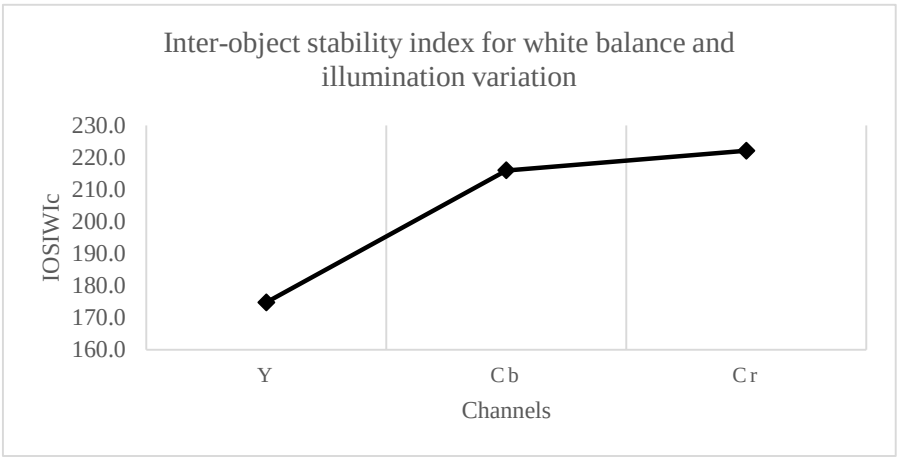

(a)

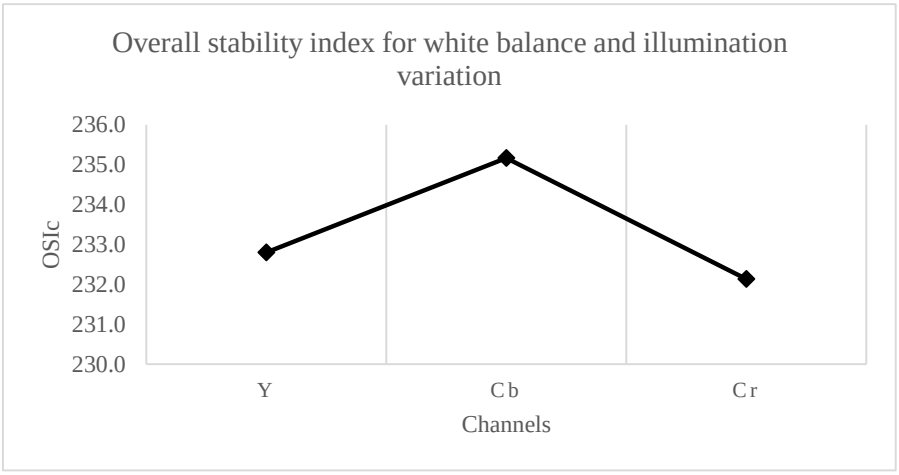

(b)

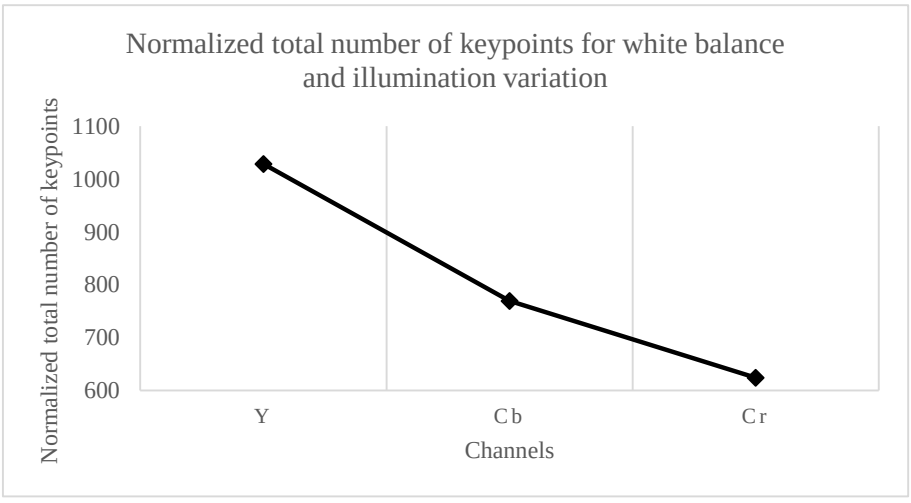

(c)

Figure 6.8: Sensitivity of color channels to change in white balance and illumination variation (a) Inter-object stability index (IOSI) (b) The overall stability index (OSI) and (c) The normalized total number of keypoints in YCbCr channel

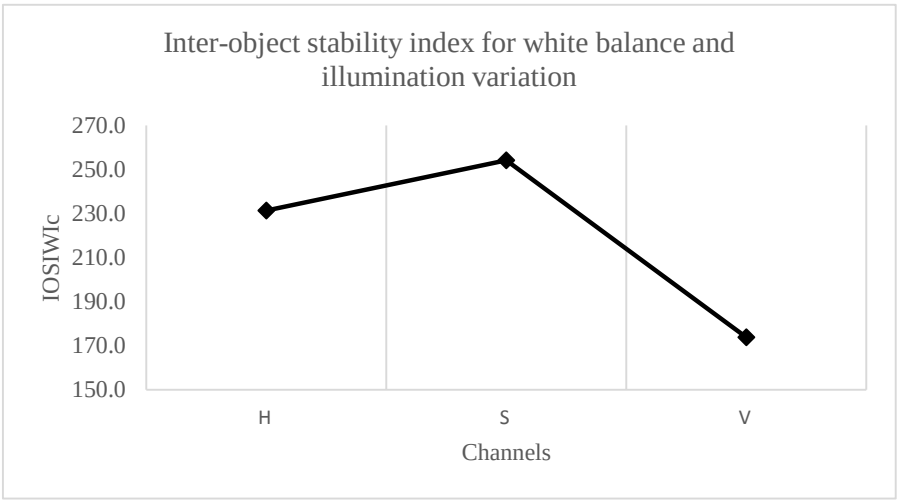

(a)

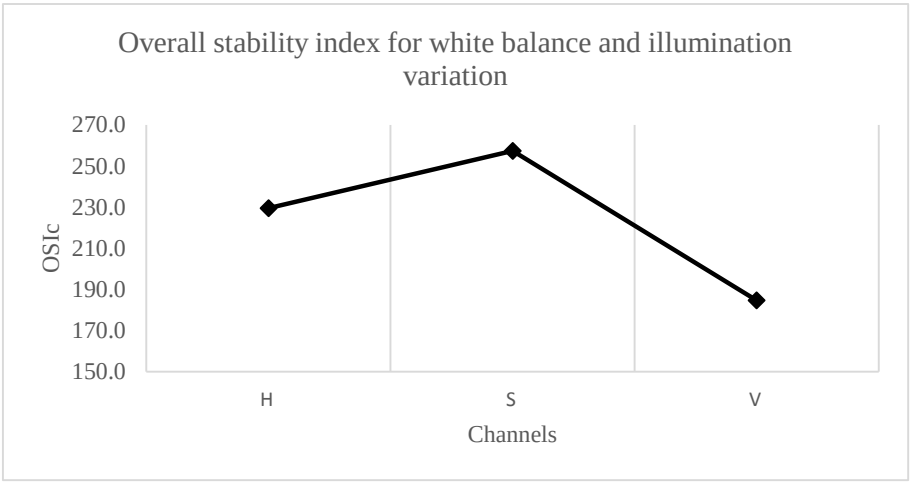

(b)

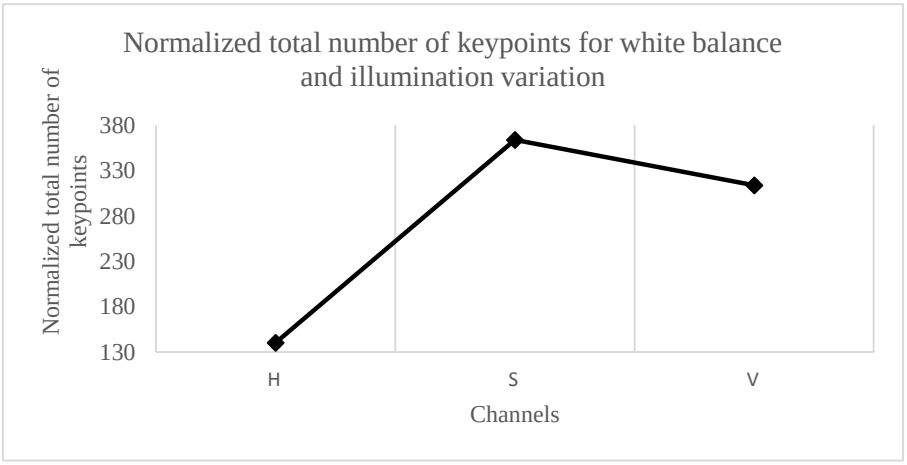

(c)

Figure 6.9: Sensitivity of color channels to change in white balance and illumination variation (a) Inter-object stability index (IOSI) (b) The overall stability index (OSI) and (c) The normalized total number of keypoints in HSV channel

Table 6.13: Inter-object stability index (IOSI) the overall stability index (OSII) for RGB color space

WB	R	G	B
H	1.5251	2.4351	33.9898
A	1.4944	1.7146	10.6337
T	1.42	2.2064	34.0034
D	1.7036	3.8842	39.9888
OSII	0.1203	0.9325	12.9909

Table 6.14: Normalized total NNDs by white balance for RGB color space

Normalized Total (WB)	H	A	T	D
R	15	15	16	18
G	14	12	12	16
B	37	23	32	34

Figure 6.10(b) gives us the comparison of different channel's sensitivity to change in illumination across the white balance conditions. The average standard deviation indicated the stability of feature dimensions rendered by the feature points of the channel. For each channel and white balance condition, the value of average standard deviation shows the sensitivity of the number of dimensions to change in illumination condition. The normalized total NNDs is shown in Figure 6.10(c). We can see that the blue channel has the most normalized total NNDs and is efficient when a global inter-object perspective is considered.

6.2.1.2 YCbCr Color Space

The results for average standard deviation in the maximum NNDs for fixed white balance and the standard deviation across white balance conditions in the YCbCr color space are shown in Table 6.15. Table 6.16 shows the normalized total NNDs categorized by white balance conditions.

Table 6.15: Inter-object stability index (IOSI) the overall stability index (OSIW) for the YCbCr color space

WB	Y	Cb	Cr
H	1.2268	5.3552	8.9269
A	1.7434	5.9259	9.1906
T	2.1215	4.0552	4.445
D	2.9555	2.1244	3.8805
OSII	0.7282	1.6865	2.8381

(b)

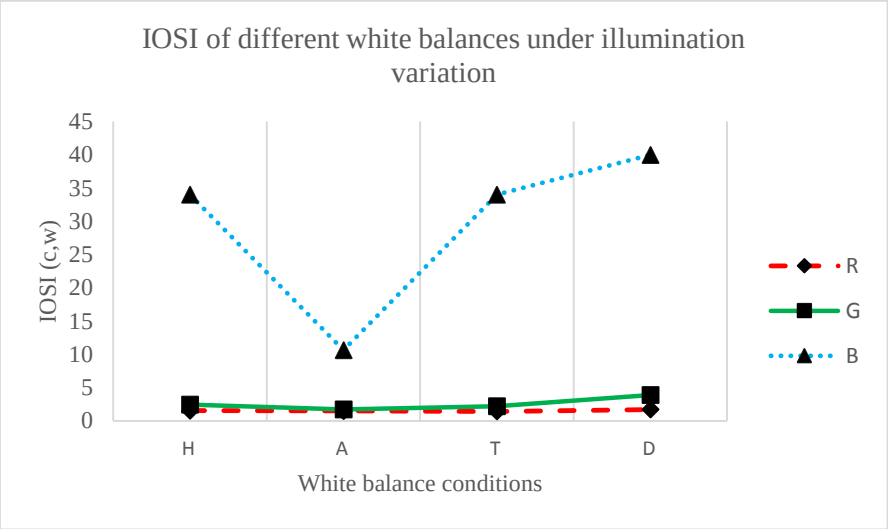

(a)

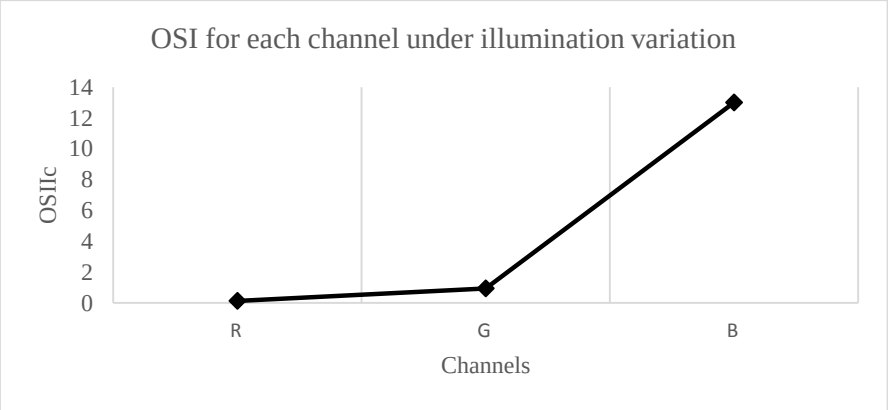

(b)

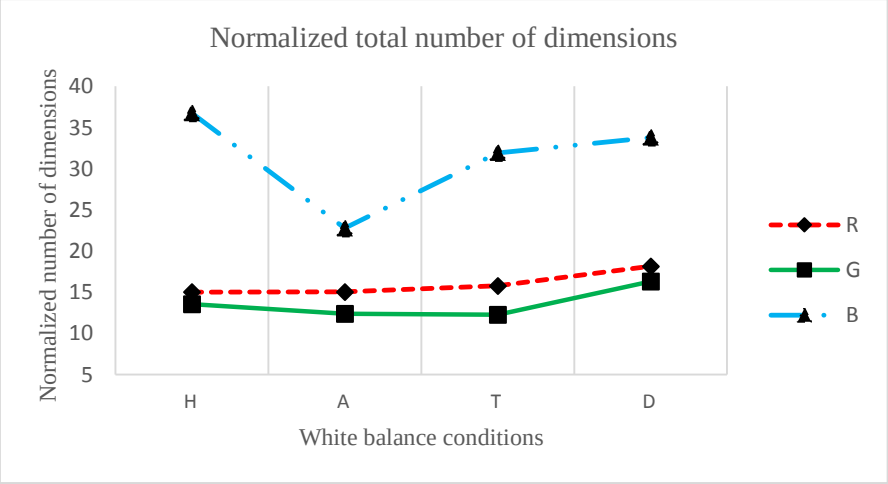

(c)

Figure 6.10: Sensitivity of individual color channels to illumination variation when white balance is constant (a) Inter-object stability index (IOSI) (b) Overall stability index (OSII) (c) The normalized total NNDs in RGB color space

Table 6.16: Normalized total NNDs by white balance for YCbCr color space

Normalized Total (WB)	H	A	T	D
Y	12	12	12	16
Cb	17	18	18	19
Cr	20	22	23	27

Figure 6.11(a) shows the average variation in the maximum NNDs under illumination change for all objects under a particular white balance condition categorized by channels of the YCbCr color space. Figure 6.11(b) gives us the comparison of different channels' sensitivity to change in illumination across the white balance conditions. We can see that Y channel has the least value of standard deviation across white balances. Hence, we can say that the dimensions in the Y channel are less sensitive to illumination change across white balance conditions. The normalized total NNDs is shown in Figure 6.11(c). The Cr channel yields the most normalized total NNDs for images in all the white balance conditions.

6.2.1.3 HSV Color Space

The results for average standard deviation in the maximum NNDs for fixed white balance and the standard deviation across white balance conditions in the HSV color space are shown in Table 6.17. Table 6.18 shows the normalized total NNDs categorized by white balance conditions.

Table 6.17: Inter-object stability index (IOSI) the overall stability index (OSIW) for HSV color space

WB	H	S	V
H	39.73	7.758	30.8314
A	39.3422	32.5002	17.091
T	30.0732	39.1723	18.2474
D	24.602	39.1218	14.9248
OSII	7.3902	14.9195	7.172

Table 6.18: Normalized total NNDs by white balance for HSV color space

Normalized Total (WB)	H	A	T	D
H	77	79	81	84
S	28	41	57	78
V	49	44	46	70

(a)

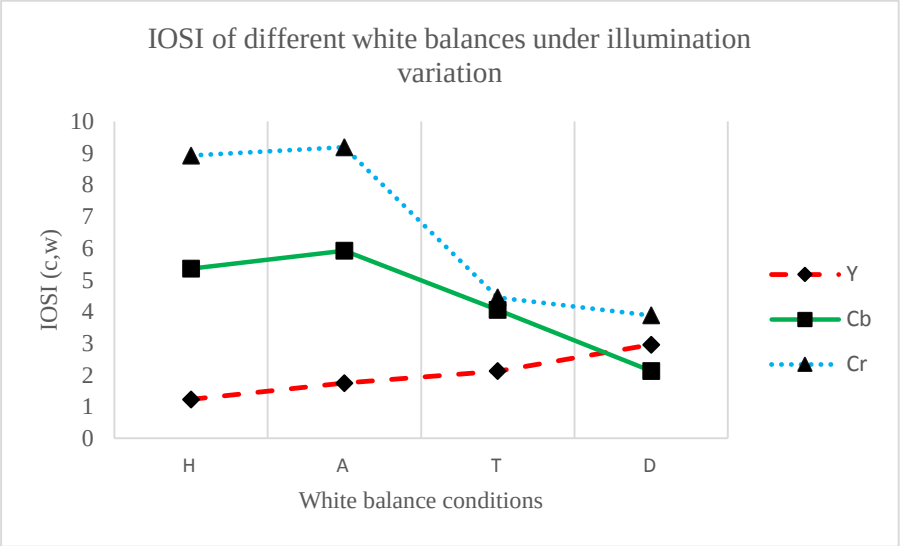

(a)

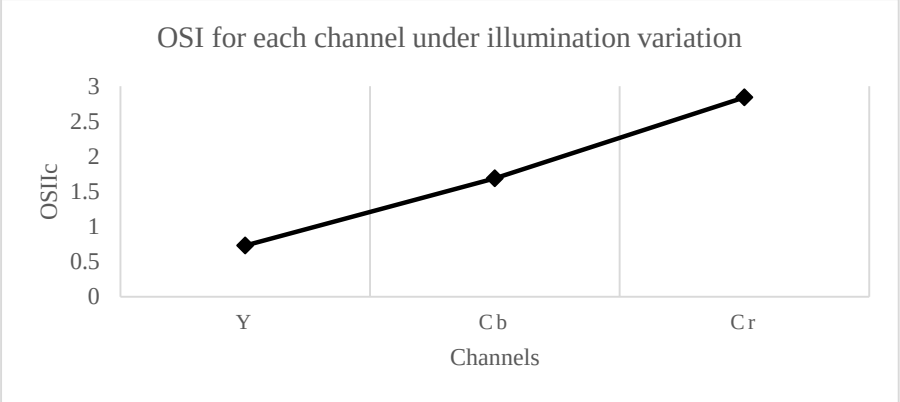

(b)

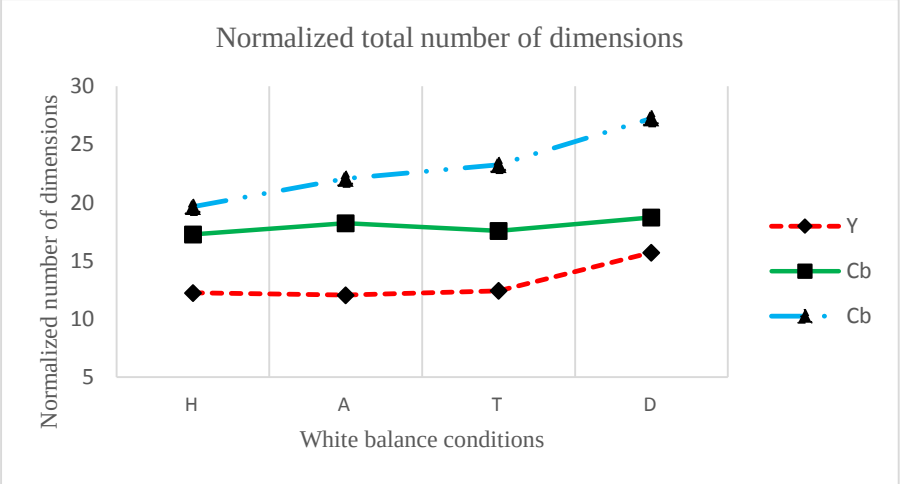

(c)

Figure 6.11: Sensitivity of individual color channels to illumination variation when white balance is constant (a) Inter-object stability index (IOSI) (b) Overall stability index (OSII) (c) The normalized total NNDs in YCbCr color space

Figure 6.12(a) shows the average variation in the maximum NNDs under illumination change for all objects under a particular white balance condition categorized by channels of the HSV color space. Figure 6.12(b) gives us the comparison of different channels' sensitivity to change in illumination across the white balance conditions. Across white balances, we can see that the dimensions from H and V channel are least sensitive to change in illumination conditions. The normalized total NNDs is shown in Figure 6.12(c). We can see that the H channel has the most normalized total NNDs for images from all the white balance conditions.

6.2.2 Effect of White Balance

6.2.2.1 RGB Color Space

Table 6.19 shows the results of average standard deviation in the maximum NNDs for fixed illumination and varying white balance conditions. It also shows the standard deviation across white balance conditions in the RGB color space. Table 6.20 shows the normalized total NNDs categorized by illumination conditions.

Table 6.19: Inter-object stability index (IOSI) the overall stability index (OSIW) for RGB color space

Illumination	R	G	B
H	1.8	3.3	35.0
A	1.7	2.5	36.1
T	1.9	1.9	9.4
D	1.6	2.8	35.5
OSIW	0.1	0.6	13.1

Table 6.20: Normalized total NNDs by white balance for RGB color space

Normalized Total (ILL)	H	A	T	D
R	17	16	16	14
G	16	13	12	13
B	34	35	20	36

Figure 6.13(a) shows the average variation in the maximum NNDs under white balance change for all objects under a particular illumination condition categorized by channels of the RGB color space.

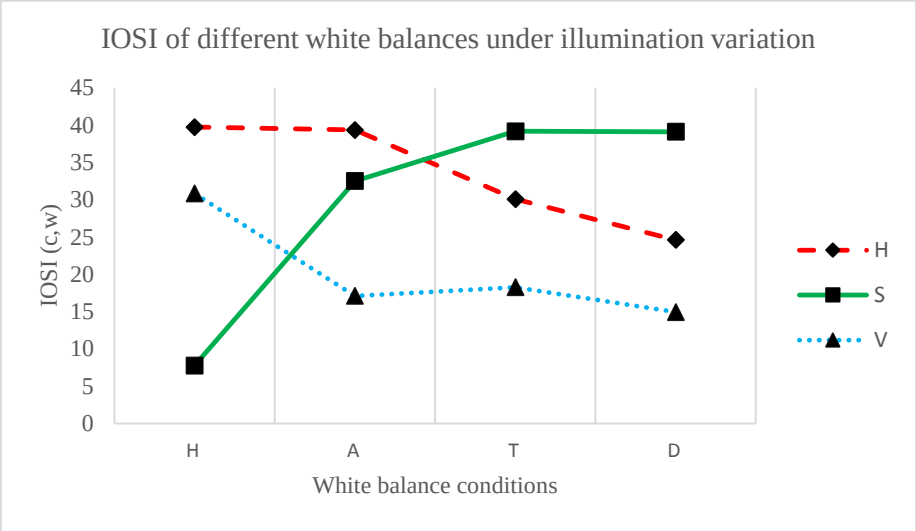

(a)

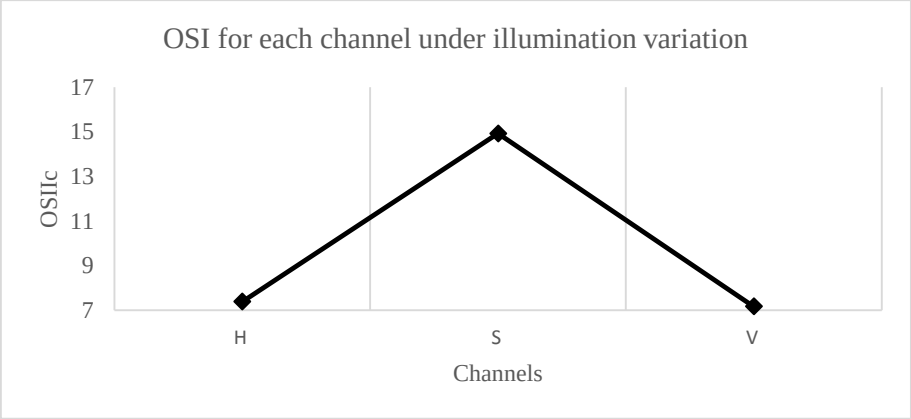

(b)

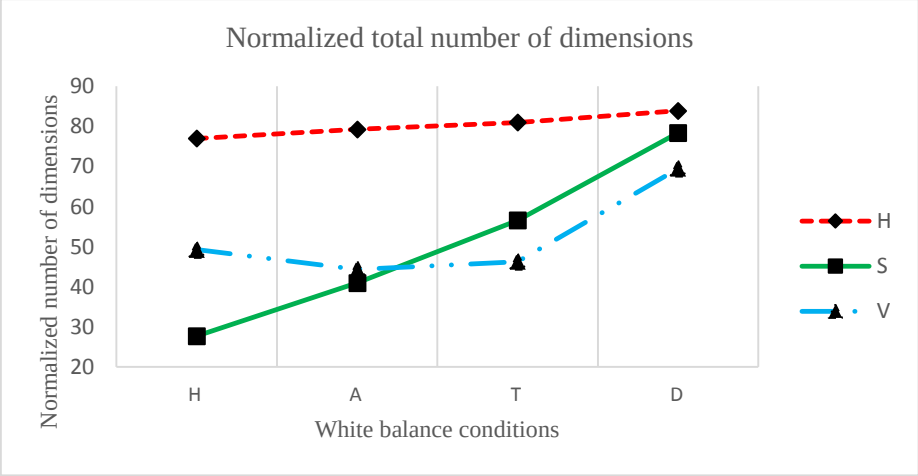

(c)

Figure 6.12: Sensitivity of individual color channels to illumination variation when white balance is constant (a) Inter-object stability index (IOSI) (b) Overall stability index (OSII) (c) The normalized total NNDs in HSV channel

Figure 6.13(b) shows us the comparison of different channels' sensitivity to change in white balance across the illumination conditions. We observe that the R and G channels have the same standard deviation across illumination conditions. The normalized total NNDs is shown in Figure 6.13(c). The B channel has the maximum normalized total NNDs for images from all the illumination conditions.

6.2.2.2 YCbCr Color Space

Table 6.21 shows the results of average standard deviation in the maximum NNDs for fixed illumination and varying white balance conditions. It also shows the standard deviation across white balance conditions in the YCbCr color space. Table 6.22 shows the normalized total NNDs categorized by illumination conditions.

Table 6.21: Inter-object stability index (IOSI) the overall stability index (OSIW) for YCbCr color space

Illuminations	Y	Cb	Cr
H	2.5	2.9	4.4
A	2.2	3.2	4.1
T	2.0	3.2	7.8
D	1.2	4.8	8.9
OSIW	0.6	0.9	2.4

Table 6.22: Normalized total NNDs by white balance for YCbCr color space

Normalized Total (ILL)	H	A	T	D
Y	16	13	12	11
Cb	20	20	18	14
Cr	28	25	21	19

Figure 6.14(a) shows the average variation in the maximum NNDs under white balance change for all objects under a particular illumination condition categorized by channels of the YCbCr color space. Figure 6.14(b) shows us the comparison of different channels' sensitivity to change in white balance across the illumination conditions. We observe that the Y channel is least sensitive to change in white balance conditions across illuminations. The normalized total NNDs is shown in Figure 6.14(c). The Cr channel has the most normalized total NNDs for images from all the illumination conditions.

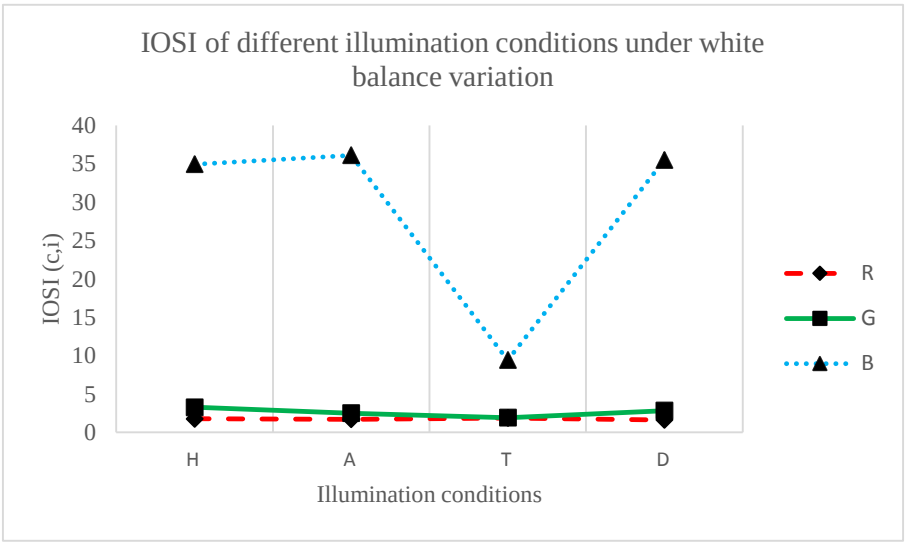

(a)

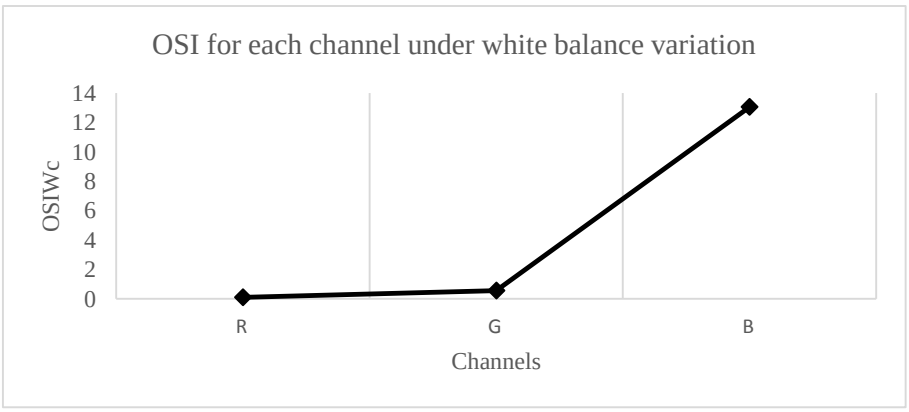

(b)

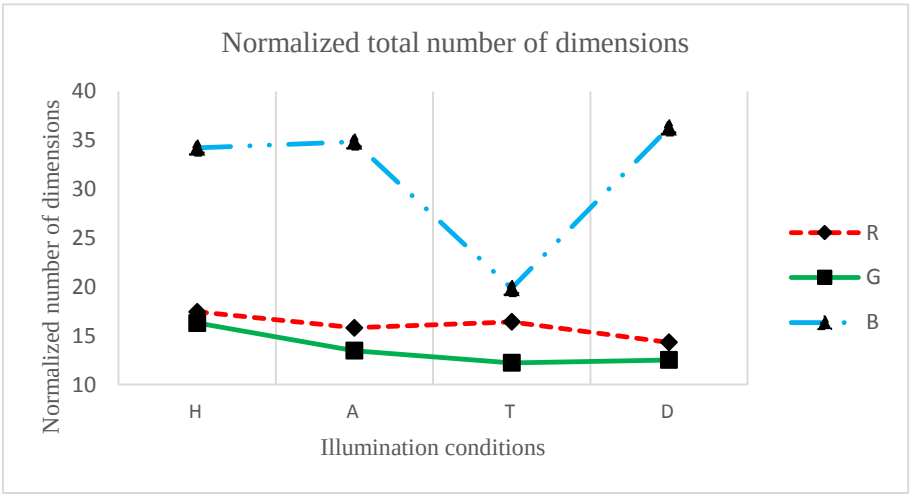

(c)

Figure 6.13: Sensitivity of individual color channels to white balance variation when illumination is constant (a) Inter-object stability index (IOSI) (b) Overall stability index (OSIW) (c) The normalized total NNDs in RGB color space

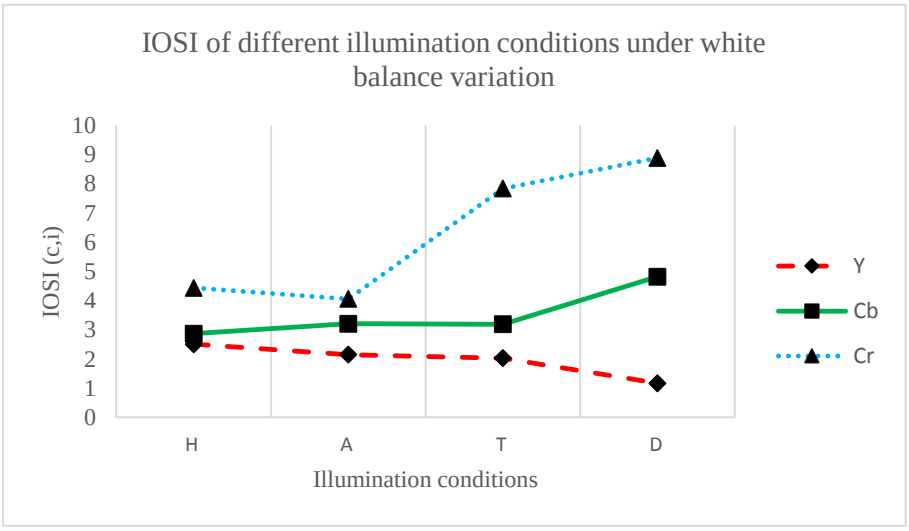

(a)

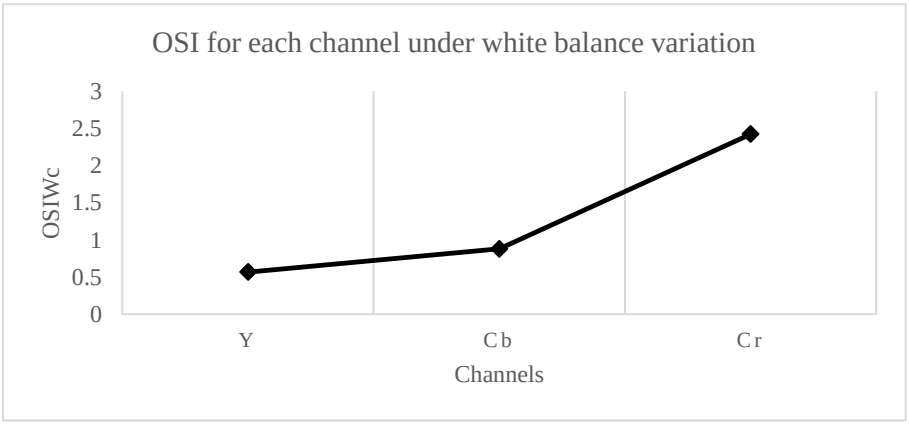

(b)

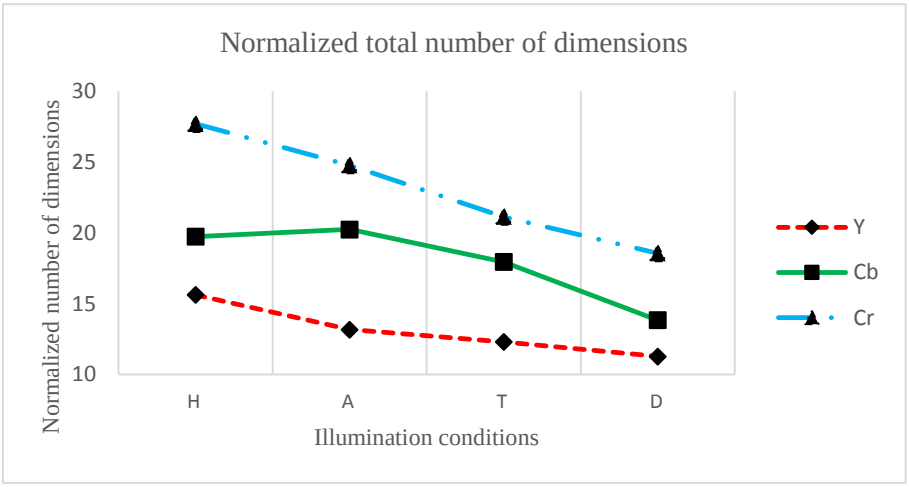

(c)

Figure 6.14: Sensitivity of individual color channels to white balance variation when illumination is constant (a) Inter-object stability index (IOSI) (b) Overall stability index (OSIW) (c) The normalized total NNDs in YCbCr channel

6.2.2.3 HSV Color Space

Table 6.23 shows the results of average standard deviation in the maximum NNDs for fixed illumination and varying white balance conditions. It also shows the standard deviation across white balance conditions in the HSV color space. Table 6.24 shows the normalized total NNDs categorized by illumination conditions.

Table 6.23: Inter-object stability index (IOSI) the overall stability index (OSIW) for HSV color space

Illumination	H	S	V
H	21.305	35.1132	13.5155
A	44.6551	41.7379	15.3135
T	39.3371	36.0671	28.1078
D	25.6331	5.9853	29.9638
OSIW	11.0568	16.0949	8.5073

Table 6.24: Normalized total NNDs by white balance for HSV color space

Normalized Total (ILL)	H	A	T	D
H	86	72	78	85
S	77	55	44	27
V	64	51	46	48

Figure 6.15(a) shows the average variation in the maximum NNDs under white balance change for all objects under a particular illumination condition categorized by channels of the HSV color space. Figure 6.15(b) shows us the comparison of different channels' sensitivity to change in white balance across the illumination conditions. The stability of features in the V channel are seen to be the best for variation in white balance across illumination conditions. The normalized total NNDs is shown in Figure 6.15(c). The H channel has the highest normalized total for the images from all the illumination conditions.

6.2.3 Effect of White Balance and Illumination

6.2.3.1 RGB Color Space

Figure 6.16 (a) shows the overall standard deviation for the maximum NNDs in the RGB channel

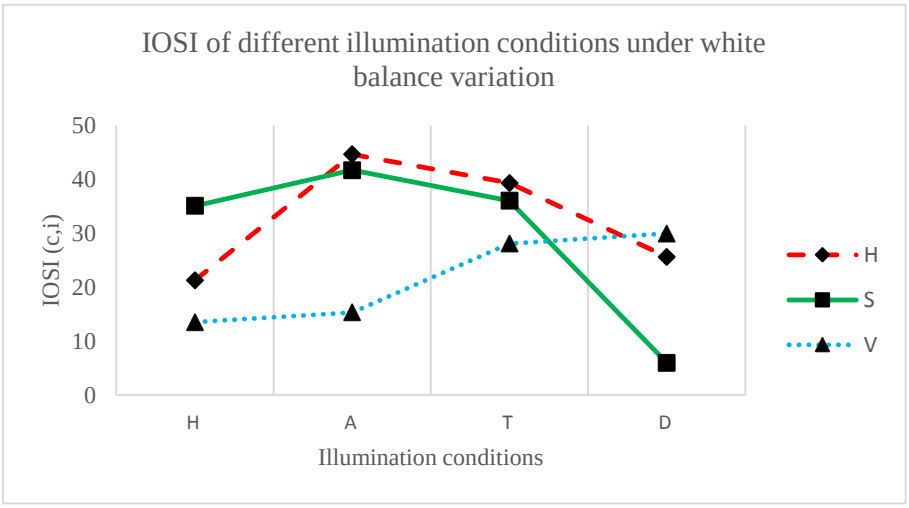

(a)

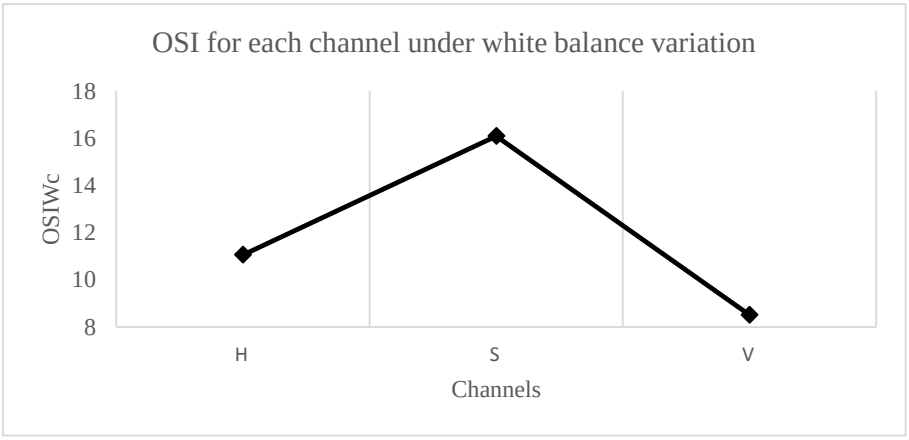

(b)

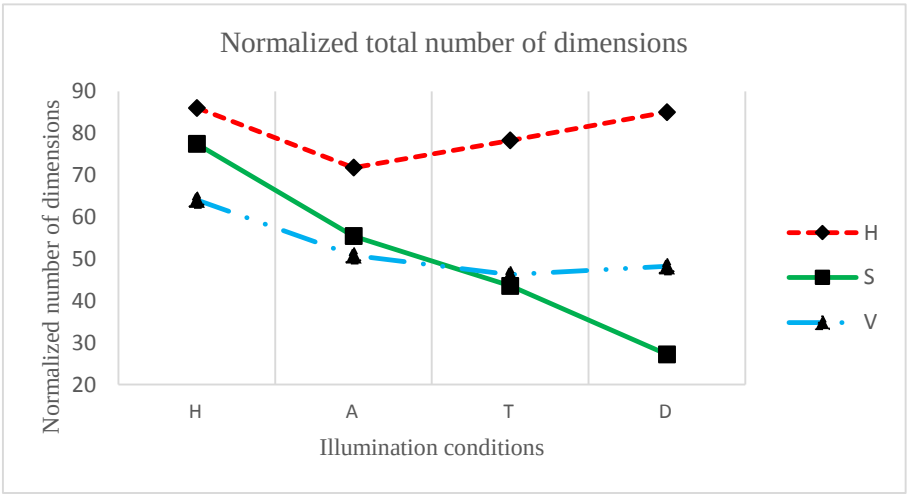

(c)

Figure 6.15: Sensitivity of individual color channels to white balance variation when illumination is constant (a) Inter-object stability index (IOSI) (b) Overall stability index (OSIW) (c) The normalized total NNDs in HSV channel

considering both white balance and illumination change. This shows the most global perspective of looking at the variation in the maximum NNDs. It can be seen that both R and G channels have the least value of standard deviation and are considered stable when the inter-object perspective is considered. The most global analysis is given by the overall standard deviation in Figure 6.16(b). Here the variation in the maximum NNDs are considered for all illuminations and white balances, we see that the overall inter-object stability of R and G channels are best compared to the B channel. Figure 6.16(c) shows the global perspective with the normalized total number of keypoints. It can be seen that the B channel yields the maximum normalized total maximum NNDs.

6.2.3.2 YCbCr Channel

Figure 6.17(a) shows the overall standard deviation for the maximum NNDs in the YCbCr channel considering both white balance and illumination change. This shows the most global perspective of looking at the variation in the maximum NNDs. It can be seen that Y channel has the least value of standard deviation and is considered stable when the inter-object perspective is considered. The most global analysis is given by the overall standard deviation in Figure 6.17(b). Here the variation in the maximum NNDs are considered for all illuminations and white balances, we see that the overall inter-object stability of Y channel is the most. Figure 6.17 (c) shows the global perspective with the normalized total number of keypoints. It can be seen that the Cr channel yields the maximum normalized total maximum NNDs.

6.2.3.3 HSV Channel

Figure 6.18(a) shows the overall standard deviation for the maximum NNDs in the HSV channel considering both white balance and illumination change. It can be seen that V channel has the least value of standard deviation and is considered stable when the inter-object perspective is considered. The most global analysis is given by the overall standard deviation in Figure 6.18(b). Figure 6.18(c) shows the global perspective with the normalized total number of keypoints.

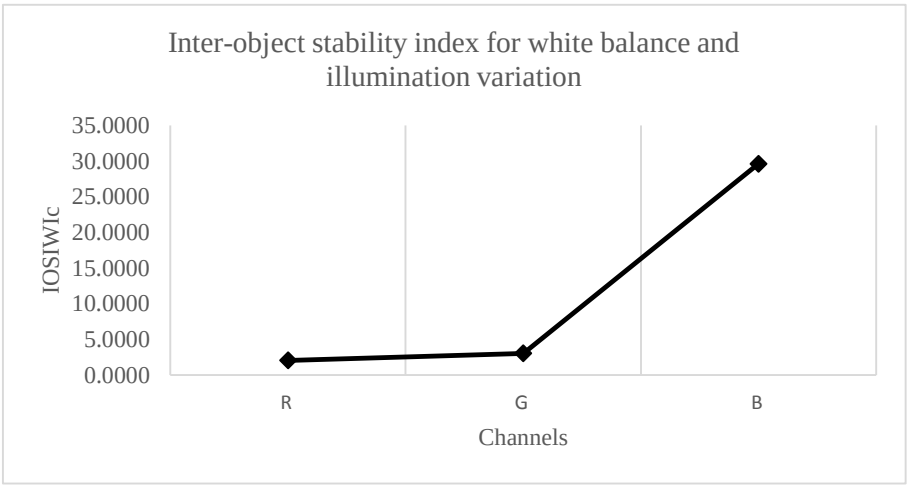

(a)

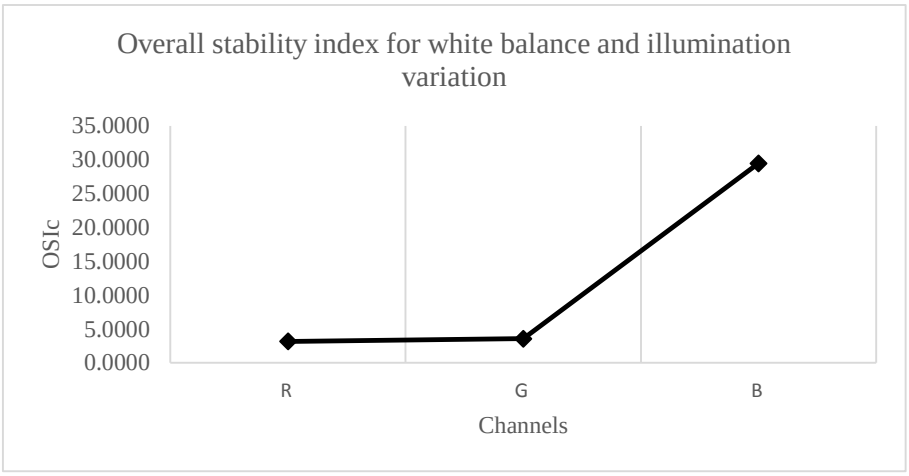

(b)

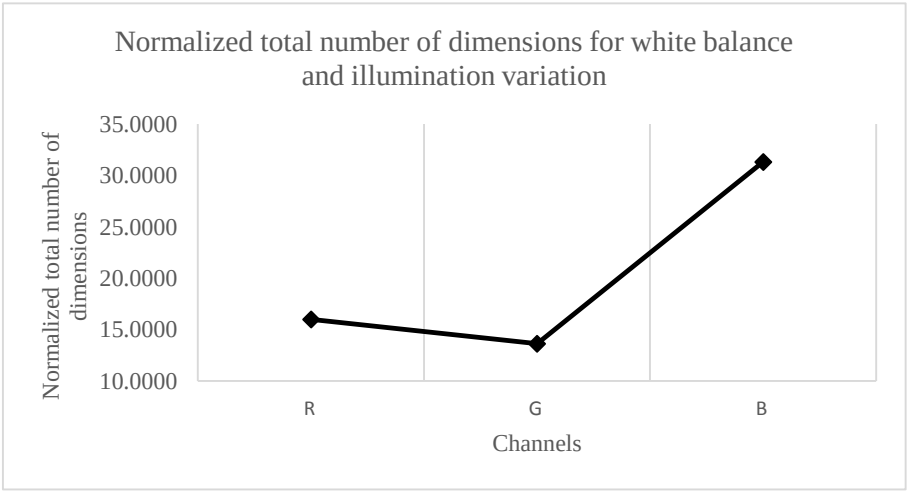

(c)

Figure 6.16: Sensitivity of color channels to change in white balance and illumination variation (a) Inter-object stability index (IOSI) (b) The overall stability index (OSI) and (c) The normalized total number of keypoints in RGB channel

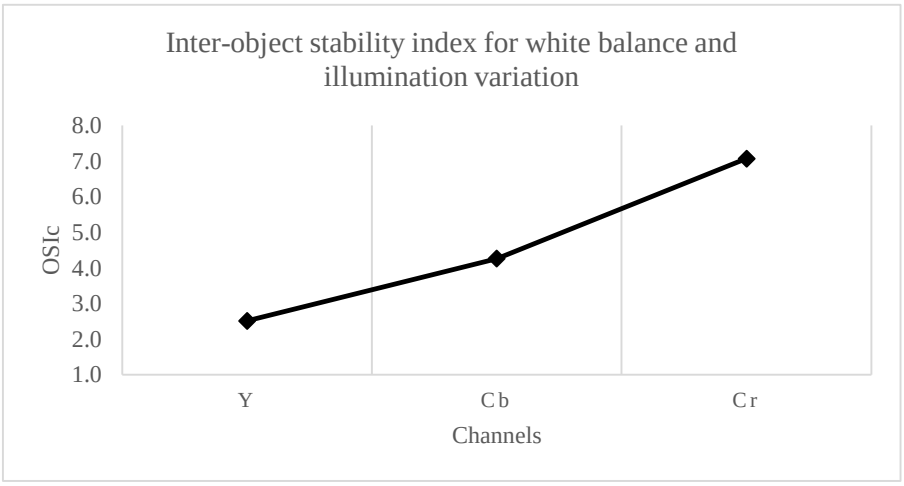

(a)

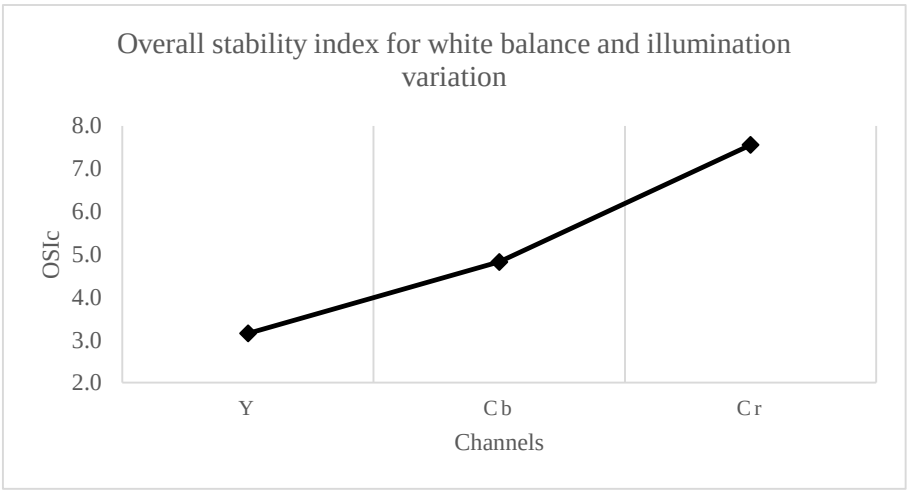

(b)

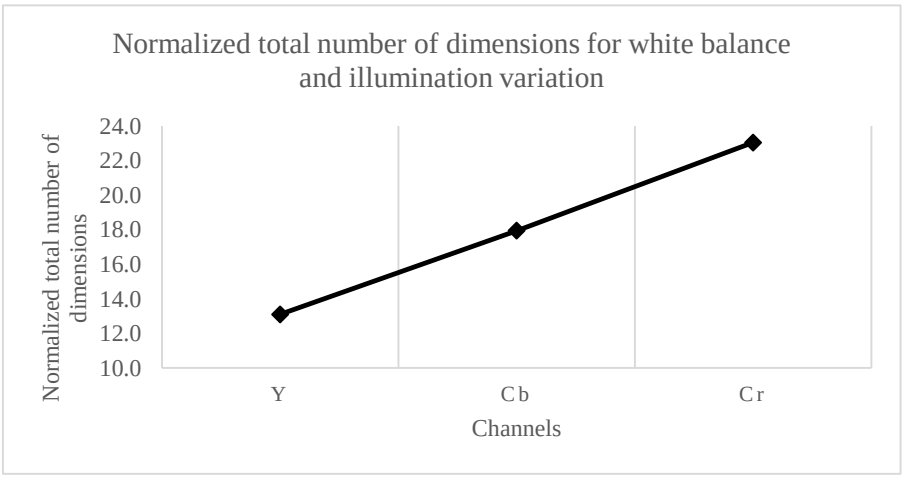

(c)

Figure 6.17: Sensitivity of color channels to change in white balance and illumination variation (a) Inter-object stability index (IOSI) (b) The overall stability index (OSI) and (c) The normalized total number of keypoints in YCbCr channel

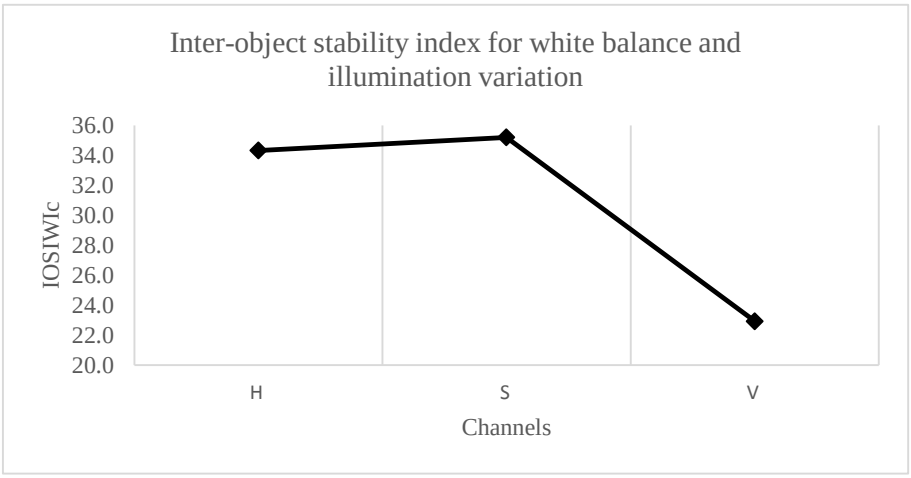

(a)

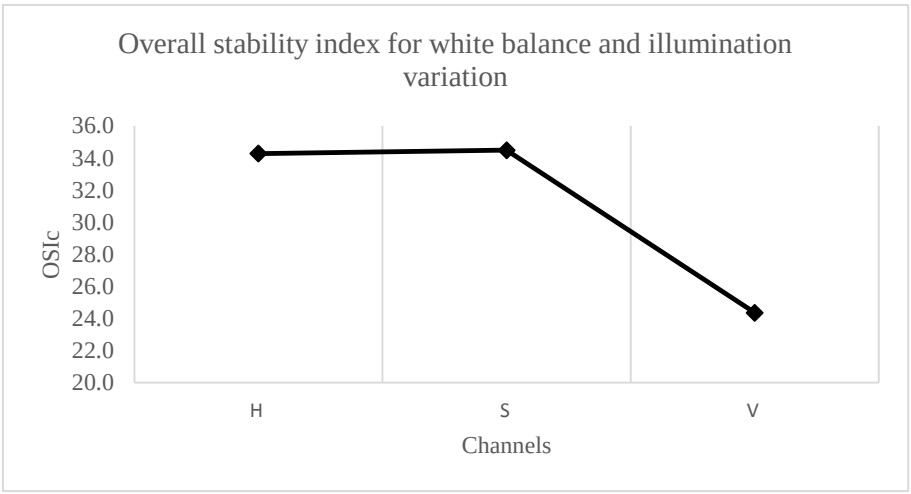

(b)

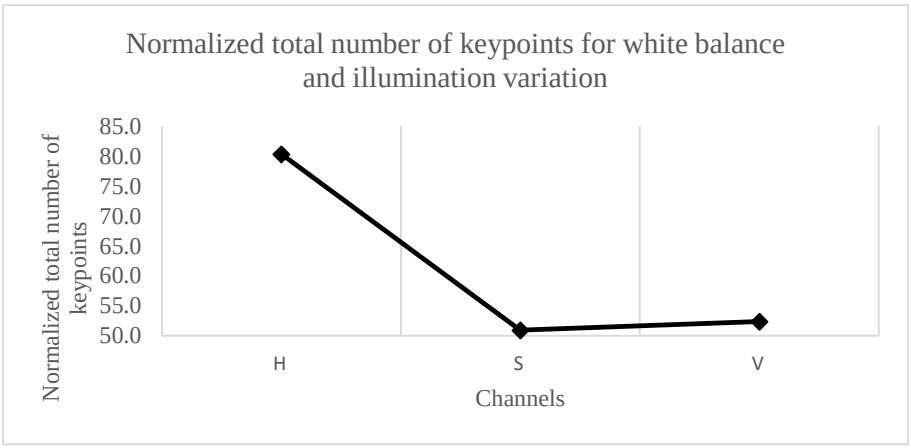

(c)

Figure 6.18: Sensitivity of color channels to change in white balance and illumination variation (a) Inter-object stability index (IOSI) (b) The overall stability index (OSI) and (c) The normalized total number of keypoints in HSV channel

Here the variation in the maximum NNDs are considered for all illuminations and white balances, we see that the overall inter-object stability of V channel is the most. It can be seen that the H channel yields the maximum normalized total maximum NNDs.

6.3 Results for Salient Keypoints in Combination of Color Channels

The method of ranking as discussed in section 4.4.2.3 is essence of finding the salient keypoints in a combination of color channel. For two channels in a color space, the lowest number of matches indicates most salient points and we assign rank 1 to it. The channel combination with highest number of matches is assigned rank 3. We will analyze the color spaces on the basis of this ranking method. All the images belonging to one white balance conditions are analyzed together to get the overall ranking. Further, the images are categorized by illumination conditions and the percentages are computed for each illumination condition.

6.3.1 RGB Color Space

Table 6.25 shows the ranking for the combination of channels in the RGB color space. For the overall analysis. We can see that RB channel has highest percentage of rank in all the white balance conditions. This indicates that the RB channel combination has the most salient keypoints. The percentages for individual illumination condition for each white balance conditions are shown in Table 6.25.

6.3.2 YCbCr Color Space

Table 6.26 shows the ranking for the combination of channels in the YCbCr color space. For the overall analysis. We can see that CbCr channel has highest percentage of rank in all the white balance conditions. This indicates that the CbCr channel combination has the most salient keypoints. The percentages for individual illumination condition for each white balance conditions are shown in Table 6.26.

Table 6.25: Ranking percentages for salient keypoints in the RGB color space channel combinations

For images in H white balance			
Overall			
Rank	RG(%)	GB(%)	RB(%)
1	0	3	97
2	1	96	3
3	99	1	0
H Illumination Condition			
Rank	RG(%)	GB(%)	RB(%)
1	0	3	97
2	0	97	3
3	100	0	0
A Illumination Condition			
Rank	RG(%)	GB(%)	RB(%)
1	0	0	100
2	0	100	0
3	100	0	0
T Illumination Condition			
Rank	RG(%)	GB(%)	RB(%)
1	0	0	100
2	3	97	0
3	97	3	0
D Illumination Condition			
Rank	RG(%)	GB(%)	RB(%)
1	0	9	91
2	0	91	9
3	100	0	0

For images in A white balance			
Overall			
Rank	RG(%)	GB(%)	RB(%)
1	0	1	99
2	13	86	1
3	87	13	0
H Illumination Condition			
Rank	RG(%)	GB(%)	RB(%)
1	0	3	97
2	0	97	3
3	100	0	0
A Illumination Condition			
Rank	RG(%)	GB(%)	RB(%)
1	0	0	100
2	0	100	0
3	100	0	0
T Illumination Condition			
Rank	RG(%)	GB(%)	RB(%)
1	0	0	100
2	51	49	0
3	49	51	0
D Illumination Condition			
Rank	RG(%)	GB(%)	RB(%)
1	0	0	100
2	0	100	0
3	100	0	0

For images in T white balance			
Overall			
Rank	RG(%)	GB(%)	RB(%)
1	0	8	94
2	33	59	6
3	67	33	0
H Illumination Condition			
Rank	RG(%)	GB(%)	RB(%)
1	0	31	74
2	0	69	26
3	100	0	0
A Illumination Condition			
Rank	RG(%)	GB(%)	RB(%)
1	0	0	100
2	0	100	0
3	100	0	0
T Illumination Condition			
Rank	RG(%)	GB(%)	RB(%)
1	0	0	100
2	54	46	0
3	46	54	0
D Illumination Condition			
Rank	RG(%)	GB(%)	RB(%)
1	0	0	100
2	77	23	0
3	23	77	0

For images in D white balance			
Overall			
Rank	RG(%)	GB(%)	RB(%)
1	0	41	93
2	21	38	7
3	79	21	0
H Illumination Condition			
Rank	RG(%)	GB(%)	RB(%)
1	0	94	100
2	0	6	0
3	100	0	0
A Illumination Condition			
Rank	RG(%)	GB(%)	RB(%)
1	0	66	74
2	0	34	26
3	100	0	0
T Illumination Condition			
Rank	RG(%)	GB(%)	RB(%)
1	0	3	97
2	0	97	3
3	100	0	0
D Illumination Condition			
Rank	RG(%)	GB(%)	RB(%)
1	0	0	100
2	86	14	0
3	14	86	0

Table 6.26: Ranking percentages for salient keypoints in the YCbCr color space channel combinations

For images in H white balance			
Overall			
Rank	YCb	CbCr	YCr
1	0	99	1
2	41	1	59
3	59	0	41
H Illumination Condition			
Rank	YCb	CbCr	YCr
1	0	97	3
2	3	3	94
3	97	0	3
A Illumination Condition			
Rank	YCb	CbCr	YCr
1	0	100	0
2	94	0	6
3	6	0	94
T Illumination Condition			
Rank	YCb	CbCr	YCr
1	0	100	0
2	66	0	34
3	34	0	66
D Illumination Condition			
Rank	YCb	CbCr	YCr
1	0	100	0
2	0	0	100
3	100	0	0

For images in A white balance			
Overall			
Rank	YCb	CbCr	YCr
1	2	99	0
2	27	1	71
3	71	0	29
H Illumination Condition			
Rank	YCb	CbCr	YCr
1	0	100	0
2	0	0	100
3	100	0	0
A Illumination Condition			
Rank	YCb	CbCr	YCr
1	0	100	0
2	17	0	83
3	83	0	17
T Illumination Condition			
Rank	YCb	CbCr	YCr
1	9	94	0
2	91	6	0
3	0	0	100
D Illumination Condition			
Rank	YCb	CbCr	YCr
1	0	100	0
2	0	0	100
3	100	0	0

For images in T white balance			
Overall			
Rank	YCb	CbCr	YCr
1	0	96	4
2	1	4	95
3	99	0	1
H Illumination Condition			
Rank	YCb	CbCr	YCr
1	0	86	14
2	0	14	86
3	100	0	0
A Illumination Condition			
Rank	YCb	CbCr	YCr
1	0	100	0
2	0	0	100
3	100	0	0
T Illumination Condition			
Rank	YCb	CbCr	YCr
1	0	100	0
2	6	0	94
3	94	0	6
D Illumination Condition			
Rank	YCb	CbCr	YCr
1	0	100	0
2	0	0	100
3	100	0	0

For images in D white balance			
Overall			
Rank	YCb	CbCr	YCr
1	0	87	15
2	0	13	85
3	100	0	0
H Illumination Condition			
Rank	YCb	CbCr	YCr
1	0	77	31
2	0	23	69
3	100	0	0
A Illumination Condition			
Rank	YCb	CbCr	YCr
1	0	83	17
2	0	17	83
3	100	0	0
T Illumination Condition			
Rank	YCb	CbCr	YCr
1	0	89	11
2	0	11	89
3	100	0	0
D Illumination Condition			
Rank	YCb	CbCr	YCr
1	0	100	0
2	0	0	100
3	100	0	0

6.3.3 HSV Color Space

Table 6.27 shows the ranking for the combination of channels in the HSV color space. For the overall analysis.

We can see that HV channel has highest percentage of rank for images in the H and A white balance conditions and the HS channel has the highest saliency ranking percentage for images in the T and D white balance conditions. The percentages for individual illumination condition for each white balance conditions are shown in Table 6.27.

Table 6.27: Ranking percentages for salient keypoints in the HSV color space channel combinations

For images in H white balance			
Overall			
Rank	HS	SV	HV
1	19	6	78
2	44	30	22
3	36	64	0
H Illumination Condition			
Rank	HS	SV	HV
1	49	0	51
2	51	0	49
3	0	100	0
A Illumination Condition			
Rank	HS	SV	HV
1	11	11	80
2	49	26	20
3	40	63	0
T Illumination Condition			
Rank	HS	SV	HV
1	17	0	86
2	77	6	14
3	6	94	0
D Illumination Condition			
Rank	HS	SV	HV
1	0	11	94
2	0	89	6
3	100	0	0

For images in A white balance			
Overall			
Rank	HS	SV	HV
1	44	4	59
2	36	19	36
3	21	77	6
H Illumination Condition			
Rank	HS	SV	HV
1	86	0	26
2	14	0	74
3	0	100	0
A Illumination Condition			
Rank	HS	SV	HV
1	37	0	77
2	63	0	23
3	0	100	0
T Illumination Condition			
Rank	HS	SV	HV
1	51	17	31
2	26	14	46
3	23	69	23
D Illumination Condition			
Rank	HS	SV	HV
1	0	0	100
2	40	60	0
3	60	40	0

For images in T white balance			
Overall			
Rank	HS	SV	HV
1	76	9	41
2	16	12	38
3	8	79	21
H Illumination Condition			
Rank	HS	SV	HV
1	69	31	46
2	0	17	11
3	31	51	43
A Illumination Condition			
Rank	HS	SV	HV
1	91	0	40
2	9	0	60
3	0	100	0
T Illumination Condition			
Rank	HS	SV	HV
1	51	0	74
2	49	0	26
3	0	100	0
D Illumination Condition			
Rank	HS	SV	HV
1	91	6	6
2	9	31	54
3	0	63	40

For images in D white balance			
Overall			
Rank	HS	SV	HV
1	65	11	47
2	25	6	29
3	10	83	24
H Illumination Condition			
Rank	HS	SV	HV
1	69	17	46
2	6	3	23
3	26	80	31
A Illumination Condition			
Rank	HS	SV	HV
1	83	26	37
2	3	9	14
3	14	66	49
T Illumination Condition			
Rank	HS	SV	HV
1	86	0	20
2	14	14	66
3	0	86	14
D Illumination Condition			
Rank	HS	SV	HV
1	23	0	86
2	77	0	14
3	0	100	0

6.3.4 HSV with RGB Color Space

The results for hybrid color spaces are presented in this section for channels belonging to the combination of HSV and RGB color space.

Using the ranking technique described earlier, we can see that the HB channel combination outperforms all other channel combinations in Table 6.28.

Similarly, SB and VB channels yield most salient keypoints as seen in Table 6.29 and Table 6.30.

1. H with RGB Color Space

Table 6.28: Hybrid channel ranking percentages for salient keypoints in the HSV and RGB color space channel combinations

For images in H white balance			
Overall			
Rank	HR	HG	HB
1	0	0	100
2	88	8	0
3	12	92	0
H Illumination Condition			
Rank	HR	HG	HB
1	0	0	100
2	71	17	0
3	29	83	0
A Illumination Condition			
Rank	HR	HG	HB
1	0	0	100
2	97	3	0
3	3	97	0
T Illumination Condition			
Rank	HR	HG	HB
1	0	0	100
2	86	9	0
3	14	91	0
D Illumination Condition			
Rank	HR	HG	HB
1	0	0	100
2	97	3	0
3	3	97	0

For images in A white balance			
Overall			
Rank	HR	HG	HB
1	0	0	100
2	73	17	0
3	27	83	0
H Illumination Condition			
Rank	HR	HG	HB
1	0	0	100
2	46	29	0
3	54	71	0
A Illumination Condition			
Rank	HR	HG	HB
1	0	0	100
2	60	29	0
3	40	71	0
T Illumination Condition			
Rank	HR	HG	HB
1	0	0	100
2	100	0	0
3	0	100	0
D Illumination Condition			
Rank	HR	HG	HB
1	0	0	100
2	86	11	0
3	14	89	0

For images in T white balance			
Overall			
Rank	HR	HG	HB
1	4	11	86
2	46	10	0
3	50	79	14
H Illumination Condition			
Rank	HR	HG	HB
1	3	26	63
2	0	17	0
3	97	57	37
A Illumination Condition			
Rank	HR	HG	HB
1	11	20	80
2	17	9	0
3	71	71	20
T Illumination Condition			
Rank	HR	HG	HB
1	3	0	100
2	66	14	0
3	31	86	0
D Illumination Condition			
Rank	HR	HG	HB
1	0	0	100
2	100	0	0
3	0	100	0

2. S with RGB Color Space

Table 6.29: Hybrid channel ranking percentages for salient keypoints in HSV and RGB channels

For images in H white balance			
Overall			
Rank	SR	SG	SB
1	0	0	100
2	66	33	0
3	34	67	0
H Illumination Condition			
Rank	SR	SG	SB
1	0	0	100
2	100	0	0
3	0	100	0
A Illumination Condition			
Rank	SR	SG	SB
1	0	0	100
2	100	0	0
3	0	100	0
T Illumination Condition			
Rank	SR	SG	SB
1	0	0	100
2	66	31	0
3	34	69	0
D Illumination Condition			
Rank	SR	SG	SB
1	0	0	100
2	0	100	0
3	100	0	0

For images in A white balance			
Overall			
Rank	SR	SG	SB
1	0	0	100
2	69	29	0
3	31	71	0
H Illumination Condition			
Rank	SR	SG	SB
1	0	0	100
2	77	14	0
3	23	86	0
A Illumination Condition			
Rank	SR	SG	SB
1	0	0	100
2	100	0	0
3	0	100	0
T Illumination Condition			
Rank	SR	SG	SB
1	0	0	100
2	100	0	0
3	0	100	0
D Illumination Condition			
Rank	SR	SG	SB
1	0	0	100
2	0	100	0
3	100	0	0

For images in T white balance			
Overall			
Rank	SR	SG	SB
1	5	6	88
2	76	4	0
3	19	90	12
H Illumination Condition			
Rank	SR	SG	SB
1	20	26	51
2	6	14	0
3	74	60	49
A Illumination Condition			
Rank	SR	SG	SB
1	0	0	100
2	100	0	0
3	0	100	0
T Illumination Condition			
Rank	SR	SG	SB
1	0	0	100
2	100	0	0
3	0	100	0
D Illumination Condition			
Rank	SR	SG	SB
1	0	0	100
2	100	0	0
3	0	100	0

3. V with RGB Color Space

Table 6.30: Hybrid channel ranking percentages for salient keypoints in HSV and RGB channels

For images in H white balance			
Overall			
Rank	VR	VG	VB
1	0	0	100
2	56	44	0
3	44	56	0
H Illumination Condition			
Rank	VR	VG	VB
1	0	0	100
2	0	100	0
3	100	0	0
A Illumination Condition			
Rank	VR	VG	VB
1	0	0	100
2	31	69	0
3	69	31	0
T Illumination Condition			
Rank	VR	VG	VB
1	0	0	100
2	100	0	0
3	0	100	0
D Illumination Condition			
Rank	VR	VG	VB
1	0	0	100
2	91	9	0
3	9	91	0

For images in A white balance			
Overall			
Rank	VR	VG	VB
1	0	0	100
2	49	51	0
3	51	49	0
H Illumination Condition			
Rank	VR	VG	VB
1	0	0	100
2	0	100	0
3	100	0	0
A Illumination Condition			
Rank	VR	VG	VB
1	0	0	100
2	0	100	0
3	100	0	0
T Illumination Condition			
Rank	VR	VG	VB
1	0	0	100
2	97	3	0
3	3	97	0
D Illumination Condition			
Rank	VR	VG	VB
1	0	0	100
2	100	0	0
3	0	100	0

For images in T white balance			
Overall			
Rank	VR	VG	VB
1	0	0	100
2	24	76	0
3	76	24	0
H Illumination Condition			
Rank	VR	VG	VB
1	0	0	100
2	0	100	0
3	100	0	0
A Illumination Condition			
Rank	VR	VG	VB
1	0	0	100
2	0	100	0
3	100	0	0
T Illumination Condition			
Rank	VR	VG	VB
1	0	0	100
2	0	100	0
3	100	0	0
D Illumination Condition			
Rank	VR	VG	VB
1	0	0	100
2	94	6	0
3	6	94	0

For images in D white balance			
Overall			
Rank	VR	VG	VB
1	0	0	100
2	0	100	0
3	100	0	0
H Illumination Condition			
Rank	VR	VG	VB
1	0	0	100
2	0	100	0
3	100	0	0
A Illumination Condition			
Rank	VR	VG	VB
1	0	0	100
2	0	100	0
3	100	0	0
T Illumination Condition			
Rank	VR	VG	VB
1	0	0	100
2	0	100	0
3	100	0	0
D Illumination Condition			
Rank	VR	VG	VB
1	0	0	100
2	0	100	0
3	100	0	0

6.3.5 YCbCr with RGB

The results for hybrid color spaces are presented in this section for channels belonging to the combination of YCbCr and RGB color space. Using the ranking technique described earlier, we can see that the YB channel combination outperforms all other channel combinations in Table 6.31. Similarly, CbB and CrB channels yield most salient keypoints as seen in Table 6.32 and Table 6.33.

1. Y with RGB

Table 6.31: Hybrid channel ranking percentages for salient keypoints in YCbCr and RGB channels

For images in H white balance			
Overall			
Rank	YR	YG	YB
1	0	0	100
2	91	9	0
3	9	91	0
H Illumination Condition			
Rank	YR	YG	YB
1	0	0	100
2	97	3	0
3	3	97	0
A Illumination Condition			
Rank	YR	YG	YB
1	0	0	100
2	100	0	0
3	0	100	0
T Illumination Condition			
Rank	YR	YG	YB
1	0	0	100
2	100	0	0
3	0	100	0
D Illumination Condition			
Rank	YR	YG	YB
1	0	0	100
2	69	31	0
3	31	69	0

For images in A white balance			
Overall			
Rank	YR	YG	YB
1	0	0	100
2	99	1	0
3	1	99	0
H Illumination Condition			
Rank	YR	YG	YB
1	0	0	100
2	100	0	0
3	0	100	0
A Illumination Condition			
Rank	YR	YG	YB
1	0	0	100
2	100	0	0
3	0	100	0
T Illumination Condition			
Rank	YR	YG	YB
1	0	0	100
2	97	3	0
3	3	97	0
D Illumination Condition			
Rank	YR	YG	YB
1	0	0	100
2	100	0	0
3	0	100	0

For images in T white balance			
Overall			
Rank	YR	YG	YB
1	0	0	100
2	94	6	0
3	6	94	0
H Illumination Condition			
Rank	YR	YG	YB
1	0	0	100
2	77	23	0
3	23	77	0
A Illumination Condition			
Rank	YR	YG	YB
1	0	0	100
2	100	0	0
3	0	100	0
T Illumination Condition			
Rank	YR	YG	YB
1	0	0	100
2	100	0	0
3	0	100	0
D Illumination Condition			
Rank	YR	YG	YB
1	0	0	100
2	100	0	0
3	0	100	0

For images in D white balance			
Overall			
Rank	YR	YG	YB
1	0	0	100
2	61	39	0
3	39	61	0
H Illumination Condition			
Rank	YR	YG	YB
1	0	0	100
2	0	100	0
3	100	0	0
A Illumination Condition			
Rank	YR	YG	YB
1	0	0	100
2	51	49	0
3	49	51	0
T Illumination Condition			
Rank	YR	YG	YB
1	0	0	100
2	97	3	0
3	3	97	0
D Illumination Condition			
Rank	YR	YG	YB
1	0	0	100
2	97	3	0
3	3	97	0

2. Cb with RGB

Table 6.32: Hybrid channel ranking percentages for salient keypoints in YCbCr and RGB channels

For images in H white balance			
Overall			
Rank	CbR	CbG	CbB
1	0	0	100
2	91	8	0
3	9	92	0
H Illumination Condition			
Rank	CbR	CbG	CbB
1	0	0	100
2	97	0	0
3	3	100	0
A Illumination Condition			
Rank	CbR	CbG	CbB
1	0	0	100
2	97	3	0
3	3	97	0
T Illumination Condition			
Rank	CbR	CbG	CbB
1	0	0	100
2	100	0	0
3	0	100	0
D Illumination Condition			
Rank	CbR	CbG	CbB
1	0	0	100
2	71	29	0
3	29	71	0

For images in A white balance			
Overall			
Rank	CbR	CbG	CbB
1	0	0	100
2	99	1	0
3	1	99	0
H Illumination Condition			
Rank	CbR	CbG	CbB
1	0	0	100
2	97	3	0
3	3	97	0
A Illumination Condition			
Rank	CbR	CbG	CbB
1	0	0	100
2	97	3	0
3	3	97	0
T Illumination Condition			
Rank	CbR	CbG	CbB
1	0	0	100
2	100	0	0
3	0	100	0
D Illumination Condition			
Rank	CbR	CbG	CbB
1	0	0	100
2	100	0	0
3	0	100	0

For images in T white balance			
Overall			
Rank	CbR	CbG	CbB
1	0	0	100
2	93	7	0
3	7	93	0
H Illumination Condition			
Rank	CbR	CbG	CbB
1	0	0	100
2	86	14	0
3	14	86	0
A Illumination Condition			
Rank	CbR	CbG	CbB
1	0	0	100
2	86	14	0
3	14	86	0
T Illumination Condition			
Rank	CbR	CbG	CbB
1	0	0	100
2	100	0	0
3	0	100	0
D Illumination Condition			
Rank	CbR	CbG	CbB
1	0	0	100
2	100	0	0
3	0	100	0

For images in D white balance			
Overall			
Rank	CbR	CbG	CbB
1	0	0	100
2	61	38	0
3	39	62	0
H Illumination Condition			
Rank	CbR	CbG	CbB
1	0	0	100
2	0	100	0
3	100	0	0
A Illumination Condition			
Rank	CbR	CbG	CbB
1	0	0	100
2	49	49	0
3	51	51	0
T Illumination Condition			
Rank	CbR	CbG	CbB
1	0	0	100
2	100	0	0
3	0	100	0
D Illumination Condition			
Rank	CbR	CbG	CbB
1	0	0	100
2	97	3	0
3	3	97	0

3. Cr with RGB

Table 6.33: Hybrid channel ranking percentages for salient keypoints in YCbCr and RGB channels

For images in H white balance			
Overall			
Rank	CrR	CrG	CrB
1	0	0	100
2	56	43	0
3	44	57	0
H Illumination Condition			
Rank	CrR	CrG	CrB
1	0	0	100
2	14	80	0
3	86	20	0
A Illumination Condition			
Rank	CrR	CrG	CrB
1	0	0	100
2	100	0	0
3	0	100	0
T Illumination Condition			
Rank	CrR	CrG	CrB
1	0	0	100
2	100	0	0
3	0	100	0
D Illumination Condition			
Rank	CrR	CrG	CrB
1	0	0	100
2	9	91	0
3	91	9	0

For images in A white balance			
Overall			
Rank	CrR	CrG	CrB
1	0	0	100
2	57	41	0
3	43	59	0
H Illumination Condition			
Rank	CrR	CrG	CrB
1	0	0	100
2	0	100	0
3	100	0	0
A Illumination Condition			
Rank	CrR	CrG	CrB
1	0	0	100
2	34	57	0
3	66	43	0
T Illumination Condition			
Rank	CrR	CrG	CrB
1	0	0	100
2	100	0	0
3	0	100	0
D Illumination Condition			
Rank	CrR	CrG	CrB
1	0	0	100
2	94	6	0
3	6	94	0

For images in T white balance			
Overall			
Rank	CrR	CrG	CrB
1	0	0	100
2	40	59	0
3	60	41	0
H Illumination Condition			
Rank	CrR	CrG	CrB
1	0	0	100
2	0	100	0
3	100	0	0
A Illumination Condition			
Rank	CrR	CrG	CrB
1	0	0	100
2	3	97	0
3	97	3	0
T Illumination Condition			
Rank	CrR	CrG	CrB
1	0	0	100
2	57	37	0
3	43	63	0
D Illumination Condition			
Rank	CrR	CrG	CrB
1	0	0	100
2	100	0	0
3	0	100	0

For images in D white balance			
Overall			
Rank	CrR	CrG	CrB
1	0	0	100
2	3	96	0
3	97	4	0
H Illumination Condition			
Rank	CrR	CrG	CrB
1	0	0	100
2	0	100	0
3	100	0	0
A Illumination Condition			
Rank	CrR	CrG	CrB
1	0	0	100
2	0	100	0
3	100	0	0
T Illumination Condition			
Rank	CrR	CrG	CrB
1	0	0	100
2	0	100	0
3	100	0	0
D Illumination Condition			
Rank	CrR	CrG	CrB
1	0	0	100
2	11	83	0
3	89	17	0

6.3.6 YCbCr with HSV

The results for hybrid color spaces are presented in this section for channels belonging to the combination of YCbCr and HSV color space. Using the ranking technique described earlier, we can see that the YV channel combination outperforms all other channel combinations in Table 6.34. Similarly, CbV and CrV channels yield most salient keypoints as seen in Table 6.35 and Table 6.36.

1. Y with HSV

Table 6.34: Hybrid channel ranking percentages for salient keypoints in YCbCr and HSV channels

For images in H white balance			
Overall			
Rank	YH	YS	YV
1	0	0	100
2	98	2	0
3	2	98	0
H Illumination Condition			
Rank	YH	YS	YV
1	0	0	100
2	100	0	0
3	0	100	0
A Illumination Condition			
Rank	YH	YS	YV
1	0	0	100
2	91	9	0
3	9	91	0
T Illumination Condition			
Rank	YH	YS	YV
1	0	0	100
2	100	0	0
3	0	100	0
D Illumination Condition			
Rank	YH	YS	YV
1	0	0	100
2	100	0	0
3	0	100	0

For images in A white balance			
Overall			
Rank	YH	YS	YV
1	0	0	100
2	93	7	0
3	7	93	0
H Illumination Condition			
Rank	YH	YS	YV
1	0	0	100
2	100	0	0
3	0	100	0
A Illumination Condition			
Rank	YH	YS	YV
1	0	0	100
2	100	0	0
3	0	100	0
T Illumination Condition			
Rank	YH	YS	YV
1	0	0	100
2	71	29	0
3	29	71	0
D Illumination Condition			
Rank	YH	YS	YV
1	0	0	100
2	100	0	0
3	0	100	0

For images in T white balance			
Overall			
Rank	YH	YS	YV
1	18	3	92
2	66	5	3
3	16	92	5
H Illumination Condition			
Rank	YH	YS	YV
1	37	11	74
2	14	6	6
3	49	83	20
A Illumination Condition			
Rank	YH	YS	YV
1	34	0	94
2	66	0	6
3	0	100	0
T Illumination Condition			
Rank	YH	YS	YV
1	0	0	100
2	100	0	0
3	0	100	0
D Illumination Condition			
Rank	YH	YS	YV
1	0	0	100
2	86	14	0
3	14	86	0

For images in D white balance			
Overall			
Rank	YH	YS	YV
1	26	4	94
2	57	6	1
3	17	89	5
H Illumination Condition			
Rank	YH	YS	YV
1	60	9	80
2	23	3	3
3	17	89	17
A Illumination Condition			
Rank	YH	YS	YV
1	43	9	94
2	17	11	3
3	40	80	3
T Illumination Condition			
Rank	YH	YS	YV
1	0	0	100
2	89	11	0
3	11	89	0
D Illumination Condition			
Rank	YH	YS	YV
1	0	0	100
2	100	0	0
3	0	100	0

2. Cb with HSV

Table 6.35: Hybrid channel ranking percentages for salient keypoints in YCbCr and HSV channels

For images in H white balance			
Overall			
Rank	CbH	CbS	CbV
1	0	0	100
2	91	9	0
3	9	91	0
H Illumination Condition			
Rank	CbH	CbS	CbV
1	0	0	100
2	100	0	0
3	0	100	0
A Illumination Condition			
Rank	CbH	CbS	CbV
1	0	0	100
2	66	34	0
3	34	66	0
T Illumination Condition			
Rank	CbH	CbS	CbV
1	0	0	100
2	100	0	0
3	0	100	0
D Illumination Condition			
Rank	CbH	CbS	CbV
1	0	0	100
2	100	0	0
3	0	100	0

For images in A white balance			
Overall			
Rank	CbH	CbS	CbV
1	0	0	100
2	91	9	0
3	9	91	0
H Illumination Condition			
Rank	CbH	CbS	CbV
1	0	0	100
2	100	0	0
3	0	100	0
A Illumination Condition			
Rank	CbH	CbS	CbV
1	0	0	100
2	100	0	0
3	0	100	0
T Illumination Condition			
Rank	CbH	CbS	CbV
1	0	0	100
2	66	34	0
3	34	66	0
D Illumination Condition			
Rank	CbH	CbS	CbV
1	0	0	100
2	100	0	0
3	0	100	0

For images in T white balance			
Overall			
Rank	CbH	CbS	CbV
1	14	5	94
2	64	8	1
3	21	87	5
H Illumination Condition			
Rank	CbH	CbS	CbV
1	26	20	77
2	11	9	3
3	63	71	20
A Illumination Condition			
Rank	CbH	CbS	CbV
1	31	0	97
2	69	0	3
3	0	100	0
T Illumination Condition			
Rank	CbH	CbS	CbV
1	0	0	100
2	100	0	0
3	0	100	0
D Illumination Condition			
Rank	CbH	CbS	CbV
1	0	0	100
2	77	23	0
3	23	77	0

For images in D white balance			
Overall			
Rank	CbH	CbS	CbV
1	21	6	90
2	49	11	2
3	30	83	8
H Illumination Condition			
Rank	CbH	CbS	CbV
1	46	9	74
2	11	6	3
3	43	86	23
A Illumination Condition			
Rank	CbH	CbS	CbV
1	40	17	86
2	17	9	6
3	43	74	9
T Illumination Condition			
Rank	CbH	CbS	CbV
1	0	0	100
2	66	29	0
3	34	71	0
D Illumination Condition			
Rank	CbH	CbS	CbV
1	0	0	100
2	100	0	0
3	0	100	0

3. Cr with HSV

Table 6.36: Hybrid channel ranking percentages for salient keypoints in YCbCr and HSV channels

For images in H white balance			
Overall			
Rank	CrH	CrS	CrV
1	1	0	100
2	96	2	0
3	3	98	0
H Illumination Condition			
Rank	CrH	CrS	CrV
1	0	0	100
2	100	0	0
3	0	100	0
A Illumination Condition			
Rank	CrH	CrS	CrV
1	3	0	100
2	86	9	0
3	11	91	0
T Illumination Condition			
Rank	CrH	CrS	CrV
1	0	0	100
2	100	0	0
3	0	100	0
D Illumination Condition			
Rank	CrH	CrS	CrV
1	0	0	100
2	100	0	0
3	0	100	0

For images in A white balance			
Overall			
Rank	CrH	CrS	CrV
1	1	0	100
2	84	14	0
3	14	86	0
H Illumination Condition			
Rank	CrH	CrS	CrV
1	3	0	100
2	94	3	0
3	3	97	0
A Illumination Condition			
Rank	CrH	CrS	CrV
1	3	0	100
2	97	0	0
3	0	100	0
T Illumination Condition			
Rank	CrH	CrS	CrV
1	0	0	100
2	46	54	0
3	54	46	0
D Illumination Condition			
Rank	CrH	CrS	CrV
1	0	0	100
2	100	0	0
3	0	100	0

For images in T white balance			
Overall			
Rank	CrH	CrS	CrV
1	13	5	96
2	69	9	0
3	18	86	4
H Illumination Condition			
Rank	CrH	CrS	CrV
1	29	20	83
2	17	20	0
3	54	60	17
A Illumination Condition			
Rank	CrH	CrS	CrV
1	20	0	100
2	80	0	0
3	0	100	0
T Illumination Condition			
Rank	CrH	CrS	CrV
1	3	0	100
2	97	0	0
3	0	100	0
D Illumination Condition			
Rank	CrH	CrS	CrV
1	0	0	100
2	83	17	0
3	17	83	0

For images in D white balance			
Overall			
Rank	CrH	CrS	CrV
1	19	4	94
2	60	9	1
3	21	87	5
H Illumination Condition			
Rank	CrH	CrS	CrV
1	49	3	89
2	31	6	3
3	20	91	9
A Illumination Condition			
Rank	CrH	CrS	CrV
1	29	11	86
2	29	17	3
3	43	71	11
T Illumination Condition			
Rank	CrH	CrS	CrV
1	0	0	100
2	80	14	0
3	20	86	0
D Illumination Condition			
Rank	CrH	CrS	CrV
1	0	0	100
2	100	0	0
3	0	100	0

Chapter 7 : Future Work

1. The format of all the images used in our experiment were in bitmap format. This is an uncompressed image format. The scope of this framework can be broadened by analyzing the images in JPEG and other image formats.
2. We analyze the robustness of channels in a color space using our framework. However, the reason behind the variation in the number of keypoints and features is yet to be explored.
3. The classification results should be compared with the results of salient keypoints between two color channels in a color space.

Bibliography

[1] W. Zhao, R. Chellappa, P. J. Phillips, and A. Rosenfeld, "Face Recognition: A Literature Survey," *ACM Computing Surveys*, vol. 35, no. 4, pp. 399-458, 2003.

[2] Wendy L. Braje, Daniel Kersten, Michael J. Tarr, and Nikolaus F. Troje, "Illumination Effects in Face Recognition," *Psychobiology In press*, August 1998.

[3] P. J. Phillips, W. T. Scruggs, A. J. O'Toole, P. J. Flynn, K. W. Bowyer, C. L. Schott, and M.Sharpe, "FRVT 2006 and ICE 2006 Large-Scale Experimental Results," *IEEE Transactions on Pattern Analysis and Machine Intelligence*, vol. 32, no. 5, pp. 831-846, 2010.

[4] Fan Chun-nian, "Illumination Invariant and Face Recognition Based on Homomorphic Filtering and LoG Operator," *International Journal of Advancements in Computing Technology*, vol. 4, no. 21, pp. 17-24, 2012.

[5] C.-N. Fan and F.-Y. Zhang, "Homomorphic filtering based illumination normalization method for face recognition," *Pattern Recognition Letters*, vol. 32, no. 10, pp. 1468-1479, 2011.

[6] http://www.cambridgeincolour.com/tutorials/white-balance.htm

[7] Liu, Chengjun. "Comparative Assessment Of Content-Based Face Image Retrieval In Different Color Spaces." *International Journal of Pattern Recognition and Artificial Intelligence*: 873-893.

[8] Dang-Hui Liu, Kin-Man Lam, Lan-Sun Shen, "Illumination invariant face recognition," *Pattern Recognition*, Volume 38, Issue 10, October 2005, Pages 1705-1716, ISSN 0031-3203, http://dx.doi.org/10.1016/j.patcog.2005.03.009.

[9] D.G. Lowe, "Distinctive image features from scale-invariant keypoints," *International Journal of Computer Vision*, vol. 60, pp. 91-110, 2004.

[10] Lindsay I Smith, "A tutorial on Principal Components Analysis".

[11] B.Gunturk, EE7730 Image Analysis I, Class Notes.

[12] http://www.cambridgeincolour.com/tutorials/color-spaces.htm

[13] http://en.wikipedia.org/wiki/File:Barns_grand_tetons_YCbCr_separation.jpg

[14] Pietikäinen, Matti, "A physics-based face database for color research," *Journal of Electronic Imaging*, vol. 9 No. 1 pp. 32-38, 2000.

[15] T. Lindeber, "Feature detection with automatic scale selection," *International Journal of Computer Vision*, vol. 30, no.2, pp. 79-116, 1998.

[16] Mikolajczyk, K. 2002. "Detection of local features invariant to affine transformations", Ph.D. thesis, Institut National Polytechnique de Grenoble, France.

[17] Brown, M. and Lowe, D.G. 2002. “Invariant features from interest point groups,” *British Machine Vision Conference*, Cardiff, Wales, pp. 656-665.

[18] Harris, C. and Stephens, M. 1988. “A combined corner and edge detector,” *Fourth Alvey Vision Conference*, Manchester, UK, pp. 147-151.

[19] http://www.robots.ox.ac.uk/~vedaldi/code/sift.html

Appendix: Permission Letters

From University of Oulu, Computer Vison Lab

From: Abdenour Hadid <hadidab@hotmail.com>

To: Jayesh Mohan <jmohan3@tigers.lsu.edu>

Dear Jayesh Mohan,

Yes, you have granted the permission to use the UOPB face database for your thesis research.

I kindly remind you that, for legal reasons and for the privacy of the database participants, only faces 1, 3, 14, 25, 94 and 111 may be used for presentation or publication. Also, please cite one our publications to refer to the database.

All best,

Prof. Abdenour Hadid

University of Oulu

Finland

From Dr.Omer Soysal

From: Omer Soysal <omsoysal@lsu.edu>

To: Jayesh Mohan <jmohan3@tigers.lsu.edu>

Dear Jayesh Mohan,

I permit you to use the UOPB face database in accordance with the permissions from Professor Abdenour. Please follow the necessary rules and cite the reference paper.

Dr. Ömer Muhammet Soysal

Research Assistant Professor, Project Supervisor; Highway Safety Research Group (affiliated with Department of Information Systems and Decision Sciences), Adjunct Faculty; School of Electrical Engineering and Computer Science

Louisiana State University

3535 Nicholson Extension, ISDS Research Lab, Room# 100G, Baton Rouge, LA 70803

Ph: 225-578-6297 Fx: 225-578-0240 Em: omsoysal@lsu.edu Web: http://projects.bus.lsu.edu/omer

Vita

Jayesh was born in Tumkur, India. After graduating from St.Claret College in 2006, he studied electronics and communication engineering at Nagarjuna College of Engineering and Technology, Visvesvaraya Technological University, India, from 2006 through 2010 toward obtaining his Bachelor of Engineering degree. He is currently a Masters student in the Department of Electrical & Computer Engineering at Louisiana State University, Baton Rouge, where he has been a graduate student since Fall 2011.